Probing Network Dynamics in Barrel Cortex

Thesis submitted for the degree of

Doctor of Philosophy

of the University College London

Lisa Kathryn Beeren

Wolfson Institute for Biomedical Research

University College London

2012

Declaration

I, Lisa Kathryn Beeren, confirm that the work presented in this thesis is my own. Where information has been derived from other sources, this has been indicated in the thesis.

Abstract

Recent studies have demonstrated that a rat can be trained to behaviourally report the electrical stimulation of a single cortical neuron (Houweling and Brecht, 2008). Other studies have reported detection of the optogenetic stimulation of ~300 neurons (Huber et al., 2008). However, although the animal can detect the stimulation, it is unclear what effect this small perturbation is having on the network and to what degree this will alter the animal's ability to perform a task. This thesis investigates the effect on both the local network and on behaviour of several magnitudes of neuronal perturbation, from a single spike to the excitation of several thousand neurons. Finding the limitations under which a network can function provides powerful insights into how neurons interact to form meaningful networks.

I performed simultaneous intra- and multi-unit extracellular recordings from the rat barrel cortex. I introduced a single spike into the patched neuron, and monitored the evolution of network activity via the extracellular probe. I found that the introduction of a single spike in a neuron produces a detectable increase in firing rate in the local network.

To extend the investigation, channelrhodopsin-2 (ChR2), a light-sensitive membrane protein, was electroporated under visual control into a small number (1 - 10) of layer 2/3 pyramidal cells in the somatosensory cortex of the adult mouse. After exciting the ChR2-positive neurons, the resulting network activity was measured both by cell-attached and whole-cell patch-clamp recordings from nearby neurons and by monitoring up to 50 nearby cells in different cortical layers using the multi-site silicon probe. I found that excitation of a small number of neurons caused an increase in the spike rate of the local network, which lasted up to 300 ms.

On the next level, large-scale perturbations were introduced into the brain by the optogenetic excitation of several thousand neurons in the cortexof transgenic mice expressing ChR2 under the Thy1 promoter. A short (2-20 ms) pulse of blue light

produced a strong initial response, measured in both the LFP and spiking activity across supragranular layers of the barrel cortex. This initial response was often followed by ~5 bursts of spikes which resulted in an oscillation in the LFP. This oscillation was found to be of similar frequency and time-scale to an oscillation recorded in the barrel cortex resulting from the deflection of a single whisker. After pharmacologically blocking activity in the thalamus, confirmed by loss of the whisker response, the light-induced oscillations disappeared, indicating that the thalamus is necessary for their propagation. Optogenetic stimulation was also able to generate oscillations in the awake animal.

I investigated the effect of such a large perturbation on mice undergoing a simple whisker-deflection discrimination task. It was found that the performance of the mice initially dropped to chance level if a strong perturbation was delivered 100 ms before the sensory stimulation. If the strong perturbation was sustained for every trial, the performance of the mice did not improve. If the perturbing stimulation was removed and then introduced gradually, the animal was able to adapt to the stimulation and learn to perform the task despite the perturbation.

In summary, small perturbations have a measurable effect on the local network, implying the use of a rate code for at least some brain states in the barrel cortex. A large perturbation produces a strong cortical response, which often leads to a strong oscillation. The same stimulus interferes with the behaviour of a mouse undergoing a simple task, and yet the mouse can learn to perform accurately despite the noise. Together, these findings suggest a coding regime with high degrees of redundancy and robustness. Although the cortical activity patterns are easily perturbed - even a single spike causes a temporary increase in firing rate - this disturbance does not have debilitating effects on the behaviour or the experience of the animal.

Acknowledgements

Thank you to Mickey London for 4 years of supervision and support and for being so wonderfully generous with your time. Thank you for always being patient with me and for the very detailed explanations and answers you gave to my often silly questions. Thank you for your wise advice, both in life and science and for all the long and meandering talks we had while you were still in London.

Thank you to Michael Haüsser for bringing together a lab full of clever and generous people and to Peter Latham for the Maths lessons early on.

To the Hausser lab during my time there - Christian, Arnd, Ian, Alanna, Martha, Spencer, Ikuko, Christoph, Ingrid, Beverley and Tiago - thank you for all the advice and technical help you've given me over the years and especially to Christian for being an excellent rig companion. Thanks to Spencer and Ikuko for their patience with our shared laser and to Arifa for very good technical assistance.

Thank you to the PhD students from our lab; Kate, Alex, Jan, Han, James, Sarah, Sara, Matteo, Ben and Gabija and from out of the lab; Dan, Laura, Karolina, Anna, Tom, Steve, Talia, Caroline, Caroline for struggling and laughing with me and for making me feel that we were all in it together.

Thank you to my family for always supporting me and more recently, to Mum, Dad, Soph and Michael for putting up with my spiritual absence from the Christmas holidays with such kindness. Thank you to Isaac for keeping me company through the long months of writing up. Thank you to Em and Tim for giving me a room in their lovely house and for never making me feel that my huge imposition was a problem. You made these final few months so much easier.

Finally, and most of all, I thank Alexander Arenz. Thank you for your patience, your support, for understanding my never-ending changes of plan and the constant delays. Thank you for your amazingly rapid and dedicated editing and for encouraging me to see value in what I had produced. And above all, thank you for your love, it has carried me through.

Table of Contents

1 Introduction

1.1 Overview

Animals encode sensory and motor information in the action potential (AP) firing of networks of neurons. One of the great, unsolved mysteries of modern neuroscience is how individual spiking neurons interact together in order to transmit a coherent message. The scope of this fundamental question is vast, and to answer it in the traditional way, i.e. by modifying the input and trying to read changes in the output, requires a degree of control over both internal networks and external stimuli far beyond what is presently possible (Brecht et al., 2006).

Recently, several studies in the barrel cortex have been published demonstrating the ability of the brain, following training, to detect and report stimulation of one (Houweling and Brecht, 2008) or hundreds (Huber et al., 2008) of neurons. These studies are fascinating, and highlight the brain's incredible capacity to listen to a few neurons in a sea of millions - but they do not help us to understand how the brain works in its natural setting, i.e. how the brain interprets and processes sensory inputs. In fact these experiments directly stimulate the cortical neurons in a way that is independent of the sensory input flowing in from the whiskers.

A synthesis between the two approaches described above is to address this question by investigating how neurons, and networks, cope with being perturbed in their processing of information by the introduction of extraneous 'noise' signals, in the form of from one to several thousand artificially introduced APs. Finding the limitations under which a network can function will provide powerful insights into how neurons interact to form meaningful networks, how robust cortical neuronal network interactions are, how sensitive a network is to "perturbations", if this changes depending on the state of the animal and if the brain learns to compute efficiently despite such perturbations.

Layer (L) 2/3 of the rodent barrel cortex is an ideal circuit for studying controlled perturbations for several reasons. Following a whisker deflection, the electrical signal is relayed through the trigeminal ganglion and thalamus to L4 and then L2/3 of the barrel cortex where a cellular spiking response can be observed. A direct link can therefore be made between simple behaviour, such as whisker-based sensory discrimination, and some of the cortical cells that are putatively involved. Furthermore, the local network contains a substantial amount of recurrent connectivity, forming a classic recurrent network popular in random network simulations. This allows for interesting modelling comparisons and predictions to be made in future studies. The strength and frequency of these connections has been quantified (Lefort et al., 2009) and the area has been well characterised: The distribution of cell types (Feldmeyer et al., 1999; Lübke et al., 2000; Petersen and Sakmann, 2000; 2001; Feldmeyer et al., 2002; Brecht et al., 2003; Petersen et al., 2003; Manns et al., 2004; Feldmeyer et al., 2006; Kerr et al., 2007; Helmstaedter et al., 2008), the structure of the barrel and distinct cellular layers, and the encoding of frequency and vibration of whisker stimulation (Kleinfeld et al., 2006) are well-known. Finally, the cells are superficial, allowing for 2-photon imaging and targeted manipulation (Kitamura et al., 2008).

The present study will therefore focus on perturbing neurons in the barrel cortex, ranging from the addition of one extra spike, to spikes in several local neurons, to synchronous activation of several thousand neurons of one cell type. Investigations into changes in local cortical activity, larger inter-structural neuronal activity and performance in a behavioural task will be conducted, shining some light on possible mechanisms the brain might use to adapt to and perform despite these perturbations.

1.2 The perturbation of neuronal networks

1.2.1 Recording Electrical activity in the brain

This work extracts and analyses information from both the local field potential (LFP) and multiunit activity (MUA) of a recorded signal. The LFP is measured over a larger distance than the MUA, often up to a distance of a centimetre from the recording electrode (Kajikawa and Schroeder, 2011). It is believed to be an average of the synaptic activity in a neural ensemble in the vicinity of the recording electrode. (Lindén et al., 2011). The specific extracellular field generated by a single synaptic current depends on the particular cell morphology as well as the spatial positions of both the synapse and recording electrode (Lindén et al., 2011). The LFP signal is filtered from 0.2-300 Hz. The MUA represents the spiking activity of neurons within a short (< 100 μm) distance of the recording electrode. Spikes from several neurons can be detected on the one channel but can often be separated according to the size and shape of the spike. The spiking signal is filtered between 300 and 5000 Hz.

1.2.2 Neural coding – rate vs. spike timing code

One of the most intriguing questions in neuroscience is how networks of neurons work together to encode and store information. Over the past decades huge advances have been made at both the microscopic (i.e. molecules, synapses, neurons) and the macroscopic level (i.e. functional mapping) of the brain. In comparison, our understanding of the intermediate level, the local neuronal network, remains relatively limited. There are many important questions to be answered with respect to network behaviour, and in particular the schemes neural networks use to encode information: Do networks use average spike rate to process information or is the precise timing of every spike important? Is this modified by the state of the network? How many neurons are needed for accurate transmission of information (deCharms and Zador, 2000)?

The controversial issue of which aspects of the spike train carry information has been the subject of debate for many decades, with a recent increase in interest

following the publication of several high profile articles arguing the importance of a simple rate code vs. a precise spike pattern (Shadlen and Newsome, 1994; Softky, 1995; Konig et al., 1996; deCharms and Zador, 2000). One possibility is that neurons react differently and rely on different parameters of the spike train depending on the stimulus they receive and the amount of essential information to be communicated. In a series of experiments, Rob de Ruyter van Steveninck, William Bialek and colleagues showed that motion-sensitive H1 neurons of the fly visual system respond differently to constant and dynamic stimuli (de Ruyter Van Steveninck et al., 1997). When presented with a random bar pattern moving at a constant velocity across the visual system, the spike pattern of the neurons was random and varied from trial to trial, even though the firing rate was constant. When presented with a dynamic stimulus, the spike pattern was remarkably precise and reproducible and the firing rate was strongly modulated by variations in the stimulus. What components of the network and its activity state underlie these different responses?

Rate and temporal coding strategies rely on the different temporal components of the spike train to transmit information. For a rate code, the important information is the average number of spikes integrated over a certain period of time. Indeed, the precise time of each spike is irrelevant and lost in the averaging process. For a temporal code, information is encoded in the precise time of each spike and the temporal patterns formed between the timings of many spikes originating from one or a group of neurons. Oscillations contribute to coding regimes by providing a background pattern on top of which the spike times fall. The precise arrival time of an input can become important when the membrane potential of the postsynaptic neuron is undergoing an oscillation. If the excitatory input falls during the trough in the oscillation, the resulting depolarisation might not be sufficient to raise the membrane potential above threshold and therefore the information from the input could be lost. If the input arrives at the beginning of a peak, the depolarisation provided by this one input could be enough to push the membrane potential above threshold and elicit an output spike. The timing of this

input spike is therefore crucial and this neuron could be described as employing a temporal coding strategy based on precise timing.

In the anesthetised animal, distinct periods of hyperpolarised and depolarised membrane potential can often be recorded which result in a slow oscillation. These are known as up and down states and are a characteristic feature of both anaesthesia and slow-wave-sleep (Steriade et al., 1993; Destexhe et al., 2007). As described above, the presence of this slow oscillation can increase or decrease the effectiveness of an input depending on at which point it arrives in the oscillatory cycle.

Neuronal noise is a limiting factor in a network's ability to transmit accurate information (Averbeck et al., 2006). Noise arises both from a neuron's intrinsic trial-to-trial variability and random inputs from the network (deCharms and Zador, 2000). This extra noise must be essentially ignored, or overcome, for a neuron to be able to precisely communicate information to its postsynaptic targets. But how does a network distinguish what is noise and what is signal (Averbeck and Lee, 2006)? One means of investigating how a network separates noise and signal is to introduce noise artificially in the form of extra spikes and measure its degree of propagation through the network under different conditions (London et al., 2010). A single extra spike may have a large effect on information propagation in one network and no effect in the next, depending on timing, connectivity, the classes and properties of the neurons, and the sensory stimulus the network is receiving. By studying the effect of a single inhibitory or excitatory input on a spiking network, a greater understanding of how neurons and networks integrate information, and under what conditions, can be gained.

1.2.3 Single cell manipulation studies

The power of the single cell and its ability to be heard through the "chaotic" brain activity of the many thousands of cells surrounding it has fascinated neuroscientists for many years (Cohen and Newsome, 2009). In 2004, a ground-breaking study showed that the electrical stimulation of a single patch-clamped

pyramidal cortical motor neuron could evoke small movements in the whisker of a rat (Brecht et al., 2004). Recently it has been shown that juxta-cellular stimulation of a single rat neuron, in the barrel cortex can be detected by the animal and reported through its behaviour (Houweling and Brecht, 2008). One might expect stimulation of thalamic neurons to be even more readily detected, given the lower numbers of thalamic neurons and their divergent connections to the cortex (Arnold et al., 2001). Interestingly, however, when tested the animal was not able to report stimulation of single thalamic neurons above chance level (Voigt et al., 2008). Recently, it was reported that extensive (~ 3 min) stimulation of a single neuron in the superficial layers of the visual or somatosensory cortex could modify the cortical states, ie between states resembling slow-wave and rapid-eye-movement sleep (Li et al., 2009).

These studies suggest that in specific situations the activity of a single neuron is both detectable by the animal and can produce a measurable motor output. What has not yet been investigated is what effect this activity can have on the ongoing behaviour of an animal and its ability to perform a simple task. Although the animal can report stimulation of a single neuron following training, it might be that activation of a single "naïve" neuron has no noticeable effect on the network and unless an animal is trained to detect it, its altered activity will be disregarded. It is possible that many more neurons must be stimulated in order to produce an effect strong enough to evoke a behavioural output.

1.2.4 Micro-stimulation during behaviour

Until recently, the principal means of stimulating a population of neurons was by micro-stimulation (Cohen and Newsome, 2004; Reppas and Newsome, 2007). This technique is non-specific, stimulating all neurons in a particular area as well as the axons of remote neurons passing through the region, and is difficult to control spatially. It has, however, been shown to both improve behavioural performance levels under certain conditions (Salzman et al., 1990) and interfere with behavioural tasks (DeAngelis and Newsome, 2004). In monkeys trained to report the direction of moving dots presented on a screen, micro-stimulation of

clusters of directionally selective neurons in the middle temporal visual area (area MT or V5; (Salzman et al., 1990) biased the animals' perception towards the direction of motion encoded by the stimulated neurons. Varying the amplitude and frequency of the stimulation pulses delivered showed that increasing the frequency of the pulses increased the bias towards the preferred direction for all tested frequencies up to 500 Hz (Murasugi et al., 1993). Increasing the amplitude similarly increased the bias towards the preferred direction up to 80 μA, at which amplitude the animal responded at chance level. This was attributed to a larger area being stimulated, including areas of neurons of opposing orientation preferences, and thus adding uninterpretable "noise" to the system (Murasugi et al., 1993). This task to some extent enabled the exploration of the limits of perturbations the brain can withstand. Without cell-type specific activation, however, or optical control, it was impossible for the study to confirm that the decrease in performance was attributable to a wider and opposing subset of neurons being stimulated.

1.2.5 Optical control of small neuronal populations

In the past ten years, rapid advances in the development of optogenetic tools have allowed researchers to exert a very precise degree of control over the small scale manipulation of specific neuronal populations. In particular two tools, Channelrhodopsin2 (ChR2) and halorhodopsin (NpHR), as well as their many variants, have made it possible for the spiking activity of neurons to be increased or decreased, respectively, and for the effects on the local network, other brain areas and animal behaviour to be monitored.

ChR2 is a light-gated ion channel isolated from the green algae *Chlamydomonas reinhardtii* (Nagel et al., 2003). It is a nonspecific cation channel, conducting H^+, Na^+, K^+, and Ca^{2+} ions. Once expressed in neurons it is incorporated into the cell membrane where it can be opened by blue light at a wavelength of ~470 nm, thus permitting the influx of Na^+ into and efflux of K^+ ions out of the neuron with the temporal precision and resolution to produce single APs (Boyden et al., 2005; Li et al., 2005). This allows millisecond control over the firing pattern of neurons,

and is a relatively clean and non-invasive method for introducing noise into a neural circuit.

ChR2 can be introduced into the neuron *in vivo via* several different methods (Luo et al., 2008), all with various advantages and drawbacks. *In-utero* electroporation, in which plasmids containing the ChR2 DNA are electroporated into the foetuses of a pregnant animal, allows large scale introduction of the plasmid into a particular cell line depending on the precise location and timing of the electroporation, but its possibly far ranging effects on the developing embryo are unclear. Viral transfection with ChR2 plasmids, combined with the use of transgenic animals allowing cell-line specific or precisely timed up-take of the plasmids into neurons, can be performed on juvenile or adult animals and has high success rates, but it is difficult to titrate the injection with enough precision to limit the number of cells affected or to prevent the virus from spreading too far. Despite these limitations, this technique has been widely used to control small populations of neurons. One of the earliest studies demonstrated that mice can detect the introduction of ~300 spikes (either trains of five APs from an average of 61 neurons or single APs from an average of 297 neurons) into the local network (Huber et al., 2008).

Recently a technique has been developed to permit targeted introduction of ChR2 plasmids into individual cells (Kitamura et al., 2008), pushing investigations into both the detection limit of behaving animals and the subsequent effect on their behaviour even further.

This study will take advantage of the precise temporal and cell type-specific control of small numbers of neurons afforded by these recent advances in optogenetic tools that finally allow us to directly examine the robustness of sensory encoding in cortical networks.

1.3 The whisker pathway

Rodents use whiskers much in the way humans use their fingertips. When awake and actively exploring an environment, rodents actively move their whiskers back and forth (whisking). The neuronal encoding of whisker activity involves a complicated interaction between sensory signals travelling from the whisker pad to the cortex and feedback from the ongoing whisking activity. This allows the animal to form an accurate representation of the physical world surrounding it. Recently, it was discovered that cortical motor control is driven not only by the motor cortex but also directly by the somatosensory cortex. Whereas activity in primary motor cortex directly evokes exploratory whisker protraction, primary somatosensory cortex directly drives whisker retraction, providing a rapid negative feedback signal for sensori-motor integration (Matyas et al., 2010).

Sensory information encoding whisker movement begins its journey with the deflection of the whisker. This deflection is thought to open mechanogated ion channels in the sensory neurons innervating the hair follicle from the infra-orbital branch of the trigeminal nerve (Petersen, 2007). This leads to depolarisation and eventual AP firing in the sensory neurons, with each sensory neuron producing APs in response to the deflection of a specific whisker. They form excitatory synapses in the trigeminal nucleus, whose principal trigeminal neurons project to the ventral posteriomedial nucleus of the thalamus (VPM). Both the trigemino-thalamic neurons in the trigeminal nucleus and the VPM are somatotopically arranged into anatomical units called “barrelettes” (Veinante and Deschênes, 1999) and “barreloids”, respectively, each responding most strongly to input from a single whisker (Simons and Carvell, 1989). Neurons from the VPM project principally to L4 of the primary somatosensory cortex and also form discrete anatomical clusters, “barrels”, which respond to the stimulation of a principal whisker (Fig 1.1; Woolsey and Van der Loos, 1970). The barrel cortex can be identified using cytochrome oxidase staining due to the direct relationship between the activity of the enzyme and neuronal activity (Fig 1.1b; Wong-Riley and Welt, 1980).

a

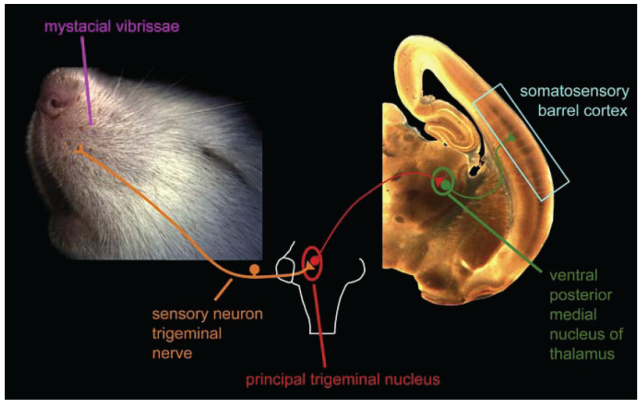

b

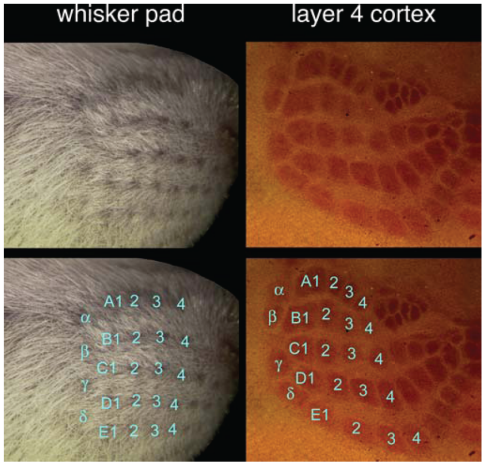

Fig 1.1 The primary signaling pathway from whisker to cortex. a) Sensory neurons of the trigeminal ganglion have nerve endings in the whisker pad. These neurons fire action potentials in response to whisker deflections, which release glutamate at brainstem synapses in the principal trigeminal nucleus. These brainstem neurons project to the VPM, whose neurons project to the primary somatosensory cortex, where they terminate in somatotopically arranged clusters in layer L4 forming barrels. **b)** The layout of the L4 barrels, which closely matches the layout of the whiskers on the rodent snout. The tangential cortical L4 sections have been stained for cytochrome oxidase, which gives a clearly delineated pattern of barrels. Adapted from Petersen, 2003).

While the pathway described above (termed the "lemniscal" pathway) has been identified as the major route for whisker-related information, information can also arrive at the barrel cortex *via* other secondary pathways, believed to encode the

information in a broader and less specific manner, with greater cortical feedback (Koralek et al., 1988). The secondary pathways deviate from the principal one as early as the trigeminal sensory neurons, which send excitatory connections to the spinal trigeminal brainstem nuclei. This nucleus is also arranged into barrelettes and can be divided into two subregions. The caudal part carries the little known "extralemniscal" pathway to the ventrolateral part of the VPM where it continues to the secondary somatosensory cortex (S2) and to the regions between the barrels, called "septa", of L4 of the primary somatosensory cortex (S1; Pierret et al., 2000). The rostral part of the spinal trigeminal brainstem nucleus carries the "paralemniscal" pathway to the posterior medial nucleus of the thalamus (POM) and then to L1 and 5A of S1, S2 and the motor cortex (Yu et al., 2006). This pathway receives particularly strong excitatory feedback from the cortex (Diamond et al., 1992), suggesting a role of sensorimotor integration (Petersen, 2007).

The striking similarity between the barrel map observed in the primary somatosensory cortex and the layout of the whiskers in the whisker pad makes the whisker system ideal to study how simple sensory inputs are translated into neural code. Furthermore the whisker information, as it passes through this pathway, undergoes two interesting transformations. Firstly, while whisker stimulation is recorded faithfully and reproducibly in the trigeminal ganglion (Arabzadeh et al., 2005), the representation of whisker related information increases remarkably in variability as it passes through the thalamus and to the cortex. While in the thalamus the information is still relatively reliable, by the time it reaches the cortex identical stimuli produce great trial-to-trial variability in their cortical neuronal responses (Petersen et al., 2003; Arabzadeh et al., 2005). Secondly, in the barrel cortex the receptive fields of each individual whisker extends to more than one barrel (Petersen, 2003). Upon deflection of a whisker, a weaker but measurable response can be recorded in the barrels surrounding the barrel corresponding to that particular whisker. This is in contrast to both the trigeminal ganglion and the thalamus, in which each somatotopically defined region responds to a single whisker. Clearly, the cortex is providing a function in which

it combines whisker responses with both other sensory responses and feedback from other regions, transforming the simple whisker deflections into an integrated sensory experience for the animal.

1.3.1 The thalamus

With few exceptions, all sensory input passes through the thalamus on its way to the cortex. This assigns the thalamus a crucial "gateway" role, with the opportunity to either passively relay information or to selectively modify certain parts of the sensory experience. It can increase the importance of select pieces of information, or restrict the pathway of other information. This opportunity to filter information, as well as strong feedback loops between the cortex and the thalamus (Fig 1.2a), suggest a potentially important role for the thalamus in attention (Sherman and Koch, 1998). In this work, the key role of the thalamus lies in translating whisker information from the faithful representation of each identical whisker stimulation it receives, to the spiking patterns recorded in the cortex which change with each repetition (Ahissar et al., 2000). Understanding how and why the thalamus makes these transformations is crucial to understand how sensory information is encoded and interpreted by the brain.

The thalamus consists of three major divisions: the dorsal, ventral and epi-thalamus. The dorsal thalamus is the largest part and is often referred to simply as the thalamus (and will be also in this work). It consists of many distinct nuclei, which form reciprocal connections with specific areas of the cortex. The ventral thalamus does not innervate the cortex directly, but receives innervation from the cortex and forms reciprocal connections with the dorsal thalamus. The epithalamus is more closely connected with the hypothalamus and has no direct connections with the cortex (Jones, 1985).

The dorsal thalamus can be divided into several independent nuclei (Fig 1.2): the lateral geniculate nucleus relays sensory input from the retina to the visual cortex; the medial geniculate nucleus sends information from the inferior colliculus to the auditory cortex; the ventral lateral nucleus receives input from the deep cerebellar

nuclei and projects to the primary motor cortex; the basal ventral medial nucleus projects gustatory input to the primary somatosensory cortex; and the ventral posterolateral nucleus (VPL) and VPM both project to the somatosensory cortex but receive input from the body and the head, respectively (Jones, 1985).

One of the nuclei of the ventral thalamus, the reticular nucleus of the thalamus (RT), deserves particular attention in this work. This nucleus forms a thin shell-like structure around the anterior and dorsal parts of the dorsal thalamus (Fig 1.2). It is itself made up of a number of subnuclei, each of which is reciprocally connected to a specific nucleus (e.g. VPL, VPM) of the dorsal thalamus. (Sherman and Koch, 1998).

The thalamus receives both excitatory and inhibitory inputs. The main excitatory inputs come from the various primary sensors such as the retina *via* the optic tract and the whisker pad *via* the trigeminal nerve. There are also strong feedback connections mainly from L6 but also from L5 of the cortex whose axons also send collateral branches to the RT. The brainstem formation sends cholinergic, noradrenergic and serotonergic axons. The major inhibitory inputs come from the specific subnuclei of the RT and local interneurons.

The nuclei of the thalamus consist principally (roughly 75%) of relay neurons, which send axons to form excitatory connections to neurons in L4 of the cortex with collaterals to L5 and L6. These connections also send branches to innervate the RT as they pass by.

Neurons of the thalamus have two distinct modes of firing, either burst spiking when activated from negative resting potentials or tonic firing when activated from more depolarized potentials (~> -60 mV; Llinás and Jahnsen, 1982).

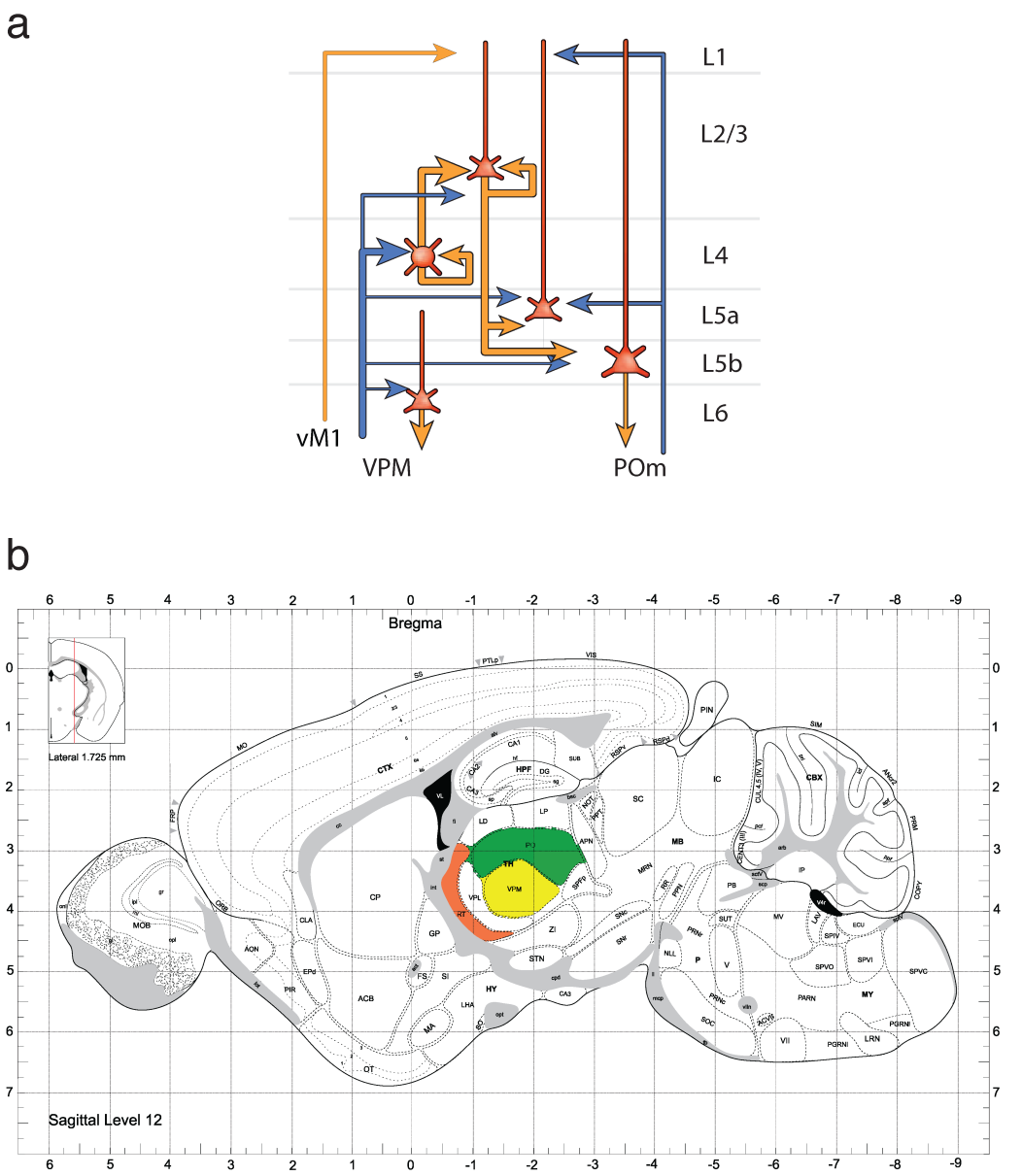

Fig 1.2 Connections and location of the whisker-related thalamus. **a)** Circuit diagram of thalamo-cortical excitatory connections. Blue lines depict the ascending thalamo-cortical input from the ventral posterior medial nucleus (VPM) and the medial subdivision of the posterior nucleus (POM). The orange lines show intracortical connections including inputs from the whisker-related motor cortex (vM1) and descending projections. The red lines depict dendritic arborizations. Adapted from (O'connor et al., 2009) **b)** Sagittal section highlighting position of VPM (yellow), POM (green) and reticular nucleus of the thalamus (RTN; orange). The medio-lateral position of this section is indicated in the inset. Slice images adapted from "The Mouse Brain in Stereotaxic Coordinates" edited by Paxinos and Franklin (Paxinos and Franklin, 2007).

For the whisker system, the two key nuclei of the thalamus are the VPM and POM, which carry information in the lemniscal and paralemniscal pathways, respectively. They are situated next to each other, both medial to the VPL, which is, in turn, medial to the RT and internal capsule. The intrinsic membrane properties of neurons from the two nuclei are similar (Landisman and Connors, 2007) however many other properties vary between them. POM neurons fire fewer spikes, have a lower firing frequency during a burst, have larger unitary EPSPs and more variable and generally longer response latencies than neurons in the VPM (Landisman and Connors, 2007). The receptive field size for neurons in POM is five whiskers whereas for VPM it is one whisker (Chiaia et al., 1991; Diamond et al., 1992). As discussed previously, the VPM is organised into discrete barreloids whereas the anatomy and connectivity of POM is more diffuse (Bourassa et al., 1995).

One possibly crucial difference between VPM and POM neurons is the presence of a $GABA_B$ component in the inhibitory responses of POM neurons to cortico-thalamic stimulation (*via* the RT). These $GABA_B$ responses were hypothesised to be responsible for the more sluggish nature of the POM response. Cells may be kept hyperpolarised for longer periods of time, making them less responsive to whisker stimulation. This could be a key feature of the temporal coding strategies of POM (Golomb, 2006). The slow responsiveness of POM neurons could suggest that they integrate inputs over long period of time, making the POM more likely to receive and transmit information in the form of a rate code rather than a code based on precise spike timing.

1.3.2 Whisker-related pathways between the barrel cortex and the thalamus

Cortico-thalamic feedback connections, while being less studied and characterized than their thalamo-cortical counterparts, often greatly outnumber the thalamo-cortical feed-forward connections, in some cases by 40 to 1 (Sherman and Koch, 1998). Similar to the input from the trigeminal nucleus, the feedback from the

cortex is somatotopically organised in the thalamus (Temereanca and Simons, 2004).

Importantly, the cortical connections onto POM and VPM suggest very different functionality for these two thalamic nuclei. The VPM receives thin axons from L6 which are thought to have only a modulatory role (Diamond et al., 1992). The POM receives both thin axons from lower L6, and large axons from L5 (Reichova, 2004). These larger inputs are thought to be of driving nature with an important influence on POM activity. The RT receives excitatory input *via* axon collaterals from corticothalamic neurons originating in layer 5 and layer 6 (Thompson 2010). It receives further axon collaterals from thalamocortical neurons.

1.3.3 The barrel cortex

After passing through the thalamus, the information encoding whisker stimulation reaches the barrel cortex. Unsurprisingly, given the importance of the whiskers to the rodents sensory experience, the barrel cortex forms the largest part of the somatosensory cortex in rodents and its circuitry and anatomy have been well documented (for review see Brecht, 2007; Petersen, 2007) .

Like other primary sensory cortices such as the auditory and visual cortices, the barrel cortex is divided into several layers, based on anatomical location, cell type composition and connections. There are six horizontal layers in total, named on the basis of their proximity to the surface, with 1 being the most superficial. Traditionally, L2 and 3 have been grouped together functionally and L5 has been separated into 5A and 5B. Input from the lemniscal whisker pathway makes connections onto neurons in L4 of the barrel cortex from the VPM of the thalamus. It is this layer after which the barrel cortex is named, being divided into aggregates of approximately 2000 (in mice; Lefort et al., 2009) cells called barrels, each of which receive input from one principal whisker (Van der Loos, 1976).

From here information travels up to L2/3 and down to L5A, L5B and L6. These inputs carry information related to whisker deflections and have both short response latencies and small receptive fields (Diamond, 1995). Paralemniscal

input enters the cortex instead at L5A, L1 and the septal parts of L4 between the barrels (in rats). The receptive fields of paralemniscal neurons are large and have long response latencies and are thought to integrate sensory and motor inputs, as well as feedback from the cortico-thalamic inputs. This pathway is therefore unlikely to be involved in precise sensory signalling but rather in aiding with sensorimotor coordination during active whisking (Brecht, 2007; Petersen, 2007).

There are several different barrel cortex outputs with varying degrees of lemniscal and paralemniscal integration (Petersen, 2007). Cortico-cortical connections are sent from L1, 2 and 3 to promote intercolumnar integration. Lemniscal outputs travel principally to other parts of S1 whereas paralemniscal travel to M1. Lemniscal and paralemniscal outputs from L5 are integrated and travel primarily to the midbrain, striatum and various subcortical targets. L6 provides the principal cortico-thalamic outputs to provide feedback to the paralemniscal pathway.

A recent connectivity study highlighted the extensive long-range connections that S1 makes to other brain areas (Aronoff et al., 2010). S1 sends a high density of axonal innervation to S2 and there are also direct monosynaptic excitatory connections from S1 to M1. Interestingly, the connections between S1 and M1 are not across corresponding layers, but rather crossing the vertical length of the cortex. Supragranular S1 L2/3 pyramidal neurons showed the densest innervation of deeper layers in M1 whereas the infragranular pyramidal neurons in S1 preferentially innervated the superficial layers of M1, with a prominent innervation of the most superficial layer 1. Further reciprocal projections to other cortical regions are seen: bilateral projections to perirhinal cortex as well as projections to the ipsilateral orbital cortex, the contralateral somatosensory cortex and contralateral motor cortex (Aronoff et al., 2010).

In each barrel column of the mouse, there are approximately 8,000 neurons, with approximately 10% of these being inhibitory, the rest excitatory (Fig 1.3; Lefort et al., 2009). L4 has the highest number of neurons with approximately 2000, followed by L6 with ~ 1500.

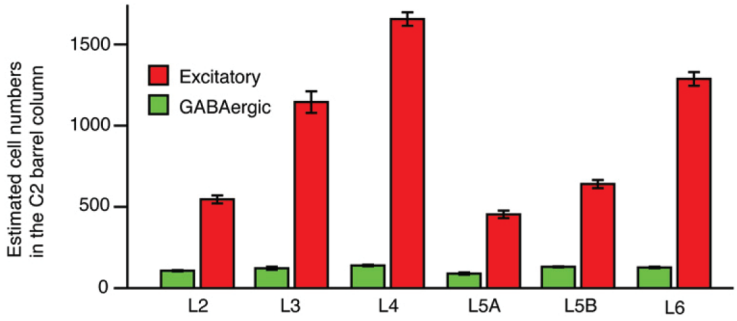

Fig 1.3 Distribution of neurons from each layer in the mouse C2 Barrel Column. Estimated numbers (mean ± SEM) of excitatory and inhibitory cells in different layers of the mouse C2 barrel column.

1.3.4 Whisker representation in the barrel cortex

Neurons in the barrel cortex are direction selective (Bruno et al., 2003; Andermann and Moore, 2006) as well as velocity sensitive, acceleration sensitive and position sensitive (Diamond et al., 2008). Overall the response in the barrel cortex is thought to be sparse, i.e. there is a relatively low firing frequency in response to whisker stimulation. For example, one thorough study found that, on average, the AP responses to a single whisker deflection in the caudal direction in the anesthetized rat during the first 100 ms post stimulus, after correction for spontaneous activity, were 0.11, 0.41, 0.15 and 0.64 APs for L2/3 cells, L4 cells, thin-tufted L5 and thick-tufted L5 cells, respectively (de Kock et al., 2007).

There has been limited work investigating the responses to controlled whisker deflections during active whisking. However, when the whiskers encounter an object, they often undergo a slip-stick movement, which is characterised by sparse, temporally precise, synchronous spiking in the barrel cortex (Jadhav et al., 2009).

In the awake state the animals actively explore their environment by moving their whiskers back and forth at ~10 Hz in an ongoing whisker cycle (Kleinfeld et al., 2006). It is the interaction between the phase of the whisking cycle and the contact between a particular whisker and an object which allows the animal to build up a clear picture of its surrounding environment, with precise locations of

environmental objects. Information reporting contact between whisker and object appears in the barrel cortex as a brief burst of APs coincident with mechanical forces on the whiskers (Curtis and Kleinfeld, 2009). Since the animal is actively whisking at the time of these bursts, the timing of these APs within the whisk cycle could therefore encode horizontal location (Diamond et al., 2008).

1.4 Sensory-evoked oscillations

1.4.1 Features

The deflection of a whisker in an anesthetised rat is often followed by several rhythmic bursts of APs observed in all layers of the barrel cortex and also in the whisker-related nuclei of the thalamus (Dinse et al., 1997). In the LFP these bursts are represented as clear oscillations of 7-14 Hz, beginning more than 100 ms after the initial response to the stimulation and stopping within a second. Their function is poorly understood but they appear to be the result of an unexpected sensory perturbation. This idea is supported by the ability of micro-stimulation to induce oscillations very similar to those evoked by sensory stimulation (Fig 1.4; Contreras and Steriade, 1996; Contreras et al., 1997; Venkatraman and Carmena, 2009). Also in this case, the brain reacts to this large, sudden, and in this case artificial rather than sensory, perturbation by producing an oscillation. Why the brain does this is still an open question.

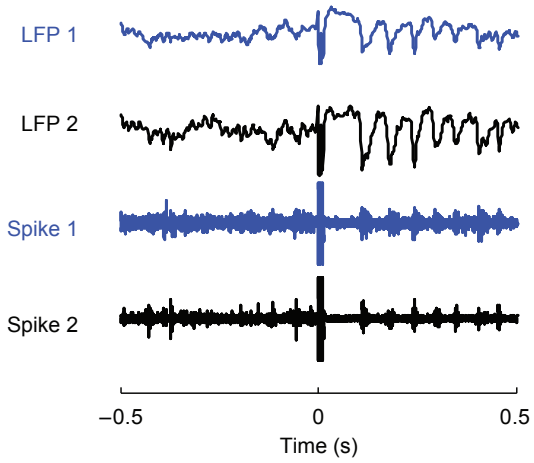

Fig 1.4 Electrical stimulation-evoked oscillations recorded in the barrel cortex of the rat. 1–200 Hz local field potential (LFP) and 0.5–10 kHz multiunit activity (Spike) recorded from two electrodes in the infragranular layer (L5/6) of the barrel cortex of awake rats. Microstimulation was delivered at 0 s. Adapted from (Venkatraman and Carmena, 2009).

Low frequency oscillations (below 20 Hz) associated with sensory stimulation were first observed as early as 1936 (Bishop and O'Leary, 1936) and have since been reported in rats, cats and rabbits (Dinse et al., 1997) and more recently in the thalamic reticular neurons of freely moving mice (Halassa et al., 2011). They can be initiated by auditory, olfactory, somatosensory and visual sensory stimuli (Spengler and Dinse, 1994) The oscillatory periods range for between 500 and 800 ms and have frequencies of 6-20 Hz, depending on the animal and the cortical area. In the whisker system of mice, there has been very little investigation into these oscillations, however in the barrel system of rats they have been well characterised (Muthuswamy et al., 1999; Ahissar and Kleinfeld, 2003).

1.4.2 Origin and Pathway

Sensory-evoked oscillations have clear similarities to spindle waves found to be present in the early stages of sleep and under anaesthesia (Steriade et al., 1990;

1993; Mccormick and Bal, 1997; Steriade, 2005). They have a similar frequency range of 7-14 Hz, a similar duration of ~ 1 s and have been found to be present in both the cortex and the thalamus.

While studies investigating the origin and pathway of sensory-evoked oscillations are limited, there is a long-standing debate as to the origin of spontaneous spindles. Two opposing hypotheses have been proposed. One purports that the generation of spindle waves depends exclusively upon RT activity. This idea was based on early *in vivo* studies that thalamic neurons disconnected from the RT cannot exhibit spindle waves (Steriade et al., 1985) whereas the RT alone can generate spindle waves (Steriade et al., 1987; Destexhe et al., 1994). *In vitro* studies have also shown that intrinsic properties of RT neurons allow them to generate rhythmic bursts at the spindles frequency (Avanzini et al., 1989; Bal and Mccormick, 1993).

The second hypothesis is that spindle waves result from the interplay between RT neurons and thalamic relay neurons, supported by more recent *in vitro* experiments (Bal et al., 1995a; 1995b). According to this hypothesis, burst firing of GABAergic neurons in the RT results in inhibitory postsynaptic potentials (IPSPs) in thalamic relay cells. These IPSPs de-inactivate the I_T current in thalamic relay cells resulting in a burst of APs. This burst firing once again activates I_T in the RE cells, thus generating the next burst of the spindle wave.

In a more recent study, investigating the structures involved in the generation and maintenance of tone-evoked oscillations in the auditory system, it was found that both the auditory RT and the medial geniculate body (MGB) were required for the presence of the tone-evoked oscillations (Cotillon and Edeline, 2000). This suggests that interactions between these two structures are necessary and supports the second hypothesis. Furthermore, the presence of I_T was reported in all the anatomical MGB divisions (Hu et al., 1994; Hu, 1995; Tennigkeit et al. 1996, 1999; Bartlett & Smith, 1999).

On the other hand, several studies have shown that the cortex is not required for the generation of spindle waves (Cotillon and Edeline, 2000; Andersen et al., 1967; Timofeev and Steriade, 1996; Contreras et al., 1997), but was required for their large synchronization (Contreras and Steriade, 1996; Contreras et al., 1997). Moreover, it was shown that the frequency of the oscillations is not modulated by cortical networks, at least in the auditory system (Brecht et al., 2006). Unlike spindle waves, tone-evoked oscillations were found not to be synchronized over large distances (Cotillon and Edeline, 2000; Cotillon et al., 2000). They can be observed simultaneously at neighbouring electrodes, but not in different structures. The more localized aspect of stimulus-evoked oscillations seems to reflect the lack of cortical involvement.

1.4.3 Presence of oscillations in awake animals

Cortical micro-stimulation in sensory areas has been shown to elicit an oscillatory response, similar to the sensory-evoked oscillations described, in both anesthetized and awake animals (Margrie et al., 2002). While the occurrence of stimulus-evoked oscillations in anesthetized animals has been well documented, experiments on awake animals have yielded conflicting results, with some studies claiming that they do not occur in awake animals (Cotillon-Williams and Edeline, 2003; 2004) and others claiming to have observed bursting of these neurons leading to oscillations in wakefulness (Ramcharan et al., 2000; Swadlow and Gusev, 2001). Epochs of vibrissa-locked oscillatory activity have been observed in freely behaving rats (Fee et al., 1997). They have recently been induced with micro-stimulation in awake behaving rats (Venkatraman and Carmena, 2009). Therefore the mechanisms for the generation of oscillations are present and active in the awake state. The conflicting data on the presence of oscillations following a more natural sensory stimulation, however, suggests that generating a natural stimulation with sufficient strength might be difficult in a brain receiving increased levels of external stimulation.

1.5 Aim of this work

This thesis uses a wide range of techniques to introduce perturbations of increasing magnitudes into the brain of an anesthetised and awake animal and while it is performing a simple task. How the brain reacts to such perturbations, whether they be a single spike or a strong, synchronous burst from thousands of neurons, will give important insight into the adaptive and coding mechanisms used by the brain to encode information.

Despite an increasing body of work into the animal's ability to detect and report neuronal and network stimulation, it is still not known whether it requires a small or large neuronal disruption to prevent the sensory signal from being relayed from the thalamus through the barrel cortex and into higher cortical areas. Common sense suggests that very large-scale perturbations, e.g. removal of the thalamus, will sabotage the animal's ability to detect whisker stimulation. On the other extreme, very weak perturbations such as one extra spike in one neuron, will most likely have no effect. But between these two extremes lie many levels of perturbation. Although it would be impossible to pinpoint exactly how many cells or how many spikes lie on this limit, it is important to be able to estimate the magnitude of minimum 'noise' which would occlude the real signal, and how this varies when the brain is in different states of awareness. This would give further understanding of how a brain region such as the cortex could be operating.

The overall and long-term aim of this project is to investigate the level of interference or perturbation needed in order to disrupt the encoding of sensory stimuli in the rodent barrel cortex. This investigation can be divided into three stages. Firstly it is necessary to investigate and quantify the effect that perturbation of one cell can have on network dynamics. To investigate this, I have performed simultaneous intra- and extra- cellular recordings in the barrel cortex of the anaesthetised rat. Following perturbation of one cell through the injection of positive current, the effect on the local network spiking activity can be quantified. Next, I performed similar experiments with up to 20 neurons using optogenetics tools.

Secondly, I introduced larger-scale perturbations by both optogenetically stimulating several thousand ChR2-expressing neurons in the barrel cortex and by deflecting the principal whisker and characterising the subsequent oscillations produced by the brain as a result of these perturbations. These were performed in both anesthetised and awake animals. I further investigated these oscillations by removing activity in the thalamus pharmacologically and recording the changes to both the whisker response and the ChR2-evoked oscillations.

Finally I extended the large-scale perturbation study to investigate the effect of such perturbations on a performing animal undergoing a simple whisker deflection task. Large-scale perturbations result in a decrease in the animal's performance. I altered the parameters of the stimulation to study whether or not the animal could learn to perform accurately despite the presence of the perturbation. This helps us to understand how the brain can adjust its encoding of information to adapt to changes and disruptions and still perform efficiently.

This work uses the specific structure and function of the barrel cortex to study the effect of adding extra noise, in the form of erroneous spikes, to a network. Through a combination of electrophysiological and behavioural experiments I investigated the magnitude of noise to which the transmission of sensory information, namely whisker movement, is sensitive. This gives important clues towards understanding the way in which networks transmit information.

2 Materials and Methods

2.1 Overview

Experiments in this thesis were performed in the barrel cortex (and thalamus) of rats and mice. The study was begun in rats, however it became necessary to change species for two reasons. Firstly, electroporation was more difficult in rats due to the thickness of the dura mater. Secondly, later experiments required transgenic animals, and therefore the use of mice was obligatory. The specific animals and surgeries required for each type of experiment are detailed at the beginning of each chapter as well as techniques specific to those experiments.

The care and experimental manipulation of the animals was carried out in accordance with institutional and national guidelines. When experiments required anaesthesia, body temperature was maintained at 37° C with a feedback-controlled heating blanket (FHC Inc, USA). Three different anaesthetic regimes were used: Urethane, ketamine/xylazine and isoflurane. Urethane was used for all experiments in rats. Ketamine/xylazine was used for recovery electroporation experiments in mice. This regime included analgesia and the recovery was slow, allowing the animals to adjust more gradually to the surgery. For the experiments involving intrinsic imaging, the use of isoflurane was necessary as the intrinsic signal was not detectable under ketamine. Depth of anaesthesia was monitored throughout experiments and considered sufficient when the animals did not show paw withdrawal reflexes in response to the noxious stimulus of a hind limb toe pinch. If required, anaesthesia was increased. For urethane and ketamine/xylazine the animal was topped-up with 10% of original dose i.p. For isoflurane, the concentration was increased to 1.5%.

All dissection tools were from Fine Science Tools and craniotomies were drilled with a Vmax dental drill (NSK Nakanishi, Japan). During surgeries and experiments the brain was kept moist with HEPES-buffered external solution (in

mM): 150 NaCl, 2.5 KCl, 10 HEPES, 2 $CaCl_2$, 1 $MgCl_2$; pH 7.3 (adjusted with HCl / NaOH), 300 mOsm.

2.2 Intrinsic imaging

For the perturbation of oscillation experiments, the precise position of the C2 barrel was located using intrinsic imaging of responses to the mechanical stimulation of the principal whisker (see below). All intrinsic imaging procedures and data analysis were based on experiments described in Aronoff and Petersen (Aronoff and Petersen, 2007). The experimental set-up is depicted in Fig 2.1a.

LEDs with low dome lens (LXHL-ND98 and LXHL-ND98, RS Components, UK) were used for green and red light illumination. Images were acquired using an EC1350 CCD camera (Prosilica, Allied Vision Technologies, USA) with 25mm and inverted 16mm F/1.4 C-mount lenses (Fujinon, Fujifilm, USA). Data was analysed using a custom built programme in Matlab. After the imaging disk was adhered over the barrel cortex (see section 4.2), the skull was covered with external solution. The camera and lenses were suspended approx. 3mm above the skull (Fig 2.1b) with the focus adjusted to image a circular area of ~2mm diameter. An image of the blood vessel pattern under green light was taken for later barrel location. The whisker was stimulated for 4 s in a horizontal direction with a piezo bender (see section 5.10) at 10 Hz. 640x480 pixel images were acquired 6 s before, during and 6 s post whisker stimulation under red light with a frame rate of 7.5 Hz (total 120 data points). The whisker stimulation was repeated 40 times with an ISI of 20 s. In order to select key time points for detecting changes in signal, for several experiments images were acquired for a longer duration, grouped into bins of 40 and the time course of the signal was analysed (Fig 2.1c).

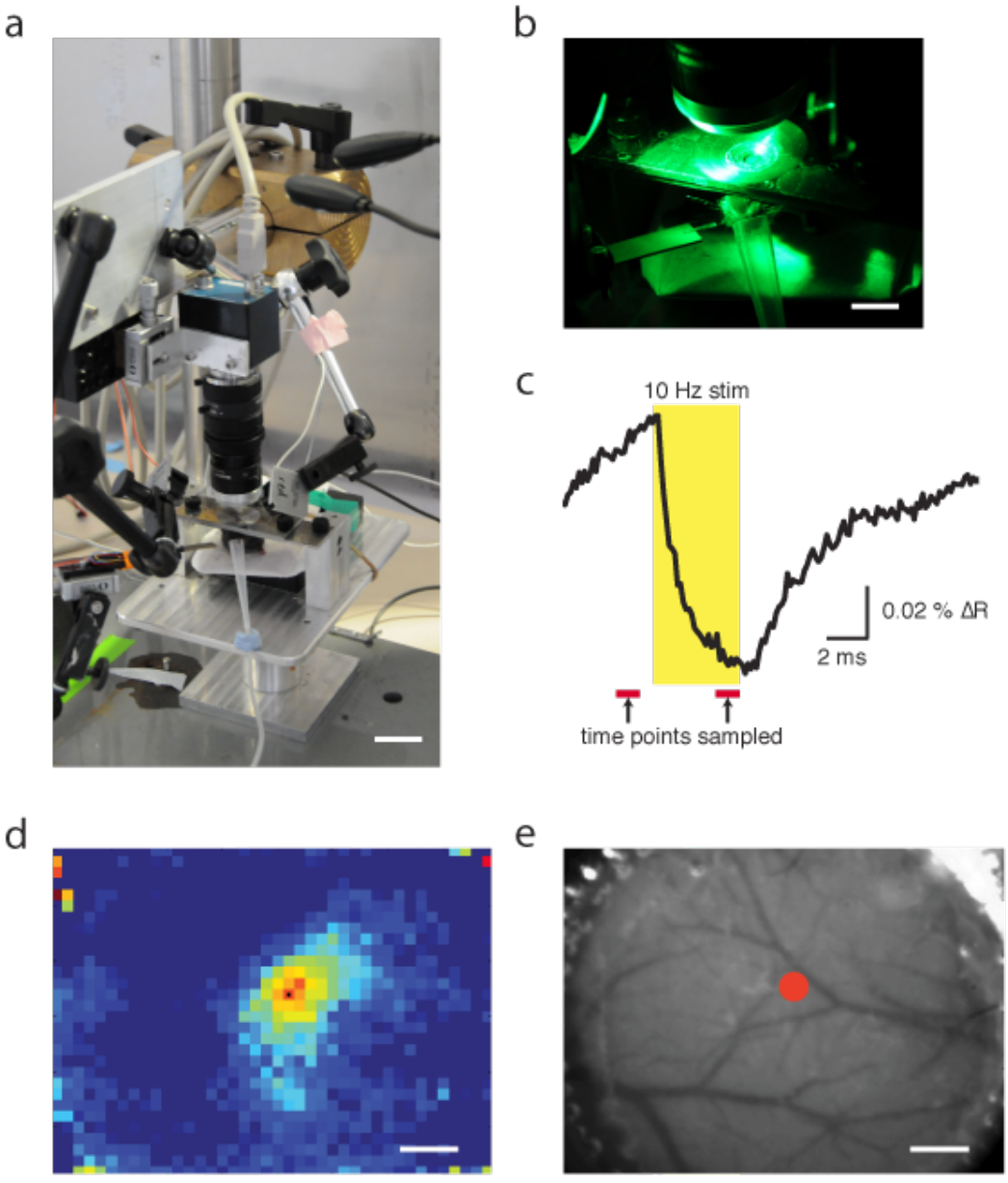

Fig 2.1. Intrinsic imaging of whisker stimulation. a) Intrinsic imaging experimental setup. Scale bar = 3 cm. **b)** Close-up of an animal with isoflurane tube, green LED and piezo whisker stimulator. Scale bar = 1cm. **c)** Time course of intrinsic imaging signal. Black line is averaged over 40 pixels. Yellow shading indicates time of whisker stimulation. Red lines indicate data time points chosen for further analysis. **d)** Imaging over C2 barrel cortex following stimulation of whisker C2. **e)** Centre of point of greatest difference in reflectance before and after whisker stimulation is plotted over blood vessel map. Scale bar for d and e = 0.4 mm.

For each experiment, all 40 images were normalised (divided by their mean) and then summed together. This data matrix was then grouped into bins of 16 pixels in each direction (to form a 30x40x120 matrix). The data points measured 3-4 s post whisker stimulation were averaged and subtracted from the data points measured 1-2 s pre whisker stimulation (Fig 2.1c). The point of maximum difference was identified and printed onto the blood vessel map to indicate position of centre of C2 barrel (Fig 2.1e). The accuracy of barrel location was confirmed with an LFP recording (pipette resistance 1 MΩ).

2.3 Targeted Single-cell electroporation

Detailed methods of the recently developed technique of targeted single cell electroporation can be found in Judkewitz et al (2009). Briefly, a pipette of 12-14 MΩ resistance containing standard external solution (see overview), 50 μM Alexa 594 (Invitrogen, UK) and 50-100 μg/ml of both ChR2-YFP plasmid DNA and either pEGFP-C1 or pTurboRFP plasmid DNA was inserted into the brain with 100 mbar pressure. Having passed successfully through the dura mater and cortical layer 1, the pressure was reduced to 20 mbar and the pipette advanced through layer 2 under visual guidance according to the shadow imaging technique (Kitamura et al 2008). Tip resistance was monitored aurally and cell contact was assessed using shadow imaging and by a 20-30% increase of tip resistance. Once contact with a cell had been made, pressure was released and a voltage pulse train was immediately applied: 50 monophasic pulses (-12 V, 0.5-1 ms duration) at 50 Hz (Judkewitz et al 2009).

After approximately 2 seconds the pipette was retracted, the pressure reapplied and another cell approached. Typically 8-10 neurons were electroporated per experiment. For online visualization, images of 256x256 pixel resolution were acquired at a frame rate of 2 Hz with 2ms per line. Alexa 594 was excited at 810nm. These images could then be compared to the expression of fluorescent protein on day 3. The external solution was removed from above the brain and replaced with silicon oil (Sigma-Aldrich, UK). A cover slip was adhered with

superglue to the lip of the imaging disk and covered with green KWIK-seal silicone sealant (World Precision Instruments, UK). The animals were housed separately for 48 hours to allow for their recovery and high expression of both the RFP or GFP and the ChR2-YFP DNA.

2.4 Electrophysiology

2.4.1 Extracellular recordings

For extracellular recordings a silicon extracellular 16 site linear probe (type A-1-16-3mm-50-177, Neuronexus Technologies, USA) was inserted into the cortex to a depth of between 900 and 1200 μm from the brain surface at an angle of 60 degrees. Several minutes were allowed for the stabilization of the recordings before the experiment commenced. A Rx5 Pentusa system (Tucker Davis, USA) was used for data collection. All data acquisition and stimulation was controlled by the Open Ex programme with custom-made protocols written in Real-Time Processor Visual Design Studio (RPvdsEx; Tucker Davis, USA). The extracellular signal was separated online into an LFP component (0-0.3 kHz) sampled at 3 kHz, and a high frequency component (0.3-5 kHz) sampled at 25 kHz. Spike detection using the latter component was done offline (see below).

2.4.2 Blind in vivo whole-cell patch-clamp recording

Whole-cell recordings were made using blind patch techniques (Margrie et al., 2002). Patch pipettes were pulled from standard borosilicate glass (thick-walled; outer diameter 1.5mm, inner diameter 0.86 mm; Harvard Apparatus, UK) on a vertical electrode puller (Narishige, Japan) to yield an electrode resistance of 5.5 MΩ. They were filled with internal solution containing the following (in mM): K-methanesulfonate 110, KCl 15, HEPES 10, Mg-ATP 4, Na_2GTP 0.3, Na-phosphocreatine 10, and 0.3% biocytin; pH 7.2, osmolarity 285 mOsm. Electrodes were quickly inserted to a depth of about 100 μm with high pressure on the back of the electrode. After reducing the pressure, the electrode was advanced in 2 μm steps until a neuron was encountered, which was indicated by an increased

apparent electrode resistance. Release of pressure often resulted in spontaneous Giga-seal formation. Rupturing of the cell membrane by short mouth-applied pulses of negative pressure achieved the whole-cell configuration. Recordings were made at a depth of ~300±200 μm from the dura mater, and neurons were identified as layer 2/3 pyramidal cells by their input resistance (~0.15 GΩ), firing properties, and by cell morphology. Access resistance was typically 20-40 MΩ at the start of the recording. Traces with access resistance above 100 MΩ were not included in the analysis. Data were filtered at 3-10 kHz and acquired at 50 kHz using Axograph software (Molecular Devices, USA) and an ITC-18 A/D converter (HEKA Instruments Inc., USA). Input resistance was calculated by fitting a linear function to the steady-state I/V curve (obtained from voltage deflections during 400 ms current steps from -300 pA to +500 pA in 100 pA steps).

2.4.3 Combined patch-clamp and extracellular recordings

A silicon extracellular 16 site linear probe (type A-1-16-3mm-50-177, Neuronexus Technologies, USA) was lowered 1200 μm from the brain surface at an angle of 60 degrees. Following the identification of clear spiking units, a patch pipette was inserted at a distance of 100-300 μm from the probe to a depth of 200 μm (distance calculated based on the distance and the angle between the two electrodes using a custom made system by Luigs & Neumann GmbH, Germany). Recordings were performed using the blind whole-cell patch-clamp recording method as described above (Margrie et al. 2002). After establishing a giga-seal and subsequently a whole-cell recording, brief current pulses (2.5-10 ms, 1-3 nA) were injected *via* the patch pipette into the recorded neuron at 200-400 ms intervals, and both the intracellular and extracellular signals were recorded using an Rx5 Pentusa system (Tucker Davis, USA). Ideally, the amplitude and duration of the current pulses would have been chosen so that each stimulus produced exactly one spike. However, because of up- and down-states, this was not possible: a stimulus strong enough to always trigger a spike in the down-state would be strong enough to regularly produce more than one spike in the up-state. Thus, the strength of the stimulus was adjusted so that it rarely produced more

than one spike. This was largely successful: out of the 13,000 stimuli delivered (in 10 experiments), only 498 (3.8%) produced 2 spikes.

2.4.4 Cell-attached recordings from electroporated cells under 2-photon visual control

48h after electroporation with RFP or GFP and the ChR2-YFP DNA, animals were anesthetized with either 1% isoflurane, supplemented with chlorprothixene (4 mg/kg; Sigma-Aldrich, UK), or Ketamine/Xylazine. The cover slip, silicon oil and dura mater were removed and the brain covered with external solution. Neurons expressing a fluorescent protein were identified using two-photon imaging. EGFP was excited at 910nm and RFP at 800 nm. Images of 256x256 pixel resolution were acquired at a frame rate of 2Hz with 2ms per line and compared to images taken of Alexa-filled cells 2 days previously.

Borosilicate glass patch pipettes (6-7 MΩ) were filled with external solution (section 2.1) and either Alexa 488 or 594 (50 mM; Sigma-Aldrich, UK) and lowered into the brain to an area near the electroporated cells. The EGFP or RFP expressing cells, or cells within 200 μm of expressing cells were then targeted under visual guidance using two-photon imaging and their activity was recorded under cell-attached configuration with a seal resistance of ~200 MΩ. The ChR2 protein also expressing in these cells was activated with a blue LED with low dome lens (LXHL-NB98; RS Components, UK). Pulses of 1-5 ms duration at 10-50 Hz frequencies were delivered and the spiking activity of the neuron recorded. Data was acquired at 25 kHz using Axograph software (Molecular Devices, USA) and an ITC-18 interface (Heka Instruments, USA).

2.5 Whisker stimulation

A multi-layer bender (PL127.10; Physik Instrumente, Germany), with a displacement of 450 μm and 380 Hz resonant frequency, was driven by a Piezo Driver (E-650.00; Physik Instrumente, Germany). For the intrinsic imaging, the bender was mounted on a plastic board and controlled with one axis of a

manipulator (Spindler & Hoyer, UK; Fig 2.2a). No attempt was made to reduce resonant vibrations. For the recording experiments a second bender was adhered to a small piece of foam, which was then attached to a metal bar (10 cm long) and controlled with a UN-3C 3D manipulator (Narashige, Japan; Fig 2.2b). Furthermore, the stimulation pulse was filtered at 1000 Hz and preceded by a ramp of 5ms. This combination of mounting and filtering greatly reduced the high frequency displacement vibrations following whisker stimulation as measured by a CMOS multi-function analogue laser sensor (Keyence, UK; Fig 2.2c).

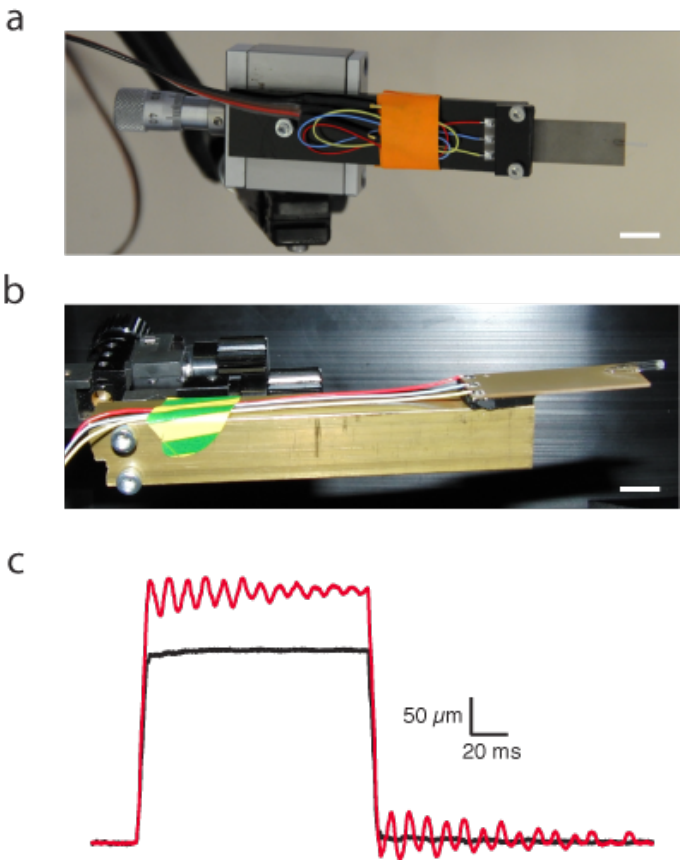

Fig 2.2. Two mounting styles of piezo benders. a. Used for intrinsic imaging. **b.** Used for recording experiments. Resonant vibrations were greatly reduced. Scale bars = ~1 cm. **c.** Displacement of Piezo bender during and after stimulation of 100 ms pulse. Red line represents piezo mounted on plastic used for intrinsic imaging. Black represents piezo mounted on foam with solid metal bar.

2.6 Light stimulation of ChR2 expressing neurons

The ChR2 +ve neurons were activated with a fibre pigtailed high brightness blue LED (Doric lenses, Canada) coupled into fibre optic cable of 0.5 NA and 1mm diameter. This was placed directly above the craniotomy (~0.5 cm) and controlled via a square pulse sent from OpenEX software (Tucker Davis, USA). A dual fibre pigtailed LED (Doric lenses, Canada) which coupled both a high brightness orange and high brightness blue LED into a 1mm diameter fibre was used to control for light activation artefacts both directly on the probe and from inadvertent stimulation of the retina.

2.7 Histology

2.7.1 Recovery of the recording site and the cell morphology after recording

During whole-cell recordings *in vivo* neurons were filled with biocytin (Sigma-Aldrich, UK) included in the intracellular solution, enabling morphological reconstructions by biocytin staining. Similarly, electroporated, ChR2 +ve neurons were co-transfected with GFP or RFP DNA and thus could be identified by their fluorescence.

Following recordings and still under deep anaesthesia, rats were perfused through the heart with 20 ml phosphate buffered saline (PBS, Sigma-Aldrich, UK), followed by 20 ml PBS with 4% paraformaldehyde (PFA, Sigma-Aldrich, UK), and decapitated. The brain was removed from the skull and incubated in PBS with 4% PFA at 4º C for a minimum of 12 hours. Once properly fixed, the brain was embedded in 3% agarose (Sigma-Aldrich, UK) and sectioned into 60-100 μm thick sections (200 μm without embedding in agarose for the thalamic inactivation experiments) either coronally or parasagitally in PBS using a vibratome tissue slicer (VT1000 S, Leica, Germany). The biocytin staining procedure was carried out as described by Horikawa and Armstrong (1988) using an ABC solution (Vectastain kit, Vector labs, UK).

For the detection of GFP expression in electroporated neurons, the fixed sections were permeabilised in Triton X (0.4%; Sigma-Aldrich, UK) for 1hr at RT. The sections were then incubated with 1μg/ml anti-GFP-Alexa-Fluor 488 (Invitrogen, UK) in PBS for two hours, and then rinsed in PBS.

Sections were then mounted on glass slides (Western Lab Service Ltd) in Moviol (Calbiochem, Merck, UK), or in Vectashield HardSet Mounting Medium with DAPI (Vector Labs, UK) as a counterstain for cell nuclei, sealed with varnish and inspected under the Spinning Disk Confocal Microscope (PerkinElmer, USA) using a wavelength of 405 nm (for DAPI) and 488 nm (for GFP).

Sections from the thalamic inactivation study were imaged with an Axio Imager A1 epi-fluorescent microscope (Carl Zeiss, Germany) under a 4x objective. Red, green, blue filters were used to image, respectively, the injection site, the ChR2-Thy1 expressing neurons and the DAPI staining. A light filter was used to record the gross anatomy of the thalamus and cortex. Images were acquired using the Axiovision software (Carl Zeiss, Germany) and pieced together with the Image Composite Editor (Microsoft, USA).

2.8 Data analysis

2.8.1 Spike detection

Spike detection was performed offline using the high frequency component of the extracellular signal. Before looking for spikes on the extracellular electrodes, we removed stimulus-induced and spike-induced artefacts. For the former, we identified null-stimuli – stimuli that did not trigger intracellular spikes (see point 1 in Fig 2.3a for an example and Fig 2.3b for an average) – and used them to compute the null-stimulus triggered average on each channel. We then subtracted each channel's null-stimuli triggered average from the channel signal (aligned on each stimulus). To remove spike-induced artefacts, we followed essentially the same procedure, except that we computed an average voltage triggered on spontaneous intracellular spikes (which induced a very small capacitive signal;

see Fig 2.3a point 2 for an example and Fig 2.3c for an average). We then subtracted each channel's spontaneous-spike triggered average from the channel signal, this time aligned on all intracellular spikes (spontaneous as well as triggered). To improve the quality of the signal, we applied a low-pass filter based on the noise spectrum. The noise spectrum was estimated from the intracellular recordings during the down states (during which there were never any spikes on the extracellular electrodes). The spectrum was then used to construct a Wiener filter (using Matlab wiener2 imaging toolbox function). Filtering the data resulted in a 15-30% improvement in signal to noise ratio for spike detection, with negligible effect on spike amplitude or shape.

Finally, to simplify the analysis, we normalized the voltage on each channel to the standard deviation of the noise on that channel. To estimate the standard deviation, we used median(|V|) / 0.6745 where V is the voltage. This estimator avoids the upward bias associated with excursions in voltage caused by action potentials. After normalization, candidate spikes were identified based on two criteria:

• There was a local minimum with amplitude greater than six standard deviations.

• There were zero-crossings less than 0.5 ms before the minimum and 1.0 ms after it. Multiple spikes – spikes occurring within 0.5 ms of each other – were often detected on neighbouring channels. When this happened, only one spike was selected (the one with the largest amplitude); the rest were discarded. This is illustrated in Fig 2.3d, where red dots are used to indicate all candidate spikes and red dots surrounded by green circles denote spikes used in the analysis.

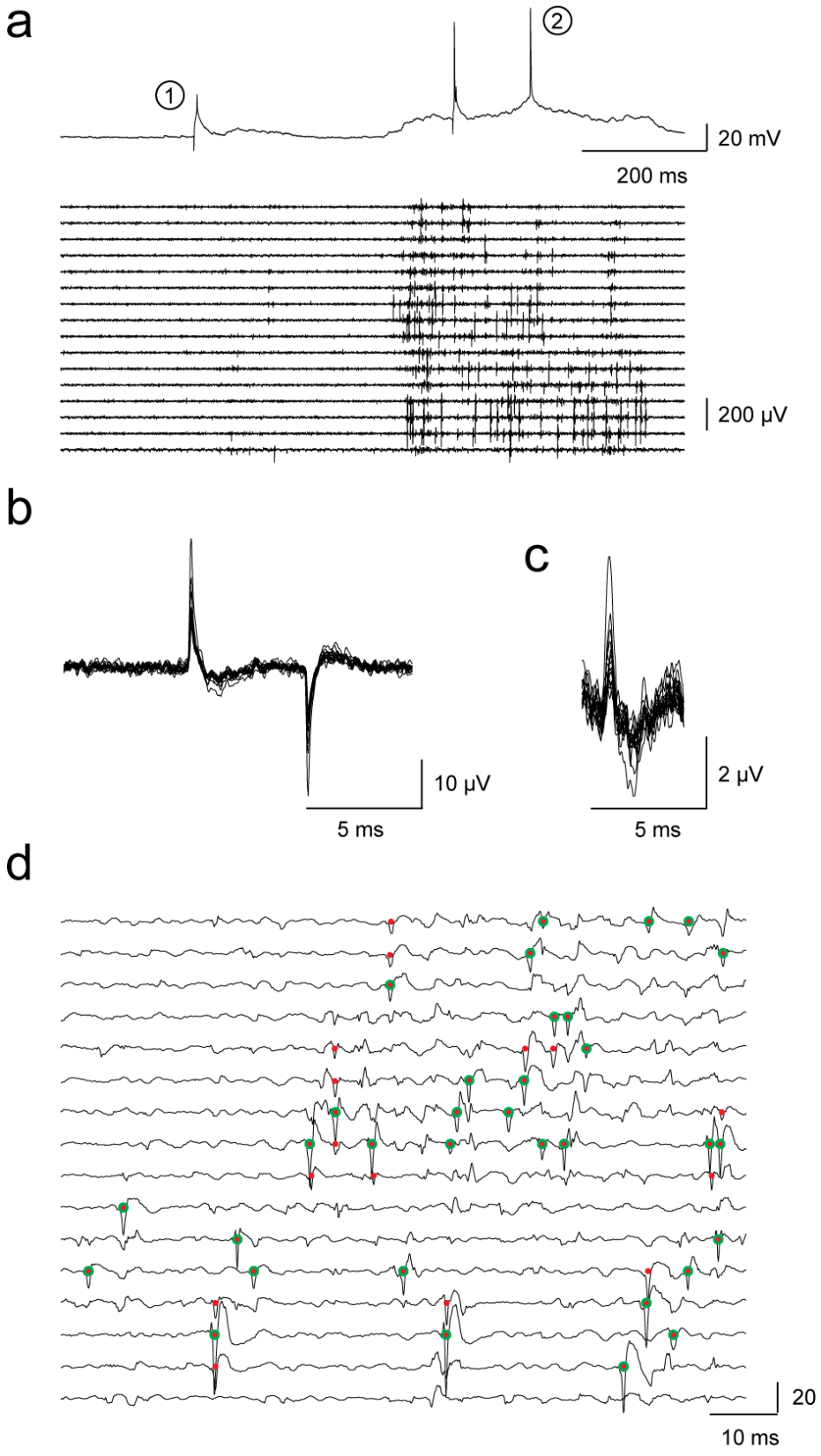

Fig 2.3

Fig 2.3 Simultaneous intracellular and extracellular recordings. a). A one second example of intracellularly recorded voltage (top) and simultaneous extracellular voltage on a 16 channel electrode (bottom, band-passed 0.3-5 kHz). Dashed red lines indicate stimulus onset. **b)**. Average extracellular voltage triggered on stimuli that did not produce a spike (point 1 in panel a). This average is a capacitive artefact, and was subtracted from the voltage on each channel. **c)**. Average extracellular voltage triggered on intracellular spikes (point 2 in panel a). This average is also a capacitive artefact (although a much smaller one), and was also subtracted from the voltage on each channel. **d)**. After subtracting the artefacts, the signal on each channel was normalized to the noise (so the vertical scale bar has units of standard deviation) and smoothed using a Wiener filter (see text). Fast, large events were considered candidate spikes (red dots). These often occurred simultaneously on neighboring channels, in which case only the largest spike (over a range of 5 channels) was included in the analysis. Included spikes are marked with a green circle; events without a green circle were discarded.

2.8.2 Peri-stimulus time histograms (PSTHs)

To ensure a flat baseline (Fig 3.3b), PSTHs were constructed triggered on stimulus onset, not on intracellular spike times. To test for significance, a cumulative PSTH was constructed by subtracting the baseline (the mean firing rate between -100 and 0 ms) from the PSTH and integrating the difference (starting from t=0 and integrating in both directions). To compute error bars, a bootstrap method was used in which I constructed surrogate PSTHs by randomly sampling 200 ms epochs from the extracellular spike trains. 10,000 surrogate PSTHs were constructed, which were then turned into cumulative PSTHs as described above. This gave a null-distribution of cumulative PSTHs at each time point; and were used those to construct the error bars shown in Fig 3.3c.

Further details of the data analysis are covered at the appropriate sections in the results.

All data are reported as mean ± standard error of the mean (SEM) unless indicated otherwise.

3 Small-scale neuronal perturbations: Can they alter the activity of the local network?

3.1 Introduction

In order to make predictions about how the introduction of a small amount of artificial noise into a sensory network will affect its ability to transmit information, we must first observe its effect on network dynamics. This will give an indication as to the magnitude of noise needed to perturb sensory encoding and possibly alter the behaviour of the animal.

To both introduce the noise and to record the changes in local network activity, I used three different techniques, each with its own individual advantages (and limitations) in power, reproducibility and scale. Firstly, I injected current into a patch-clamped pyramidal neuron in the somatosensory cortex to force it to spike, and measured changes in activity of the surrounding network with a multi-site silicon electrode. In previous related work, colleagues injected a current pulse into a similarly patch-clamped pyramidal neuron and measured the change in the spiking output of that same neuron. Results from this work suggested that artificially introducing even a single excitatory spike into the local network would result in 28 extra spikes across the neurons in the neighbourhood of the manipulated neuron and be enough to effect a short-term increase in the average network firing rate of the surrounding network of 0.04-0.08 Hz. Secondly, I electroporated plasmids encoding for Channelrhodopsin-2 (ChR2) into 2-15 excitatory neurons, forced them to spike synchronously using blue light stimulation, and measured the changes in local dynamics with the silicon probe. Finally I similarly introduced ChR2 into 2-15 excitatory neurons and measured the activity of individual surrounding neurons using patch-clamp and cell-attached recordings under 2-photon guidance.

3.2 Methods

3.2.1 Animals and surgery

Combined intra- and extracellular recordings

Sprague Dawley rats (postnatal day (P) 18 to 25, average weight 45.6 g) were anesthetized with urethane (Sigma-Aldrich, UK; 1.5 g/kg, injected i.p.). A small craniotomy (1 mm^2) in a region overlying the somatosensory cortex (S1) (centered 5.5 mm lateral, 2.5 mm caudal of Bregma) was made and a small opening (~0.1 mm^2) was made in the dura mater.

Single -cell electroporation and recording from network cells

Male wild-type C57BL/6J or GAD67-GFP mice (CIT; P30 to P60) were anesthetized with a ketamine/xylazine mix (Ketamine 120mg/kg, Pfizer Animal Health, UK; Xylazine 18mg/kg, Millpledge Veterinary, UK). A custom designed stainless-steel recording chamber (Judkewitz et al 2009) was adhered over the somatosensory cortex region of skull (centred 2 mm lateral, 2 mm caudal of Bregma) and the skull moistened with external solution. A small craniotomy (~1 mm diameter) was made in the centre of the recording chamber and the dura left intact. For the experiments involving single-cell electroporation and cell-attached network recordings, ~50 % were done with GAD67-GFP animals, and the other half were performed on wild type animals. All the experiments in which network activity was recorded with the multi-unit silicon probe were performed in GAD67-GFP animals.

3.2.2 Plasmids

For the single-cell electroporation experiments, in order to exogenously express fluorescent reporters and manipulate neuronal activity, cells were electroporated with three different plasmids. To allow introduction of action potential into specific neurons, channelrhodopsin2 (ChR2) under a CMV promoter (a gift from Juan Burrone) was introduced. This plasmid also contained a yellow florescent protein (YFP) marker. While the YFP fluorescence was possible to visualise at high magnification once the YFP positive neurons had been identified, it was not

strong enough to use for the initial identification. Therefore, to identify electroporated neurons and to provide additional confirmation of electroporation success, a plasmid containing green fluorescent protein (GFP), pEGFP-C1 (Clontech, USA), was also included. This plasmid was selected for its high expression rate, providing a very clear indication of electroporation. Finally, for animals containing GAD expressing neurons, the GFP plasmid was exchanged for red fluorescent protein (RFP) containing plasmid, pTurboRFP, under a CAG promoter (sequenced in house). Expression of the RFP plasmid on day 3 was not as visible as the expression of the GFP plasmid and this plasmid was therefore only used when made necessary by the presence of green GAD +ve neurons.

3.3 Results

3.3.1 Electrically perturbing one neuron

Pyramidal neurons from layer 2/3 of the rat barrel cortex under urethane anaesthesia were recorded from in the whole-cell patch-clamp configuration and forced to spike by the injection of current. The spiking activity from between 20 and 35 nearby cells in layers 1-4 and the LFP were recorded simultaneously using a 16-channel silicon probe inserted at an angle of 60 degrees into the brain ~100-300 μm from the patched cells (Fig 3.1a). A clear correlation in the timing of up- and down-states was observed in the membrane potential of the patched cell and the extracellular spikes of the surrounding cells (Fig 3.1b).

Current pulses of 200 ms and an amplitude of 500 pA were injected into the patched cell at 1 second intervals, and the extracellular spikes in the surrounding network were recorded before, during and after the perturbation (Fig 3.2a). In the down-state each current pulse evoked ~3 spikes, in the up-state >10 spikes were typically evoked. Following spike sorting, an increase was occasionally observed in the spikes for an individual cell (asterisks in Fig 3.2b). If the spike timings between the extracellularly recorded neuron and the patch-clamped neuron were highly similar, the spikes registered could be either a capacitance artefact (see discussion) or the extracellular recording of the spikes of the patch-clamped cell

by the probe (green asterisks) and thus were discarded from further analysis. Some neurons showing altered firing rates post stimulation, however, showed firing patterns different from the patch-clamped neuron and could thus be neurons receiving direct or indirect excitatory input from the patched neuron (red asterisks).

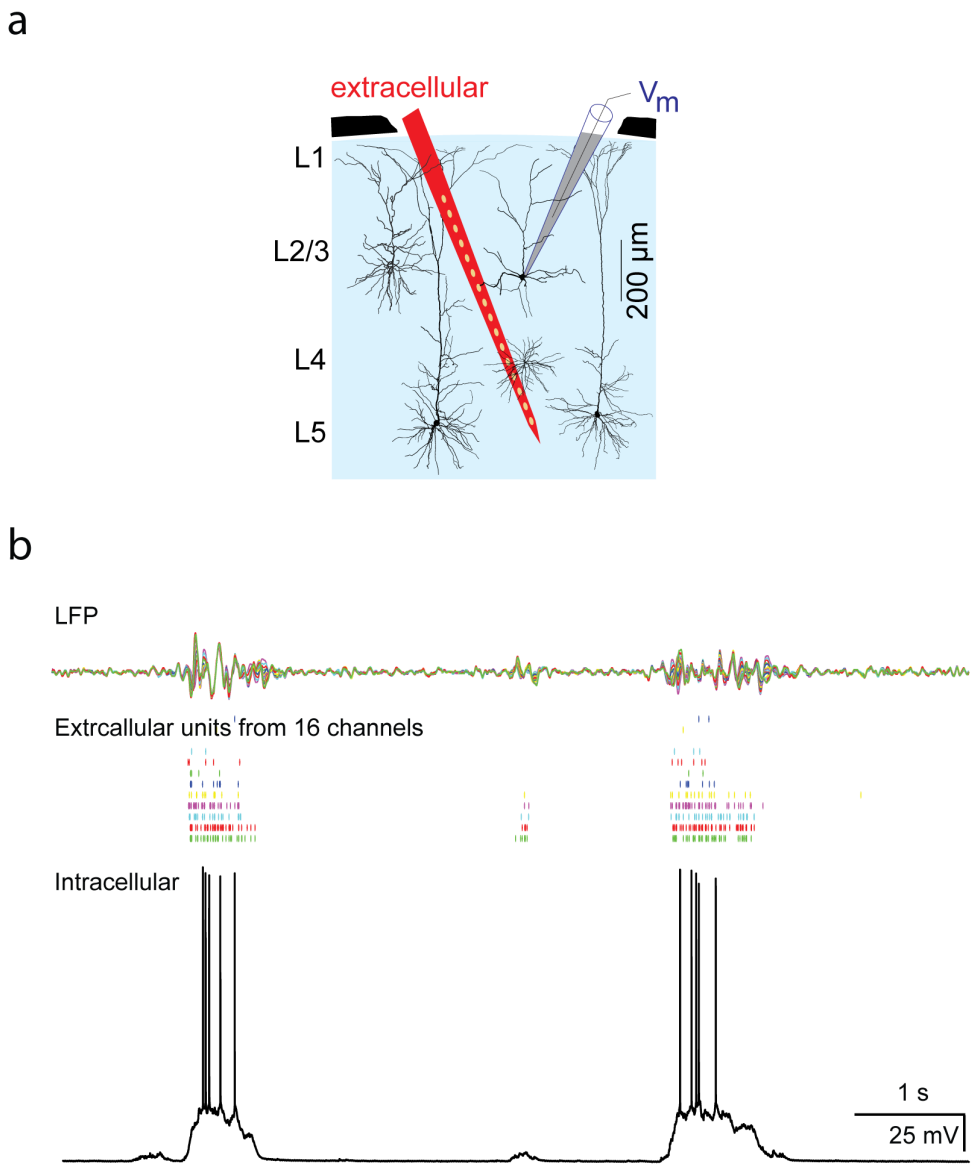

Fig 3.1 Experimental setup and sample data. a) Experimental setup showing whole-cell patch-clamp electrode (grey) and extracellular multi-site silicon electrode (red) inserted into the mouse barrel cortex (schematic diagram). **b)** Typical data sample showing correlated up and down states between a whole-cell patch-clamped cell and surrounding network.

For a typical experiment, there was a high degree of variability in the responses of the neurons to the stimulation and different baseline rates. For the increase in firing rate to be significant, therefore, all neurons were pooled for each experiment. In some cases no effect was seen in the network following perturbation (data not shown). In one experiment, a significant ($p < 0.0003$) increase in network firing rate was observed in the first 40 ms following current injection (Fig. 3.2c), indicating that perturbation of one cell can have an observable effect on network dynamics. The scale of this effect will obviously depend on the position of this cell in the network and the pattern of its connections.

Fig 3.2 Perturbing a single neuron can change the local network activity a) Experimental protocol showing both the extracellular recording of local neurons as well as the whole-cell patch-clamp recording of one neuron in response to 200 ms intracellular current injections with an ISI of 1 s into the patched cell. **b)** Sorted spikes from 24 neurons recorded from the local network by the silicon probe. The green asterisk indicates a likely extracellular recording of the patched neuron. The red asterisks highlight the possible post-synaptic neurons. **c)** PSTH across all cells triggered on the first intracellularly recorded spike from each current injection, including only isolated intracellular spikes which are not followed by another spike within at least 20ms. Error bars are SEM (assuming binary statistics).

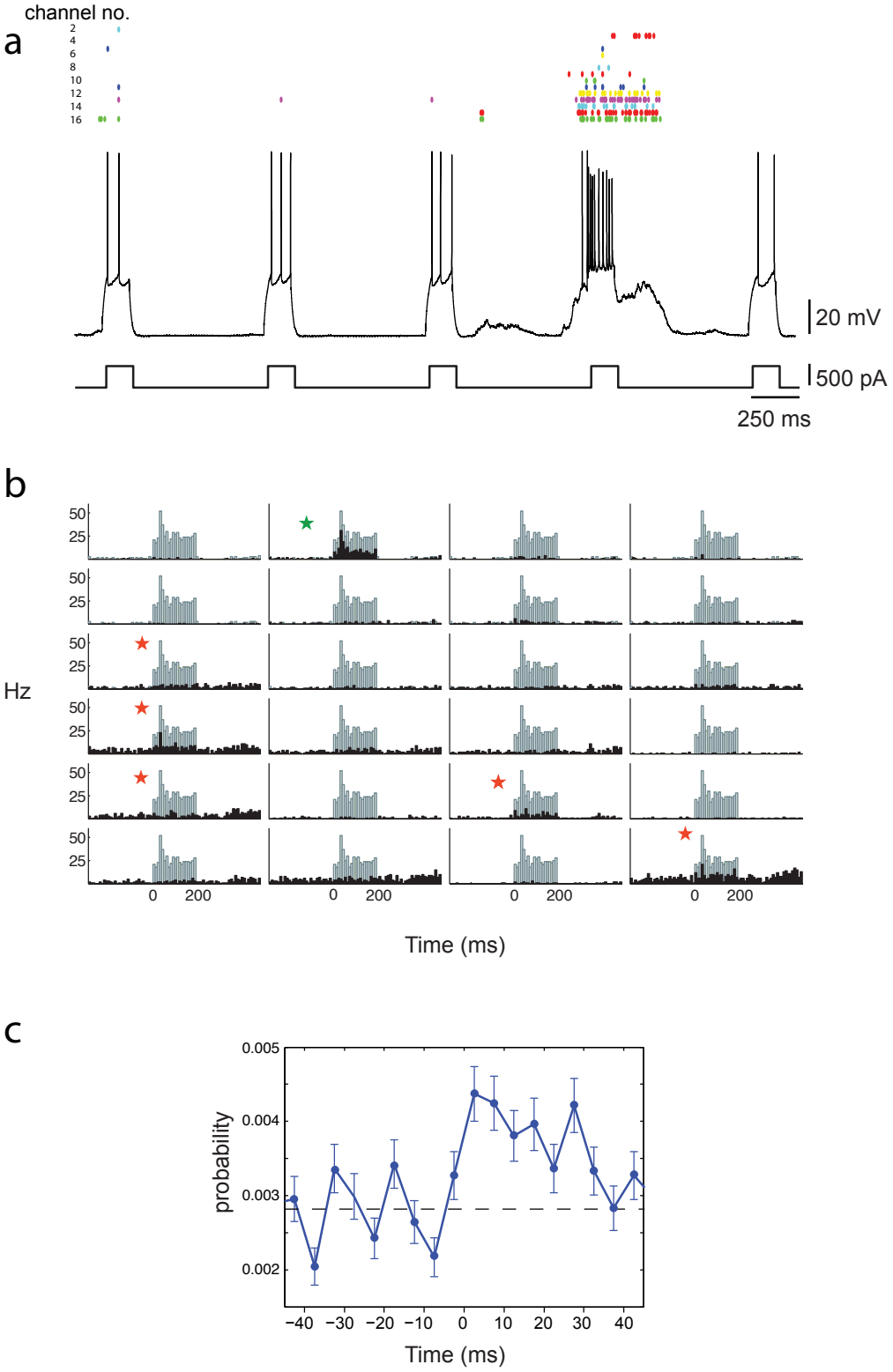
a
channel no.
2
4
6
8
10
12
14
16
20 mV
500 pA
250 ms
b
Hz
50
25
0
200
Time (ms)
c
probability
0.005
0.004
0.003
0.002
−40 −30 −20 −10 0 10 20 30 40
Time (ms)

Fig 3.2

3.3.2 Introducing one spike into the network

The length of the stimulation was decreased to between 2.5-10 ms (sufficient to induce one spike) and the inter-stimulus interval (ISI) to 200-400 ms, allowing many more trials per neuron and the possibility to average over enough repetitions to observe an effect. Previous results had already suggested that a single extra spike should have a measurable, although small and short-lived, effect on network firing rate (London et al., 2010). Introducing several spikes over 200 ms had required a larger ISI in order to allow the neurons sufficient time to recover from the stimulation and reduced the possible number of repetitions per neuron. Reducing the stimulus duration also decreased the time period over which the increase in the local network would be expected to take place, thus making the increase more likely to be detected in the peristimulus time histogram (PSTH).

The experimental design is shown in Fig 3.3a. Because the effect expected was very small, for these experiments it was very important that the spikes recorded extracellularly be included in the analysis only after careful selection. Some spikes had a signature on more than one site of the extracellular electrode and thus only one of these events should be included. A more rigorous spike-sorting algorithm was therefore applied to the neurons included in the analysis (details in Section 2.2.2).

A PSTH was constructed with bins of 5 ms of extracellular spikes triggered on the stimulus for all the spikes (recorded over all 16 electrode channels) for 10 experiments with a combined total of 13,000 stimuli (Fig 3.3b). As predicted by the results from section 3.2.1 and in previous experiments described in Section 3.1 an increase in firing rate on the extracellular electrodes was observed. In the first 10–20 ms, the increase in the firing rate was calculated to be 0.03–0.065 Hz per neuron ($n = 10$; Fig 3.b insert). The increase, as assessed by the cumulative increase in the probability of an extra spike, was statistically significant (with $p < 0.01$) for greater than 50 ms (Fig 3.3c). This indicates that a single spike is sufficient to effect a change in the local network.

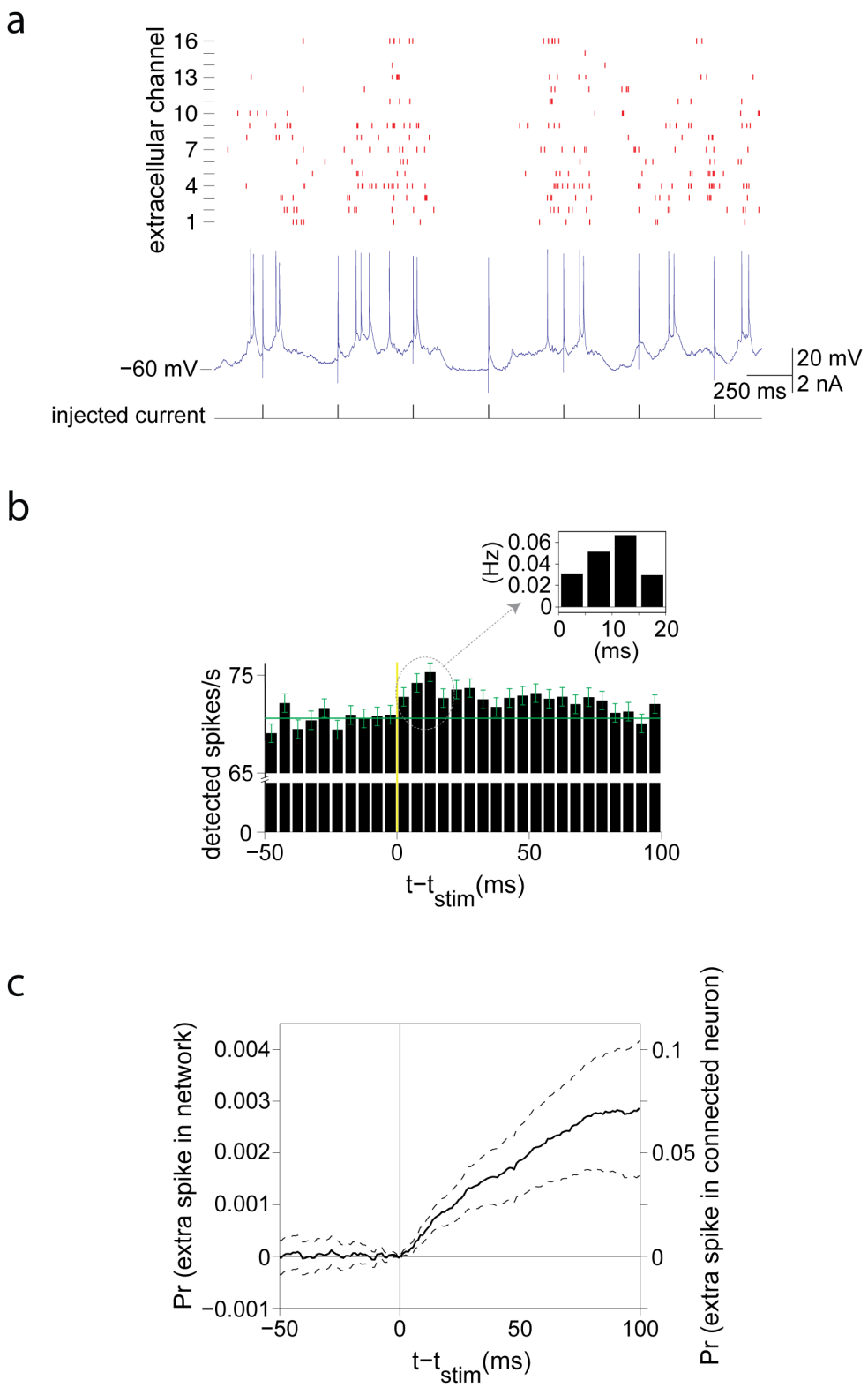
a
extracellular channel
16
13
10
7
4
1
−60 mV
20 mV
2 nA
250 ms
injected current
b
(Hz)
0.06
0.04
0.02
0
0
10
20
(ms)
detected spikes/s
75
65
0
−50
0
50
100
t−t_stim (ms)
c
Pr (extra spike in network)
0.004
0.003
0.002
0.001
0
−0.001
0.1
0.05
0
−50
0
50
100
t−t_stim (ms)
Pr (extra spike in connected neuron)

Fig 3.3

Fig 3.3. The effect of one extra spike on network activity. (a) Extracellular spikes (top) and intracellular membrane potential (bottom). **(b)** PSTH triggered on the stimulus and binned at 5 ms; includes all extracellular spikes on all electrodes from 10 experiments. Error bars are one standard deviation. Inset: change in firing rate per neuron, assuming an average firing rate of 1 Hz **(c)** Cumulative probability of an extra spike, averaged over all recorded neurons, again assuming an average firing rate of 1 Hz. Dash lines indicate one standard deviation, obtained using bootstrap sampling. Left scale: probability of an extra spike in a randomly chosen neuron. Right scale: probability of an extra spike between connected pairs, found by dividing the left side by 0.04. This corresponded to the 4% connectivity observed in the literature for the somatosensory cortex, based on pair-wise connectivity (Holmgren et al., 2003).

Because spikes were far less likely to occur in the down state than the up state, the number of spikes in the intracellularly recorded neuron was correlated with ongoing activity, and thus correlated with spikes on the extracellular electrodes. Thus, to ensure a flat baseline, I constructed PSTHs triggered on stimulus onset, not on intracellular spike times. As can be seen in Fig 3.3b, this strategy was successful, as the PSTH was indeed flat before stimulus onset.

The peak in the PSTH after stimulus onset (Fig. 3.3c) was small, but the fact that 16 consecutive 5 ms bins were more than one standard deviation above the mean suggests that it is significant. To test this, a cumulative PSTH was constructed by subtracting the baseline (the mean firing rate between -100 and 0 ms) from the PSTH and integrating the difference (starting from t = 0 and integrating in both directions). For further details of analysis see section 2.11.2.

3.3.3 Optically perturbing several neurons

Perturbing a single neuron can change the activity of the local network, but this change is small and only detectable over many repetitions. While experiments have shown that behaving mice can indeed detect and report the perturbed activity of a single sensory neuron (Houweling and Brecht, 2008) or a small population of sensory neurons (Huber et al., 2008), and that stimulation of a single motor neuron can lead to detectable movement of a whisker (Brecht et al., 2004), these studies have not investigated how perturbations in the activity of these neurons can change the animal's sensory processing. They have simply shown that

perturbing a sensory neuron can be detected and perturbing a motor neuron can lead to a motor response. To actually alter the ongoing behaviour of an animal actively engaged in a separate task to that of identifying the perturbation, it is most likely necessary to perturb more than one sensory neuron.

The next step in this study was therefore to perturb a small number of neurons in a synchronous manner. To circumvent the requirement of triple or quadruple patch-clamp recordings *in vivo* and to permit non-invasive stimulation, ChR2 encoding plasmids were electroporated into small numbers of neurons in the barrel cortex and a silicon probe was used to monitor the activity of the local network before, during and after optical stimulation of the ChR2-expressing neurons (Fig 3.4a and b).

Under 2-photon guidance ChR2 plasmids as well as an equal amount of either green fluorescent protein (GFP) or red fluorescent protein (RFP) encoding plasmids were electroporated into up to 20 pyramidal neurons in layer 2/3 of the somatosensory cortex (Judkewitz et al., 2009). Alexa 594 was also included in the electroporation pipette to provide immediate feedback on the success of electroporation (Fig 3.4c). Two days later, expression of the proteins was confirmed by visualisation under the 2-photon microscope (Fig 3.4d). A success rate of up to 80% of electroporated cells expressing ChR2/GFP or RFP was often observed, although there was large variability in the quality of the craniotomy and the clarity of visualisation.

In a subset of electroporated mice, the presence of Channelrhodopsin-2 in the neurons was explicitly confirmed with cell-attached recordings under visual control. A 50 Hz train of 3 ms light pulses was given with a blue LED through the microscope objective focussed directly onto the surface of the brain while the spiking output was recorded (Fig 3.5a). For successfully electroporated neurons, the probability of a spike following the stimulus was 100% for the second stimulus in the set, and >80% for stimuli 1,3 4 and 5 (Fig 3.5b). A longer light pulse (200 ms) elicited a train of spikes (Fig 3.5c) and a light pulse of increasing duration produced a roughly linear increase in spikes (Fig 3.5d).

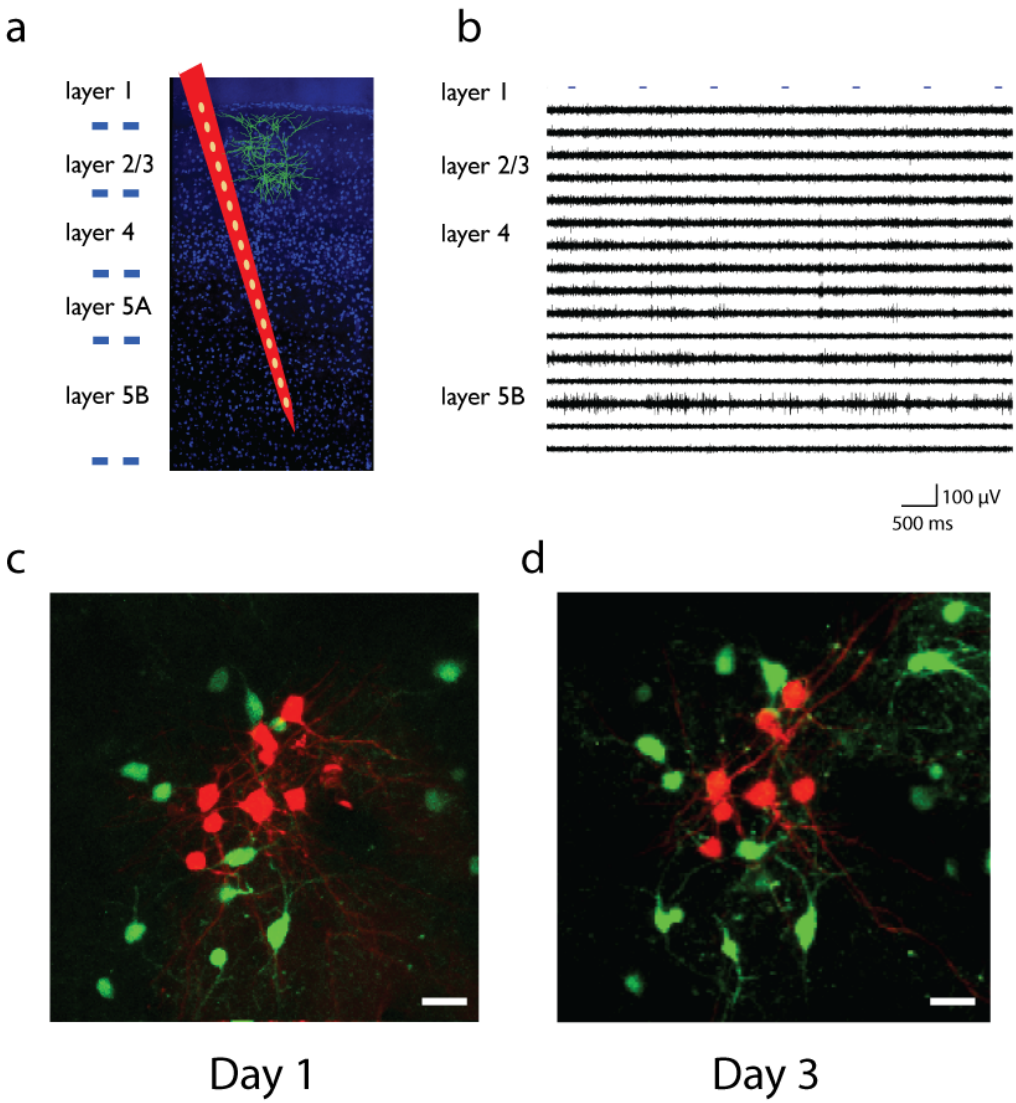

Fig 3.4. Multi-cell electroporation and multi-unit recording. a) Schematic showing a silicon probe inserted at an angle of ~20° to the vertical into layers 1-5 of the barrel cortex, as close as possible to several electroporated neurons. **b)** Sample extracellular recording from 16 channels of the silicon probe with 100 ms light stimulations every 2 s. **c)** Electroporation of RFP, ChR2 and Alexa 594 (red) into 8 layer 2/3 putative pyramidal neurons. Image taken 10 min after electroporation. Green cells are inhibitory GAD +ve neurons. **d)** Image taken 2 day after electroporation. Electroporated neurons can be visualised due to expression of RFP. By day 3 all traces of Alexa 594 are expected to have dispersed from the neurons. Scale bars: 20 µm.

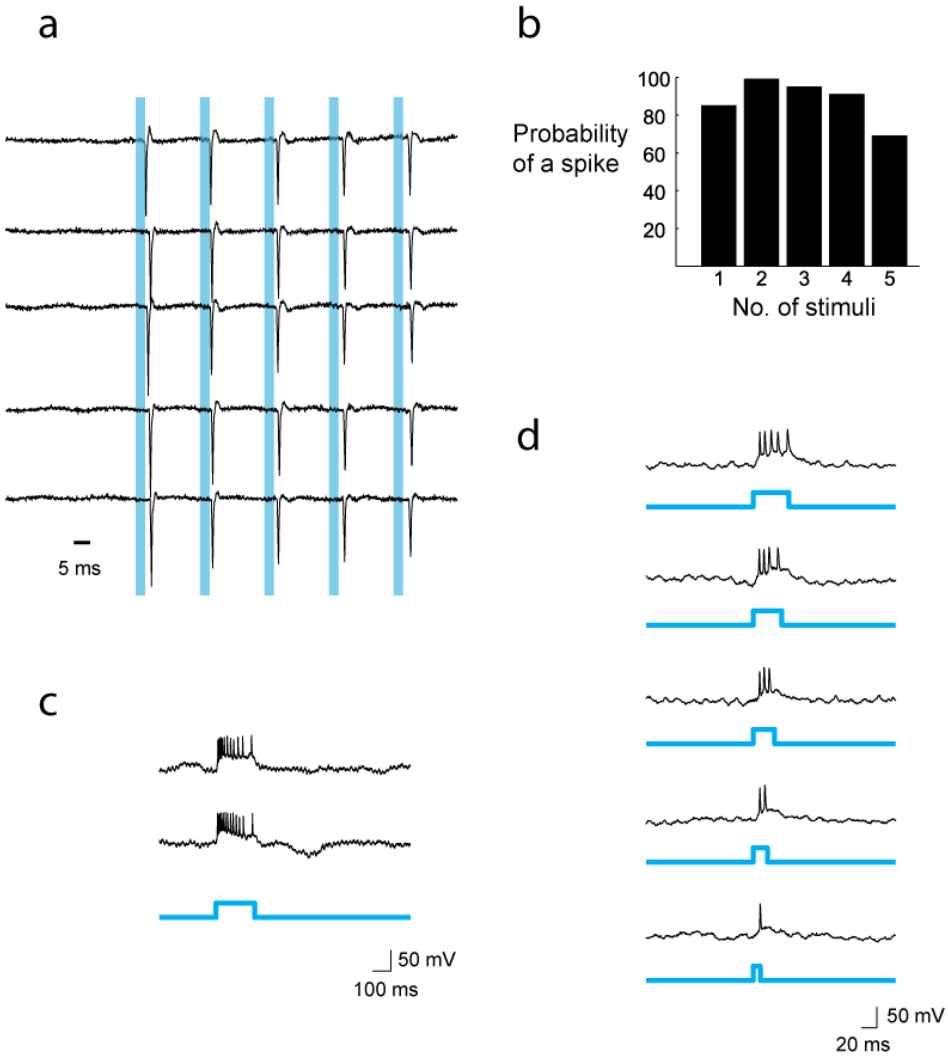

Fig 3.5 Spikes can be introduced into the network in a temporally controlled manner. a) Cell-attached recording from a ChR2 expressing pyramidal neuron. The neuron is stimulated at 50 Hz with train of 5 blue light pulses of 3 ms duration. Each light pulses elicits one spike. **b)** Bar graph showing the probability of each light pulse in the train causing a spike in the ChR2 expressing neuron. Taken over 100 trials. **c)** Two sample traces of intracellular recordings of the same neuron showing that a 200 ms light pulse elicits a train of >10 spikes of increasing ISIs. **d)** Increasing the duration of the light pulse elicits more spikes.

The expression of the fluorescent protein did not always indicate that the ChR2 DNA had been successfully expressed to a sufficient level. In ~40% of neurons GFP or RFP was clearly expressed, however no spikes were recorded following the activation of the ChR2 with blue light. For these neurons it was not possible to distinguish between the possibilities that either the ChR2 protein had failed to be expressed or that there was not enough expression to elicit a spike. While the probability of a fluorescent protein-expressing neuron also expressing sufficient ChR2 is unknown, from a large number of recordings from fluorescent protein expressing neurons in which no spikes were elicited, it was estimated to be around 60%. This proportion was far higher for interneurons (personal communication from James Cottam).

In order to examine the effect on the activity of the network of optically introducing spikes in several neurons, a 16 channel silicon extracellular electrode was used to measure activity in the local network of several electroporated neurons. The mice were placed under isoflurane anaesthesia and successful electroporation was confirmed visually under the 2-photon microscope. The silicon probe was then inserted ~150 μm from the electroporated neurons into layers 2-5 (without visual guidance) and the ChR2 positive neurons were stimulated with a 100 ms blue light stimulus, evoking ~5 spikes. To mask visual stimulation of the mice's retina by the optogenetic stimulus, a strong, flickering blue light was given directly in front of the eyes for the duration of the experiments. In pilot experiments a response to the optogenetic stimulus was observed in the local network even in control animals in which only electroporation of GFP had been carried out. This response was attributed to a visual effect in the barrel cortex (see Discussion for more details). The additional masking light removed all visual effects of the periodic blue light stimulus and no further changes in the surrounding network were observed.

Following completion of the extracellular recording, the probe was removed, covered in diI and reinserted to its original position. This permitted an accurate assessment of the position and distance of the electroporated neurons form the site of the probe and confirmation that the neurons were not damaged by the insertion

of the probe. Fig 3.6a contains a clear example of 12 electroporated neurons (green) with intact dendrites and the site of probe insertion (red). The centre of the cluster of neurons is ~120 μm from the probe site.

Experiments were carried out in 12 animals under blind conditions, with ~10 neurons of 6 mice electroporated with ChR2 and GFP plasmids and the neurons of 6 other mice electroporated with only GFP plasmids. These latter animals were used as controls. In the first 3 mice electroporated with ChR2 there was no masking light used and the results were therefore discarded due to the possibility of a visual effect.

An increase in the firing activity of the local network following light stimulation was recorded in one experiment. Spikes from 1200 trials were recorded from a stimulus of 100 ms and an ISI of 4 s. A PSTH with 5 ms bins was constructed from the spiking data from channel 3 (Fig 3.6b). A clear increase in the firing rate, which lasts for 150 ms, is seen immediately following the stimulus.

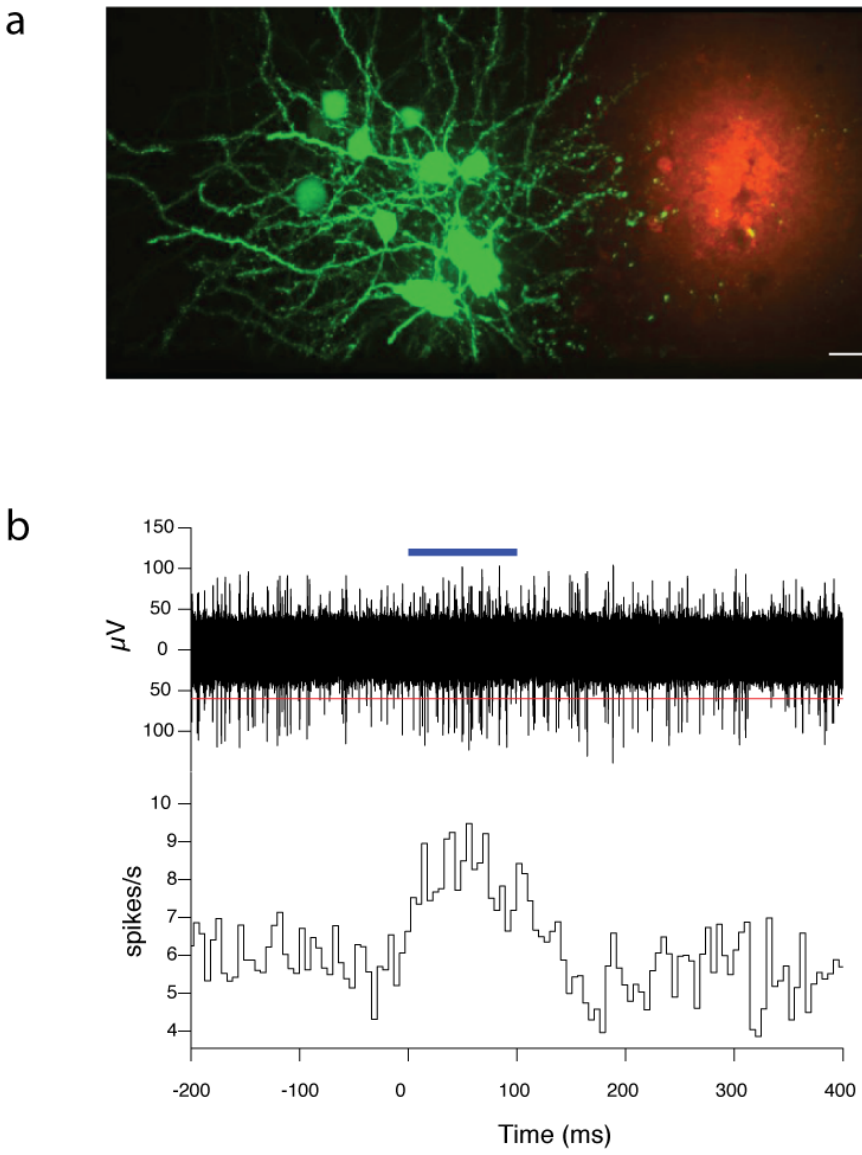

Fig 3.6 Extra spikes in 11 neurons can increase the firing rate of the local network. **a)** After recording was finished, the probe was retracted, coated in red DiI and reinserted. The staining was then used to determine the distance from the probe to the electroporated neurons (green). For this experiment the probe was ~120 μm from the centre of the group of GFP/ChR2-expressing neurons. Image is taken on a confocal microscope using a 80 μm coronal slice. Scale bar is 20 μm **b)** Top panel: raw traces overlaid from channel 3 of the silicon probe inserted into brain imaged in panel **a.** The red line indicates the threshold used to identify spikes. A 100 ms blue light stimulus (blue line) increased the firing rate of the neurons recorded on channel 3 from 6 Hz to 9 Hz for ~200 ms (bottom panel).

3.3.4 Recording from individual neurons

While recording with the extracellular silicon probe can confirm the ability of a few neurons to affect local activity, in order to gain a precise understanding of the proportion and type of neurons affected, it was important to record intracellularly from individual neurons. In addition, this gives the advantage of providing information about changes in both the membrane potential of the neuron as well as its spiking output.

Two days after electroporation of ChR2 and either RFP or GFP plasmids, neurons in the layer 2/3 local network were whole-cell patch-clamped *in vivo* under 2-photon guidance for up to one hour. The ChR2 positive neurons were stimulated every 4 s with a 100 Hz train of 10 pulses of blue light of 2-5 ms duration and the membrane potential of the patched cell recorded (Fig 3.7a). For a putatively connected neuron, the probability of spiking increased immediately following light stimulation and a response to the light pulses was observed in the membrane potential, averaged over all stimuli (Fig 3.7b). The resulting raster plot (Fig 3.7c) and PSTH also showed a peak following each light stimulus, with the highest peak following the first stimulus (Fig 3.7d) and a latency of 5 ms.

In other experiments, the firing rate and membrane potential of the patched neurons increased significantly following the stimulus but only with a long delay. This delay ranged from 200 ms (Fig 3.8a) to 1 s (Fig 3.8b). Sometimes the delayed effect on the cell's firing was inhibitory (Fig 3.9a). In one case the response of the firing rate of the neuron increased immediately following the light pulses, suggesting that the neuron was postsynaptically connected to the electroporated neurons, but also increased substantially 80 ms following the first pulse, indicating a delayed, indirect response (Fig 3.9b). Possible explanations for this delayed response to ChR2 stimulation will be suggested in the Discussion.

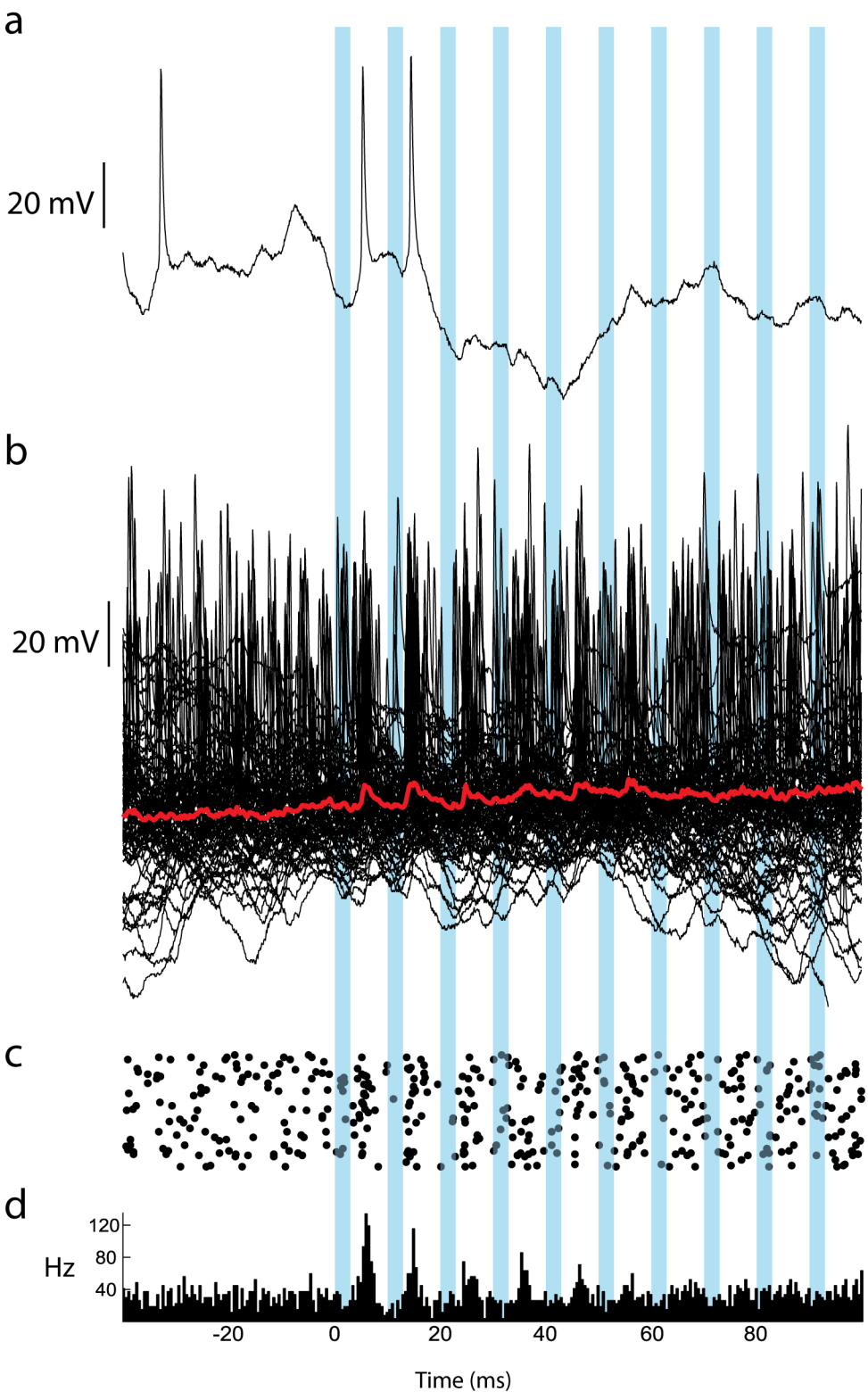

Fig 3.7

Fig 3.7 Putative postsynaptically-connected neurons are identified with ChR2 activation. a) Whole-cell patch-clamp recording from a GFP-negative (non-electroporated) pyramidal neuron in layer 2/3 of barrel cortex within 150 μm of the electroporated neurons. Blue lines indicate time of ChR2 activation. A 50 Hz train of 10 pulses with 2 ms duration was given. **b)** 100 traces from the same cell with average membrane potential in red. **c)** Raster plot over the 100 trials. **d)** PSTH from 100 trials. Clear peaks are observable following light stimuli with a latency of 5 ms.

Fig 3.8 Delayed increase in the firing rate of GFP-negative (non-electroporated) neuron following ChR2 stimulation. a) Raster plot, overlaid and mean membrane potential and PSTH from 100 trials of intracellular recording of a single cell. 5 light pulses of 2 ms at 50 Hz were given. b) Second example of delayed reaction to ChR2 stimulation. Raster plot, cell attached recording and PSTH from second neuron. Only one 2 ms pulse of light was given per trial.

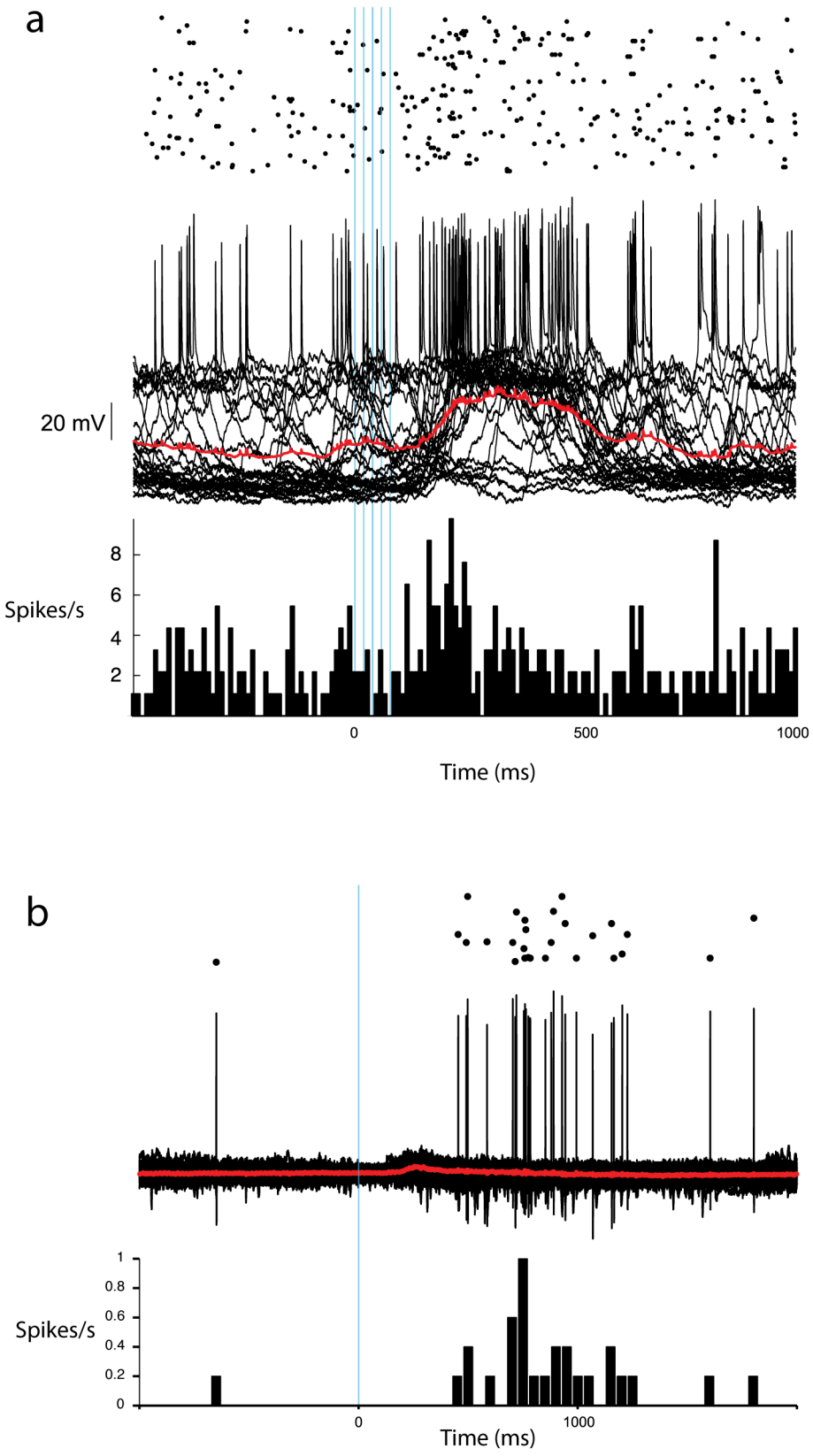
a
20 mV
Spikes/s
8
6
4
2
0
500
1000
Time (ms)
b
Spikes/s
1
0.8
0.6
0.4
0.2
0
0
1000
Time (ms)

Fig 3.8

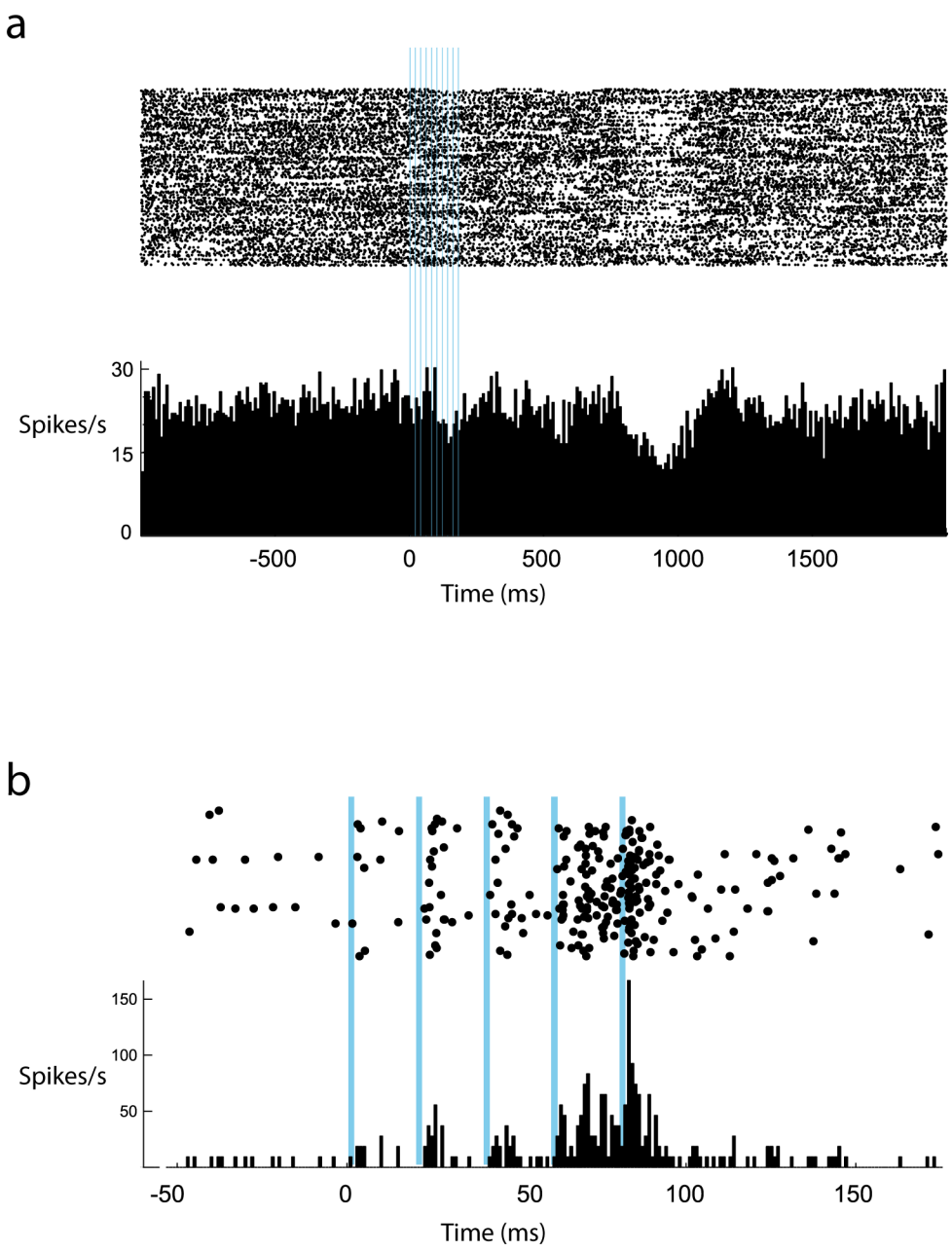

Fig 3.9 Additional delayed inhibitory and excitatory responses to light stimulation were observed. a) Raster plot and PSTH from 100 trials of a cell-attached recording. 10 light pulses of 2 ms at 50 Hz were given which resulted in an inhibitory response in the recorded neuron. **b)** Raster plot and PSTH from putative connected cell with an additional delayed response. Light stimulation consisted of 5 light pulses of 2 ms duration at 50 Hz which produced an excitatory response in the recorded neuron.

Of 51 neurons recorded from, either intracellularly or in a cell-attached configuration, 14% showed a fast excitatory response < 50 ms following the first light stimulation either in their spike rate or their membrane potential. This suggested an excitatory input from the ChR2 containing neurons (Fig 3.10a). 44% showed a delayed response, with a delay of up to 1 s. 42% showed no change in their firing rate following ChR2 stimulation of the electroporated neurons nearby.

The presence or absence of a change in the activity of the recorded neuron was possibly due to the number of ChR2 expressing neurons. The number of fluorescent protein expressing neurons for each of the three different types of experiment (no response, fast response and delayed response) was compared. The number of neurons for both the no-response experiments (mean = 2.7 ± 0.4; n = 24) and delayed response experiments (mean = 3.5 ± 0.3; n = 25) was found to be lower than the neurons expressing in the fast response experiments (mean = 5.3 ± 0.7; n = 8, $p < 0.01$ and < 0.05 respectively, t-test).

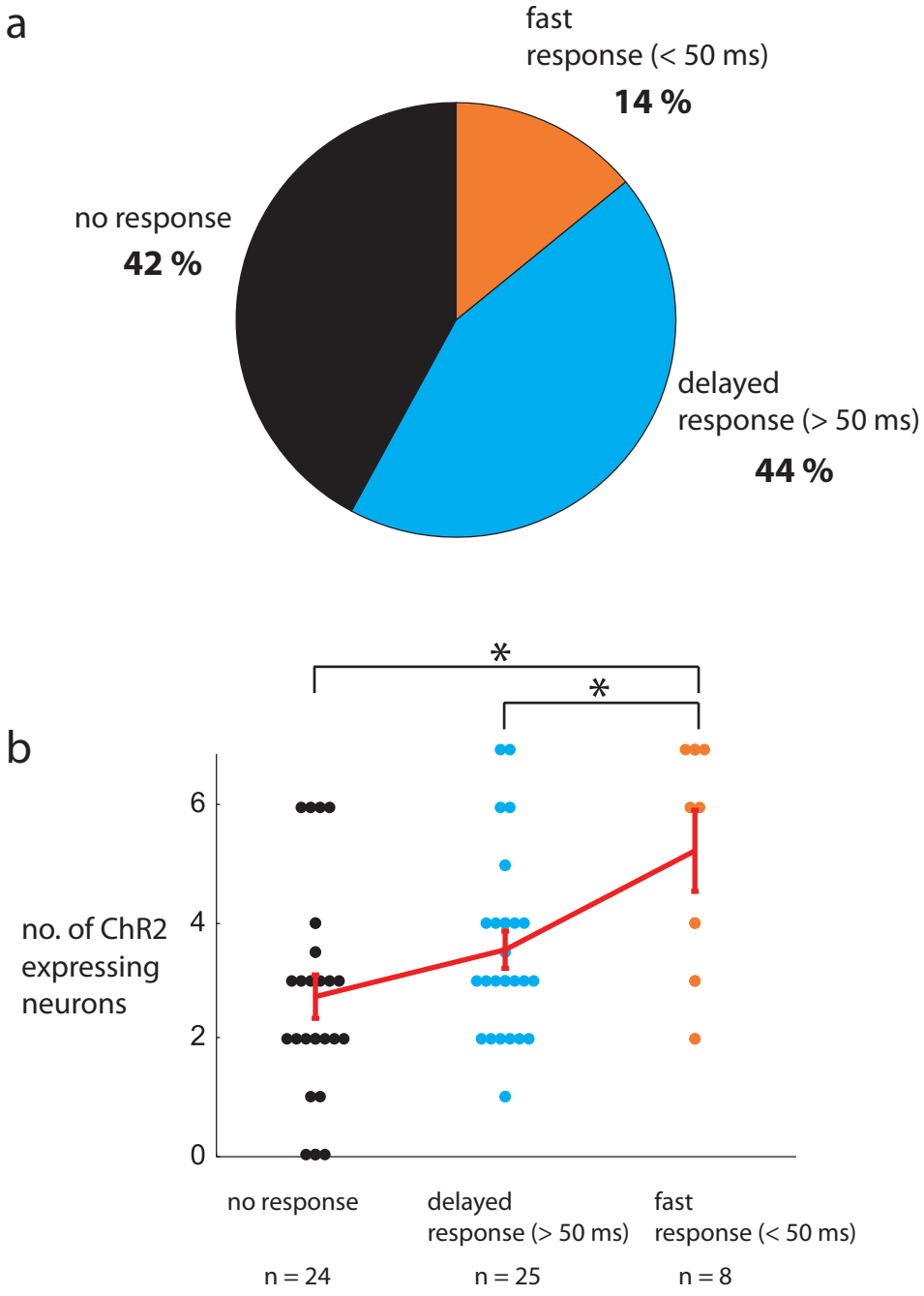

Fig 3.10 Population responses to local ChR2 stimulation a) Pie graph showing the proportion of neurons in which no response (42%), a rapid connected response (14%) and a delayed response (44%) was observed following stimulation of ChR2-expressing neurons in the local network. **b)** The number of neurons for both the no-response experiments (mean = 2.7 ± 0.4; n = 24) and delayed response experiments (mean = 3.5 ± 0.3; n = 25) was found to be lower than the neurons expressing in the connected experiments (mean = 5.3 ± 0.7; n = 8, $p < 0.01$ and < 0.05 respectively, t-test)

3.4 Discussion

The experiments presented above clearly indicate that the introduction of a small number of spikes can have a detectable effect on the firing rate of the local network. This is demonstrated quantitatively with injection of current into a single neuron and has far-reaching implications for the possible coding strategies employed by the brain to transmit information.

3.4.1 Variability in responses and baseline firing rates

In the experiments involving injection of a single spike and the recording of changes in the firing rate of the local network, there is great variability in the responses across cells and animals. In these blind experiments, the connectivity and spatial relationship between the patched cell and the cells picked up by the - cellular probe was unknown, and probably varied considerably between experiments. Furthermore, the experiments assumed a homogenous cortex, without taking into account connectivity patterns. It is possible that averaging across all the data collected in all animals could cancel out the changes in the activity of specific neuronal sub-networks.

Urethane anaesthesia is accompanied by distinct up and down states in the membrane potential of the neurons, which last for up to a second. This leads to very variable baseline firing rates, with many repetitions required to reach a stable enough baseline for meaningful changes in firing rates to be observed. It is possible that similar experiments performed under isoflurane or in the awake animal might give smoother baseline firing rates before stimulation. This would permit changes in firing rates to be observed within the recordings of individual animals, removing the need to average across all animals in order to see a change in baseline firing rate. In recordings performed under isoflourane anesthesia in this work (see Fig. 3.7 and 3.9), the up and down states are less pronounced than recordings in which urethane anesthesia was used (see Fig. 3.1) leading to a smoother baseline firing rate.

3.4.2 Is the size of the increase in firing rate expected?

The increase in the firing rate of the local network from the simultaneous intra- and extra-cellular recordings can be compared with the increase predicted in the previous single-cell current injection experiments (London et al., 2010). In these earlier experiments a single current pulse was injected into a patch-clamped pyramidal neuron in the barrel cortex and the change in the firing rate of that same neuron was measured following the injection. It was found that a single extra presynaptic spike increased the probability of a postsynaptic spike on a connected neuron by approximately 2 percent points for 5 ms, corresponding to a 4 Hz increase in firing rate (2%/5 ms = 4 Hz). The extracellular recordings described in this work, however, include spikes from neurons that are not connected. This should reduce the average increase in firing rate by a factor equal to the connection probability, which is approximately 0.04 in somatosensory cortex (Holmgren et al., 2003) . Thus, if all extra spikes occurred within 5 ms, the expected increase in firing rate would be 0.16 Hz. It is, though, unlikely that they do, for two reasons: the stimulus lasted 2.5-10 ms, spreading out the time of the extra presynaptic spike, and axonal delays, dendritic filtering, and latency to spike spread out the time of the postsynaptic spike by another 1-5 ms. Thus, the extra postsynaptic spikes should occur within 10-20 ms of the presynaptic ones, which implies an increase in firing rate of 0.04-0.08 Hz (i.e., a factor of 2-4 smaller than the 0.16 Hz increase expected if all the spikes were to occur within the first 5 ms). Assuming that the average firing rate in somatosensory cortex is 1 Hz (de Kock and Sakmann, 2009), this is very close to the 0.03-0.065 Hz increase seen in the first 10-20 ms in the inset of Fig. 3.3b. Thus, not only does a single extra spike introduced into somatosensory cortex produce a measurable effect on the network, one that lasts for more than 50 ms, it produces an effect whose size is predicted by the previous single-neuron current injection experiments.

3.5 Different scales of local network stimulation - single cell and small population

How the local network activity changes with different degrees of neuronal stimulation can be observed by comparing the results described previously in this section. The response in the local network resulting from the optogenetic stimulation of a small number of ChR2 +ve cortical pyramidal neurons can be compared to the effect of the electrical stimulation of a single cortical pyramidal neuron. Both experiments employed the use of a multi-unit silicon probe to measure changes in the firing rate of the local network. The increase in the firing rate of the local network had a greater duration (~200 ms) when 11 neurons were stimulated optogenetically to produce ~10 spikes (Fig 3.6 b) compared to when one neuron was stimulated electrically to produce 1 spike (20 ms; Fig 3.3 b). While in Fig 3.3b the firing rate stays elevated above noise for 200 ms, the large increase remains for only 20 ms. Interestingly, even though the experiment involving a greater number of stimulated neurons causes an increase of longer duration, both scales of stimulation (11 neurons or 1 neuron) result in an increase in the firing rate of ~5 spikes per second. This is surprising, as it would be expected that only 11 neurons stimulated for 100 ms would cause a larger change in the firing rate. It is possible, however, that as well as excitatory neurons, inhibitory neurons were also recruited and the extra inhibitory spikes caused the overall spike rate of the local network to decrease.

3.5.1 Response to light in control animals

The experiments involving combined electroporation and extracellular recording with silicon probes were performed blind, the neurons of half of the 12 animals involved were electroporated with only GFP and no ChR2 plasmid. Analysis of the network activity of the first 6 animals (3 control, 3 ChR2 containing animals) following ChR2 activation showed a consistent response to the light stimulation on one channel of one animal, visible on single traces as well as in the PSTH. This animal was a control and contained no ChR2, indicating that the light was altering the activity of the brain independently of ChR2 activation. This response

was interpreted as a visual response to the bright blue light. For the further 6 experiments (including the experiment featured in Fig 3.6) of which, again, 3 were control animals, a flickering light was constantly applied to the eyes to attempt to prevent the light from stimulating the animal directly. No further light artefacts were observed following the introduction of the constant flickering light.

The introduction of small perturbations with light, in general, has serious experimental complications. The presence of a visual response, however small, can occlude the observation of small changes to the network activity expected by the introduction of extra spikes into the network. While light artefacts will be negligible in experiments focusing on visual responses or large-scale cortical interference, they could prevent small changes from being observed or confuse interpretation of changes thought to be due to the increased spiking from the ChR2 experiments.

3.5.2 Non-responsive electroporated pyramidal neurons.

Expression of either RFP or GFP 2 days after electroporation was used as an indication that the neuron would also contain ChR2. However, around 40% of the electroporated pyramidal neurons which had shown clear expression of the co-electroporated fluorescent protein did not react to ChR2 stimulation, assessed in the cell attached configuration (for interneurons this proportion was much lower, J. Cottam). While problematic, this phenomenon could have several explanations.

First, it is possible that ChR2 was not expressed in every neuron that expressed the fluorescent protein. Expression of the ChR2 was driven by a PCAG promoter, whereas both the fluorescent proteins were under control of the CMV promoter which could lead to different expression efficiencies. Similarly, it is possible that the reverse case is also true. All ChR2-expressing cells might not be fluorescent, decreasing the ChR2 positive cell count in the study of the correlation between expression and effect (Fig 3.10b).

Secondly, the precise concentration of plasmid in the neuron could also influence the amount of protein produced. While great efforts were made to keep the injection concentrations consistent (with frequent concentration measurements

and intense vortexing), it was impossible to control exactly how much of each plasmid entered the neuron during electroporation. This depended upon the position of the electroporation pipette in relation to the neuron, the morphological variations between neurons and the amount of solution released from the pipette during the voltage pulse.

A greater proportion of electroporated interneurons responded to light stimulation (personal communication from James Cottam). While this could be due to individual electroporation technique, the interneurons are a much smaller cell type and have a higher baseline firing rate and are thus closer to threshold. They also have a higher input resistance and the same amount of channels opened will cause a higher depolarization and a higher likelihood of evoking a spike. It is likely, therefore, that the amount of ChR2 needed to induce the cells to spike is lower in interneurons than for pyramidal cells.

Another possible explanation for the low ChR2 response rate is that the cell-attached recording was erroneously performed on a cell adjacent to the electroporated neuron instead of the electroporated neuron containing the expressed plasmid. Often, the quality of the craniotomy 2 days following electroporation was such that accurate 2-photon guidance of the recording was impossible. Even with very high quality craniotomies it was very difficult to be certain that the electroporated neuron was indeed the one from which the cell-attached recording was being taken. Whole cell patch clamp recordings, permitting filling of the neuron with Alexa dye and therefore confirmation of cell identity, were attempted. While a number of recordings were successful, the depleted quality of the craniotomies made whole-cell recordings difficult and unsuitable to be used as a routine procedure to confirm ChR2 expression.

3.5.3 Delayed response to optogenetic stimulation in the membrane potential of patched neurons

While the firing patterns of a small number of the local neurons responded rapidly to ChR2 stimulation of the nearby electroporated neurons, the majority of the responses were delayed by as much as 1 second, and were larger than would be

expected after the short activation of only a few neurons. Although it is possible that these responses were related to the ChR2 stimulation, it is more likely that they were a direct result of the light. This is because the responses were both much larger and more delayed than would be expected from the excitation of several neurons. This response to the light could be a visual response that has arrived from the visual cortex, either reaching the retina directly or through the translucent brain. Even when the eyes were covered, however, a response was sometimes observed, suggesting that the response is not caused only by the light reaching the retina directly. The response could also be an unknown effect caused by the heating of the brain, or it could be a multisensory activation of the barrel cortex by a visual stimulus.

While the characterisation of non ChR2-activated responses was out of the scope of this thesis, several experiments were conducted in which 2-40 2 ms pulses of direct blue light (the same as that used for the ChR2 experiments) were flashed at 50 Hz in front of the animal during whole-cell patch-clamp recordings from neurons of the barrel cortex. The response was stronger than the delayed response seen in the ChR2 experiments (the light was given directly to the eyes) but the time scale was similar (Fig 3.11). This indicates that visual responses can indeed be detected in the barrel cortex and is the most likely explanation for the delayed responses observed.

3.6 Conclusion

Despite the added complications of possible visual artefacts (see 3.4.1), it is clear that many of the responses to optogenetic stimulation were indeed neuronal and due to the presence of ChR2 expressed inside the electroporated neurons. The rapid timescale of the responses and the consistency of spiking following every stimulation (Fig. 3.5) both suggest that it is the ChR2 channels causing the response rather than a visual related response, which would be delayed and inconsistent.

The introduction of a single spike into a network of neurons causes a temporary increase in the firing rate of the local neurons. The optogenetic excitation of several electroporated neurons also causes a noticeable increase in the firing rate of the local network. These two findings support the idea that groups of few neurons can have an important role in cortical coding. This has strong implications for possible coding regimes employed by the brain to transmit information. For small perturbations, however, the contribution of visual input from the optogenetic stimulation could possibly be significant and complicates interpretation of results. The next set of experiments to explore the effect of perturbations on brain function were designed to include only large-scale perturbations, which would make negligible the contribution of any light or heat stimulation artefacts.

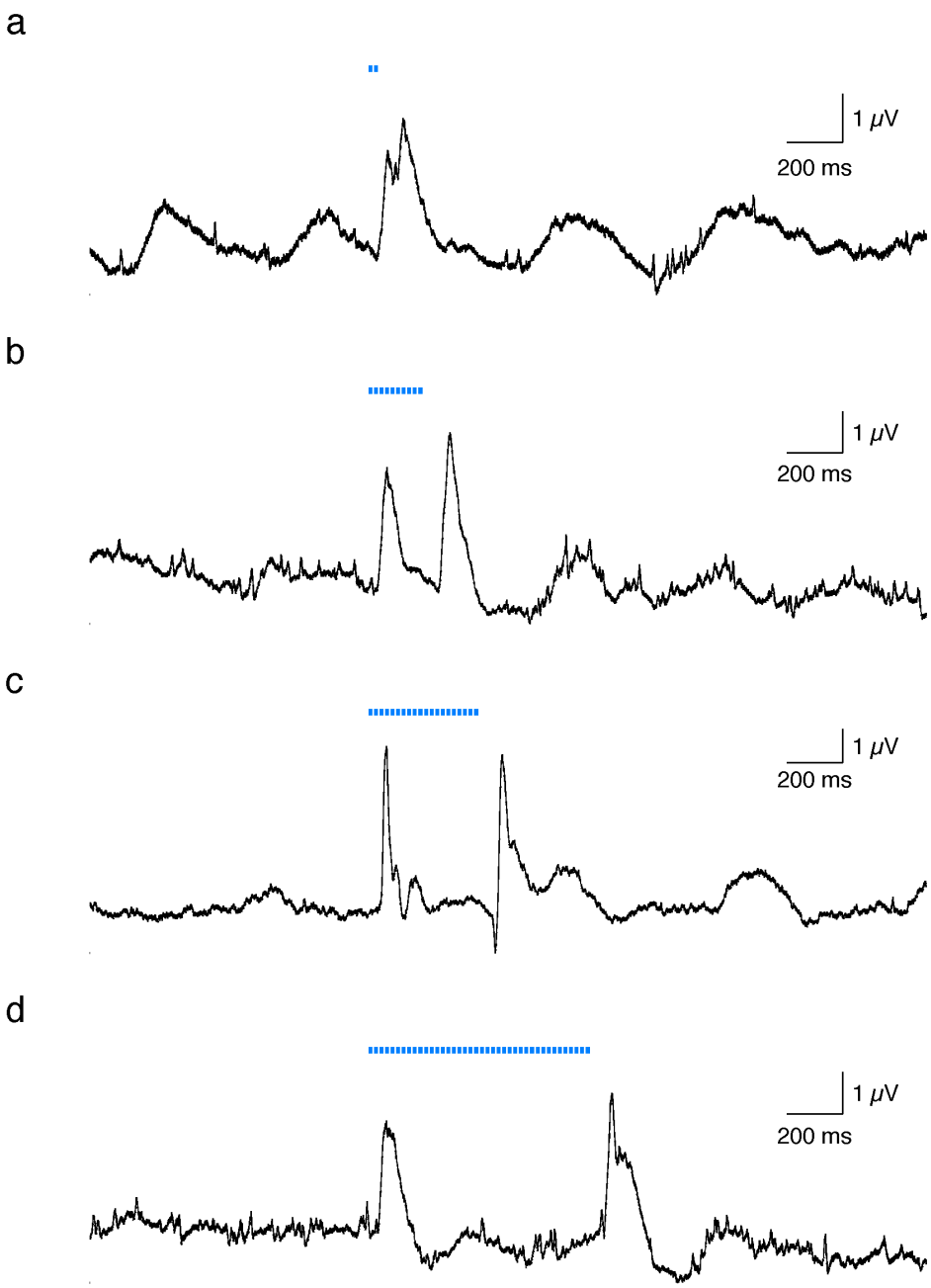

Fig 3.11 Responses to light stimulation in the barrel cortex. a) Mean cell-attached recording (n = 100) from layer 2/3 pyramidal neuron in the barrel cortex of a wild-type animal with no electroporated ChR2. Blue light stimulation (blue lines) consisted of 2 pulses of 2 ms duration at 50 Hz projected onto a screen directly in front of the eyes. **b-d)** Same as for **a** with 10, 20 and 40 pulses respectively.

4 Sensory and light-evoked oscillations produced by large-scale perturbations

4.1 Introduction

The deflection of a whisker in an anesthetised rat has been found to cause an initial strong response often followed by several rhythmic bursts of APs observed in all layers of the barrel cortex and also in the whisker-related nuclei of the thalamus (Dinse et al., 1997). In the LFP these bursts can be observed between 100 ms and 800 ms following the deflection and have a frequency of 7-14 Hz. A similar oscillation has been recorded following cortical or thalamic micro-stimulation (Fig 1.4; Contreras and Steriade, 1996; Contreras et al., 1997; Venkatraman and Carmena, 2009). These oscillations have been likened to spontaneous spindle waves, which have been observed in the early stages of sleep (Steriade, 1995; 2005). The basic parameters of these oscillations have been well characterised in rats and rabbits but so far not in mice and there has been limited work investigating their prevalence across different cortical layers. This chapter will begin by characterising whisker-evoked oscillations in the anesthetised mouse using whole-cell patch-clamp and cell-attached recording configurations.

Instead of micro-stimulation, which is not cell-type-specific, a transgenic mouse line expressing ChR2 under the promoter Thy1 (Arenkiel et al., 2007; Wang et al., 2007); Jackson Laboratories mouse strain B6.Cg-Tg(Thy1-COP4/EYFP)9Gfng/J) was used. In these mice ChR2 expressing neurons identified by a co-expressed YFP reporter protein have been observed in various layers of the cortex and in the thalamus. In this chapter I will first characterise the distribution of ChR2 expressing neurons in the barrel cortex and the thalamus. I will then use these mice to induce oscillations, similar to those observed following micro-stimulation and investigate the presence of both optogenetically- and whisker deflection-

evoked oscillations in the different layers of the cortex using extracellular recordings from a multi-site silicon electrode.

The origin and spread of sensory-induced oscillations has long been a topic of intense debate (Steriade et al., 1993; Steriade, 1995; Contreras and Steriade, 1996; Steriade, 2005). Several different hypotheses have been proposed. One hypothesis purports that the generation of spindle waves depends exclusively upon reticular nucleus activity (Steriade et al., 1985). The second hypothesis is that the oscillations result from the interplay between the thalamic reticular neurons (RT) and the specific nuclei of the thalamus, the ventral posteromedial nucleus (VPM) for the whisker system (Cotillon and Edeline, 2000). This idea was strongly supported by a study which separately knocked out the RT and the thalamus and found both of them to be essential for oscillatory activity in the auditory system of anaesthetised rats (Cotillon and Edeline, 2000).

In this chapter, I took advantage of the ability to induce an oscillation with optogenetic stimulation to further explore their origin. I blocked neuronal activity in the VPM pharmacologically and measured the effect of this blockade on the presence of the light-induced oscillations in the cortex over time. Successful thalamic knockout was confirmed by the abolition of a pre-established response to whisker deflections.

Two different drugs were selected to knockout activity in the thalamus: tetrodotoxin (TTX), a neurotoxin which blocks action potentials in neurons by binding to the voltage-gated, fast sodium channels in cell membranes (NARAHASHI et al., 1964) and muscimol, a $GABA_A$ agonist (Krogsgaard-Larsen et al., 1975). Both drugs strongly decreased the activity of the thalamic neurons.

A further controversy involving these oscillations has been whether or not they can be evoked in awake animals. Conflicting results have been reported (Cotillon-Williams and Edeline, 2003; Venkatraman and Carmena, 2009; Halassa et al., 2011). In the final part of this chapter I recorded oscillations following brief optogenetic stimulation in an active, awake animal, confirming their presence in the awake state.

4.2 Methods

4.2.1 Animals and Surgery

For all anaesthetised experiments in this chapter (except control experiments in which male C57BL/6J mice were used), male Thy1-ChR2 mice (P 30 to P60) were anesthetized with isoflurane (IsoFlo, Abbott, UK; 2.5% during surgery and 1% throughout recording). A custom-designed stainless steel recording chamber with a diameter of 11 mm (Judkewitz et al., 2009) was adhered over the barrel cortex region of skull (centered 3.5 mm lateral, 2 mm caudal of Bregma) and the skull moistened with external solution. All whiskers except C2 were cut to ~2mm from the snout. Following intrinsic imaging (see section 4.3) a small craniotomy (~1 mm^2) over the C2 barrel was made and the dura left intact.

Hemizygous B6.Cg-Tg(Thy1-COP4/EYFP)9Gfng/J (Thy1-ChR2) mice were sourced from Jackson Laboratories (http://jaxmice.jax.org/strain/007612.html) and mated with wild-type C57BL/6J mice. Genotyping of offspring was performed after the animals were weaned using transgene primers oIMR7303 and oIMR7304 and internal control primers oIMR7338 and oIMR7339 (Sigma-Aldrich, UK) according to the online PCR protocol. PCR products were run on an SDS-PAGE 1.5% agarose gel (Sigma-Aldrich, UK). 800 base pair (b.p.) transgene and 324 b.p. bands were observed. Pairs of hemizygous mice were then mated to create a homozygous colony. Both hemizygous and homozygous animals were used in experiments.

For the oscillation parameter experiments, mice are labelled 1-10. For the thalamic inactivation experiments, mice are labelled 1-11. For the awake recordings, mice are labelled 1-4. Mouse number 5 for this final section is the same anesthetised mouse 5 from the oscillation parameter experiments.

4.2.2 Injection of TTX and muscimol for thalamic inactivation

Following the craniotomy over the barrel cortex for insertion of the silicon probe, another smaller (~0.5 mm craniotomy was drilled 1 mm medial and 1 mm posterior to the first craniotomy. The position of this craniotomy was calculated to

allow the tip of a glass pipette to reach the VPM without damaging the ventricle or colliding with the silicon probe. A glass pipette (~1 MΩ) with a broken tip was filled with mineral oil (Sigma-Aldrich, UK) and inserted into a nanoject (Drummond Scientific Comp., USA). ~3 μl of the oil was ejected and replaced with a filtered solution of 10 μM TTX (Invitrogen, UK) and 0.375% tetramethylrhodamine dextran (Invitrogen, UK). For some experiments the TTX was replaced with 26 μM Muscimol hydrobromide (Sigma-Aldrich, UK), a GABA agonist, and the rhodamine was replaced with 2.5% fluorescein dextran (Invitrogen, UK). The silicon probe was placed just above its intended area of insertion, in the centre of the craniotomy. The TTX-filled pipette was lowered into the brain from a point 0.9 mm lateral and 0.3 posterior to Bregma, at an angle of 12º and 22º to the vertical plane, in the medial and posterior direction respectively. It was inserted to a depth of 4.1 mm to reach a final position of 1.8 mm posterior and 1.61 mm lateral to bregma and 3.75 mm deep, the position of the centre of the ventroposterior medial nucleus of the thalamus (Fig 4.17). The extracellular multiunit probe was then inserted shortly after. Following 10 - 30 min. of successful recordings of oscillations evoked by both light and whisker stimulation, TTX was injected into the VPM with the micro-injector. To begin with, 5 single pulses of 20 nl were injected, one pulse every 15 seconds. If a noticeable decrease in whisker response was detected before the 5 injections had been administered, no further liquid was injected. After the 5 pulses, recordings were made for several minutes. If after at least 5 minutes no decrease in whisker response was detected, a further 5 injections were made, also with 15 sec between injections. Further groups of 5 injections were made as necessary. Total amount of TTX injected is shown in Table 4.1

4.3 Results

4.3.1 Oscillations were recorded intracellularly following whisker deflection

Oscillations in membrane potential were recorded following deflection of the C2 whisker under isoflurane in whole-cell patch-clamped pyramidal neurons in layer

2/3 of the barrel cortex of wild-type mice (Fig 4.1). The oscillations had a frequency of ~12 Hz and a duration of ~700 ms. Previously similar oscillations in the cortex had been reported in both the LFP and intracellular recordings in other species, most particularly in rats and rabbits (Dinse et al., 1997) but had so far not been reported in mice. From recordings in 11 animals, in whole-cell patch-clamp and cell-attached configurations, oscillations were recorded in 16 / 37 neurons (43%). The average depth of the neurons in which oscillations were observed was 302 ± 99 μm (s.d.) and the depth of neurons in which there were no oscillations was 237 ± 76 μm (s.d.). These values are not significantly different, indicating no depth dependence within L2/3 and L4.

4.3.2 Transgenic mice expressing ChR2 under the Thy1 promoter

Oscillations induced with neuronal electrical stimulation have been reported, which show very similar characteristics to those following sensory stimulation (Steriade et al., 1990; Venkatraman and Carmena, 2009). In order to compare the whisker-evoked oscillations with oscillations evoked directly, I took advantage of the recent development of the transgenic mouse line expressing ChR2 under the promoter Thy1 (Arenkiel et al., 2007; Wang et al., 2007; Jackson Laboratories mouse strain B6.Cg-Tg(Thy1-COP4/EYFP)9Gfng/J). In these mice ChR2 expressing neurons identified by YFP reporter protein co-expression have been observed in various layers of the cortex and the thalamus.

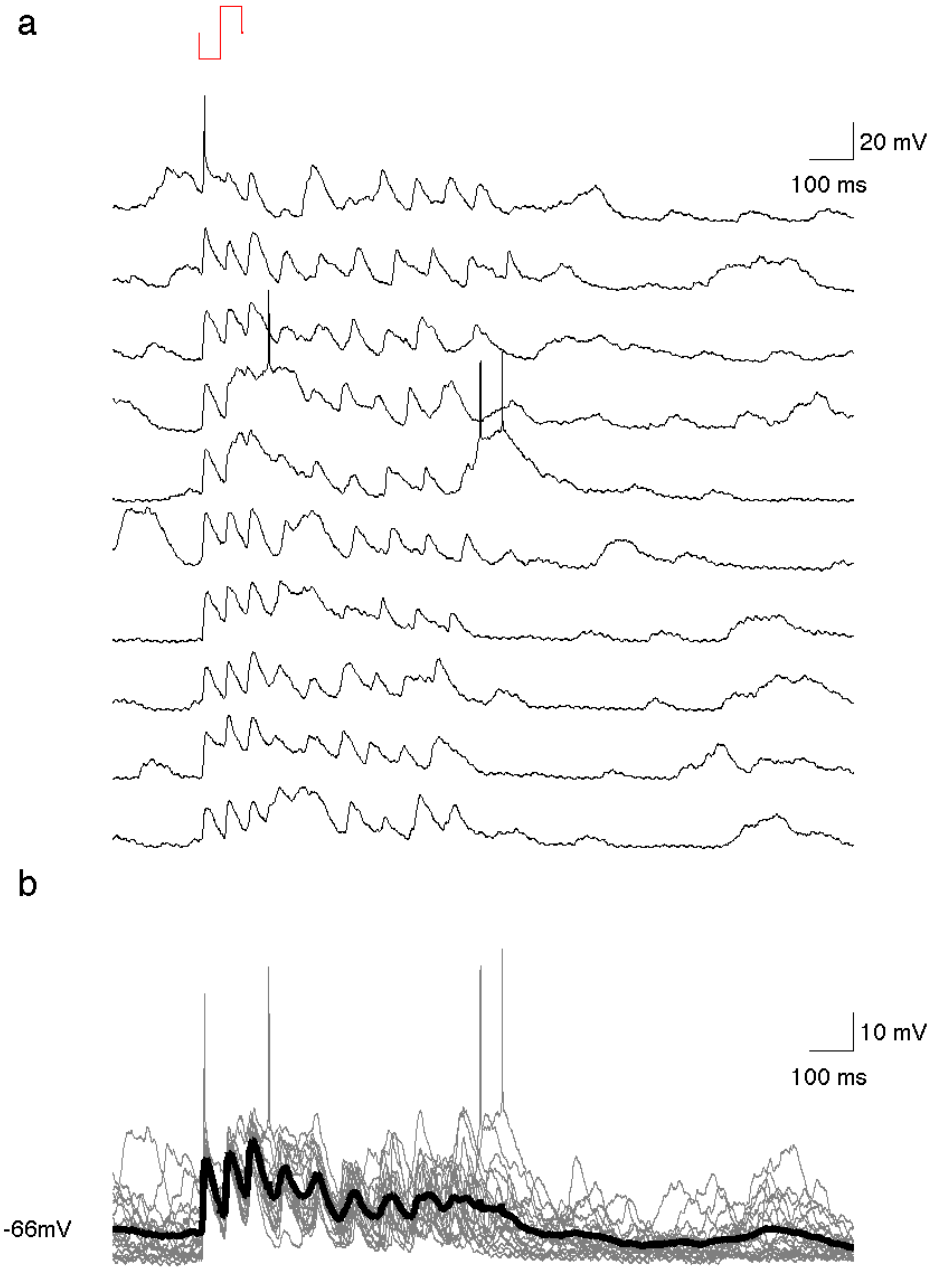

Fig 4.1 Membrane potential oscillations follow a whisker deflection in the barrel cortex. a) 10 individual traces of the membrane potential of a pyramidal neuron in layer 2/3 of the mouse barrel cortex. Whisker deflection (red) is an down-up-down movement with a total duration of 100 ms. b) 20 traces overlaid with the average membrane potential (black). The oscillations recorded in the membrane potential of this neuron had a frequency of 12.5 Hz.

To determine the precise location and extent of the ChR2 expression in these mice, the endogenous YFP expression in 100 μm sections of several mice was observed with a confocal microscope (Fig 4.2). The YFP expression was strong enough to observe without amplification of the signal with antibodies. In the cortex, there was strong staining in L2/3 and L5. In the thalamus, the VPM and POM were strongly stained, as well as the RT. In previous detailed studies of the expression in different cell types of these mice, it was found that almost all the pyramidal neurons in L2/3 and L5 expressed ChR2 whereas very few interneurons showed expression (Arenkiel et al., 2007; Wang et al., 2007). Due to the high concentration and specificity of ChR2 expressing neurons in this mouse strain, it was considered suitable for the induction of oscillations.

4.3.3 The characterisation of sensory and light-evoked oscillations

To further investigate both sensory and optogenetically-evoked oscillations across all layers and at a much larger scale than was feasible with patch-clamping, large-scale extracellular recordings were performed. The spiking activity and the LFP were recorded using a 16 channel silicon extracellular probe in the mouse barrel cortex of Thy1-ChR2 positive mice following both a 10 ms whisker deflection (Fig 4.3a) and a 2-20 ms optogenetic cortical stimulation with blue light (Fig 4.3b). Both types of oscillations had a frequency of approximately 12 Hz, continued for around 800 ms and were only activated in a fraction (~20-80%) of trials, despite identical stimuli being used. The oscillations recorded in the LFP are comparable in their frequency and duration to the oscillations recorded in the spiking activity in the middle channels of the extracellular probe (Fig 4.3 c,d). Comparisons between LFP and spiking data will be discussed in greater depth over the course of the chapter. In the following analysis, only the LFP measured from site 6 (~450 μm deep) of the extracellular probe was included.

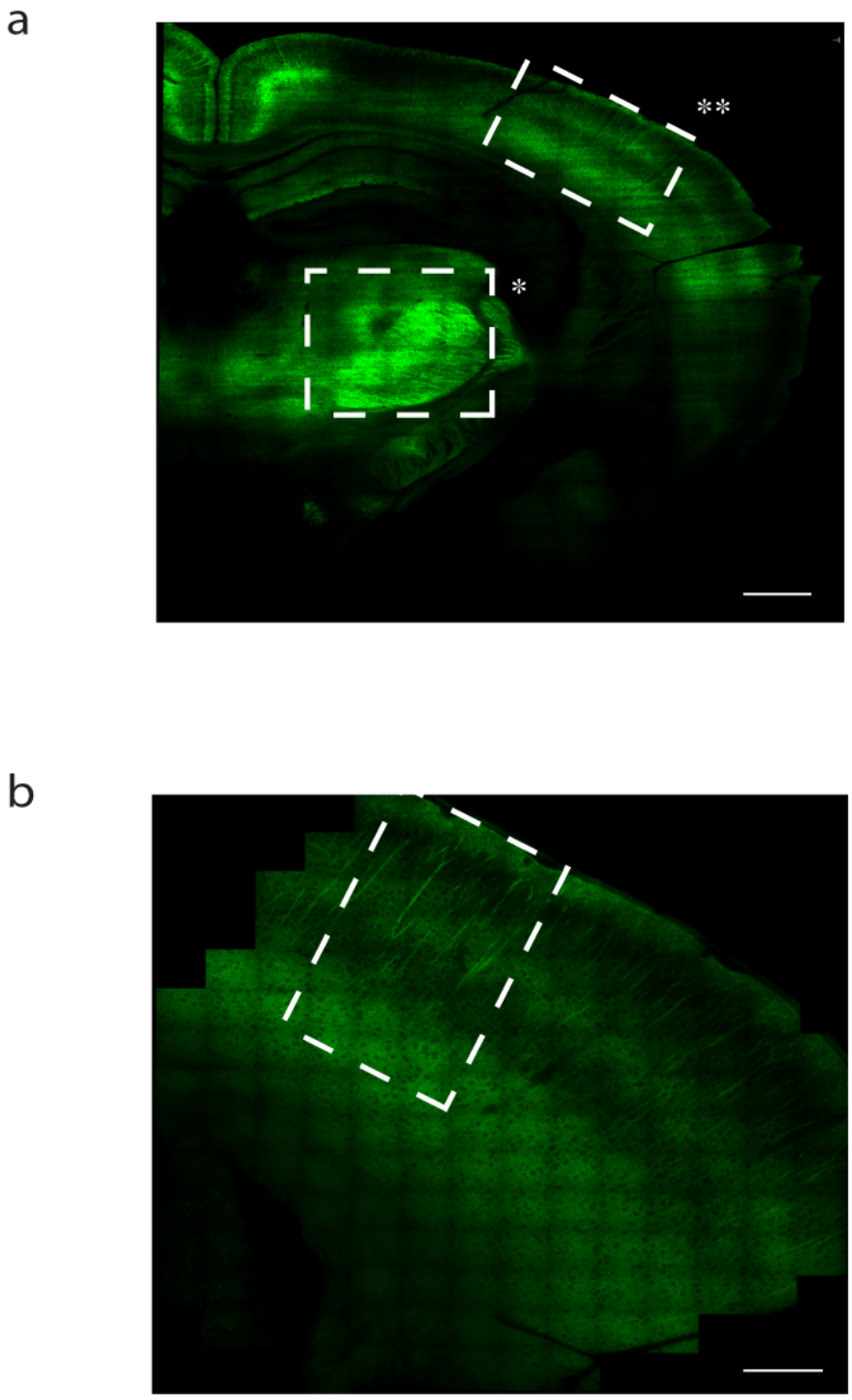

Fig 4.2 Distribution of YFP-expressing neurons in the Thy1-ChR2 mouse. a) Confocal image of a 100 µm coronal brain slice showing YFP fluorescence in the thalamus (one asterisk) and cortex (2 asterisks; see Fig 4.17 for a schematic diagram). Scale bar = 600 µm. **b)** Confocal image from the same slice as in **a,** showing clear dendrites in the superficial layers of the cortex**.** Scale bar = 200 µm.

For a typical experiment, the light and whisker trials were interleaved randomly and the trials had an inter-stimulus interval (ISI) of 4 s. The fast Fourier transform (FFT) was calculated for each segment of the LFP taken over the interval of 800 ms duration starting 100 ms post-stimulus and ending 900 ms post-stimulus for both the light and whisker stimuli (Fig 4.4 section II). The initial response (0-100 ms post-stimulus; Fig 4.4 section I) was not considered to be part of the oscillation and was not included in the oscillation analysis. As a control we used the FFT for an interval of the same duration taken at 1000 - 1800 ms after the stimulus, by which time the oscillation had subsided (Fig 4.4a section III). The FFT of the control recording was compared to the post stimulus response, and the difference between the two was attributed to the oscillation.

For each animal, the mean FFT for all whisker-induced response, light-induced response and control segments were compared (example animal, Fig 4.4b). To find the frequency of highest power, the control was subtracted from the whisker and light response (Fig 4.4c). This resulting maximum peak falls at the most common frequency of the dominant oscillation. For the example animal, selected for high trial number and consistent oscillations, both the light- and whisker-induced oscillations have an average frequency of 12.7 Hz.

By examining its FFT, each trial was classified as either containing or not containing an oscillation. Firstly, an FFT was performed on each of the control sections of recording, taken 1000-1800 ms after the stimulus. The power at the dominant frequency (12.7 Hz for the example mouse) was calculated for each trial (Fig 4.5a top panel). The power value 2 standard deviations above the mean was set as threshold (blue line, Fig 4.5a). An FFT was then performed on all trials containing light and whisker stimulation and the power at the dominant frequency calculated. Power values above the threshold were classified as containing an oscillation (Fig 4.5a bottom two panels).

For the example mouse, 87% of the light-stimulated trials (421 of 485 trials) and 59% of the whisker-induced trials contained an oscillation (259 of 439 trials; Fig 4.5b).

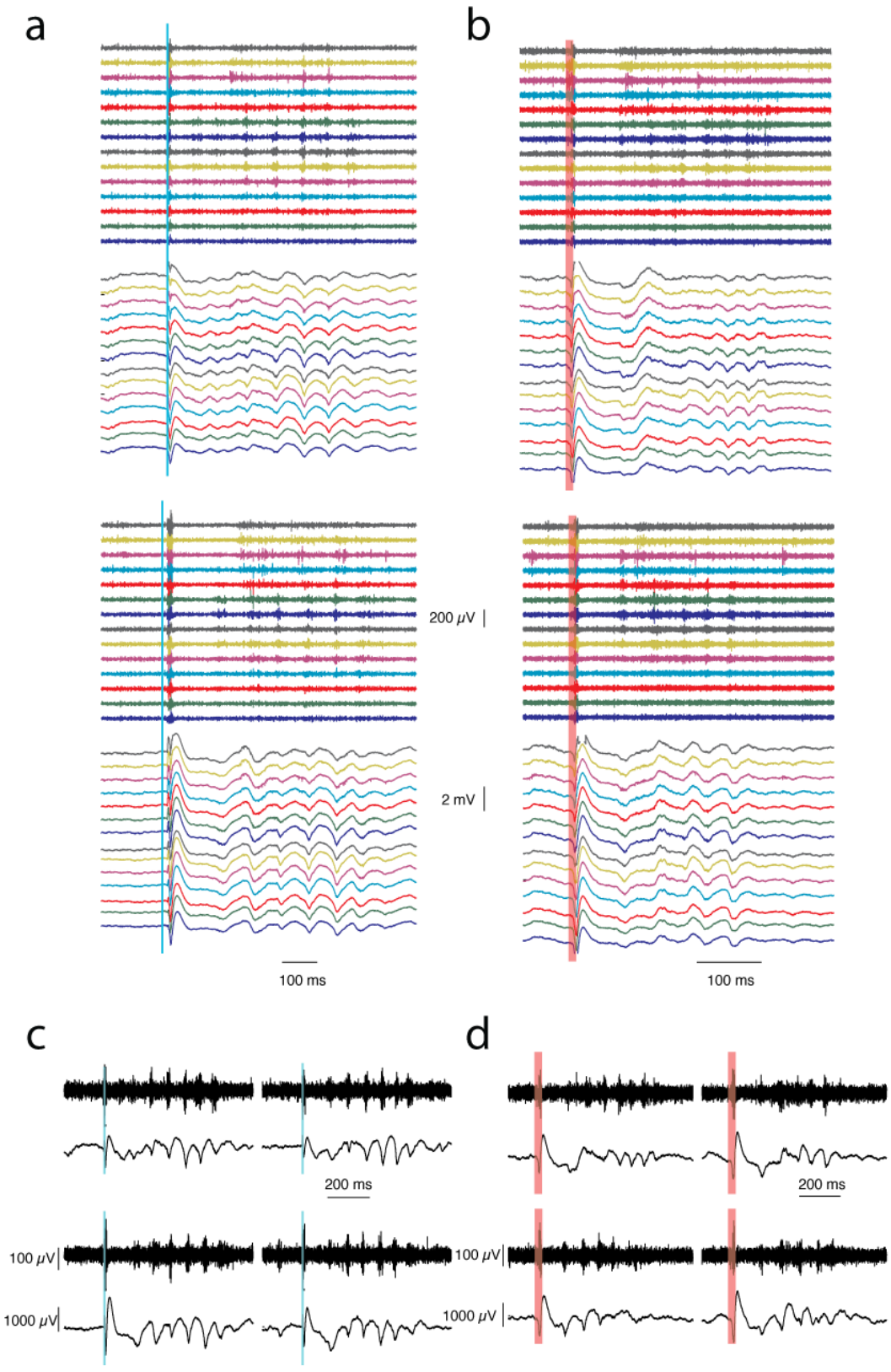
a
b
200 μV
2 mV
100 ms
100 ms
c
d
200 ms
200 ms
100 μV
1000 μV
100 μV
1000 μV

Fig 4.3

Fig 4.3 Example traces of light- and whisker-induced oscillations. a) Recording of 14 channels from a 16-channel extracellular silicon probe, placed into layers 2-4 of the barrel cortex, at a 60° angle to the surface of the brain. Each colour represents a different channel. Top panels: spiking data filtered at 300-5000 Hz. Bottom panels: Low frequency component / local field potential (LFP) filtered at 0.2-300 Hz. Each example shows one trial and the 3 ms ChR2 stimulation is indicated with a blue line. **b)** Two trials over 14 channels with a 10 ms whisker deflection (red line). **c)** Examples of raw spike data (top panels) and LFP (bottom panels) from channel 6 for four different trials containing a light stimulation. **d)** Four examples of whisker stimulation trials from channel 6.

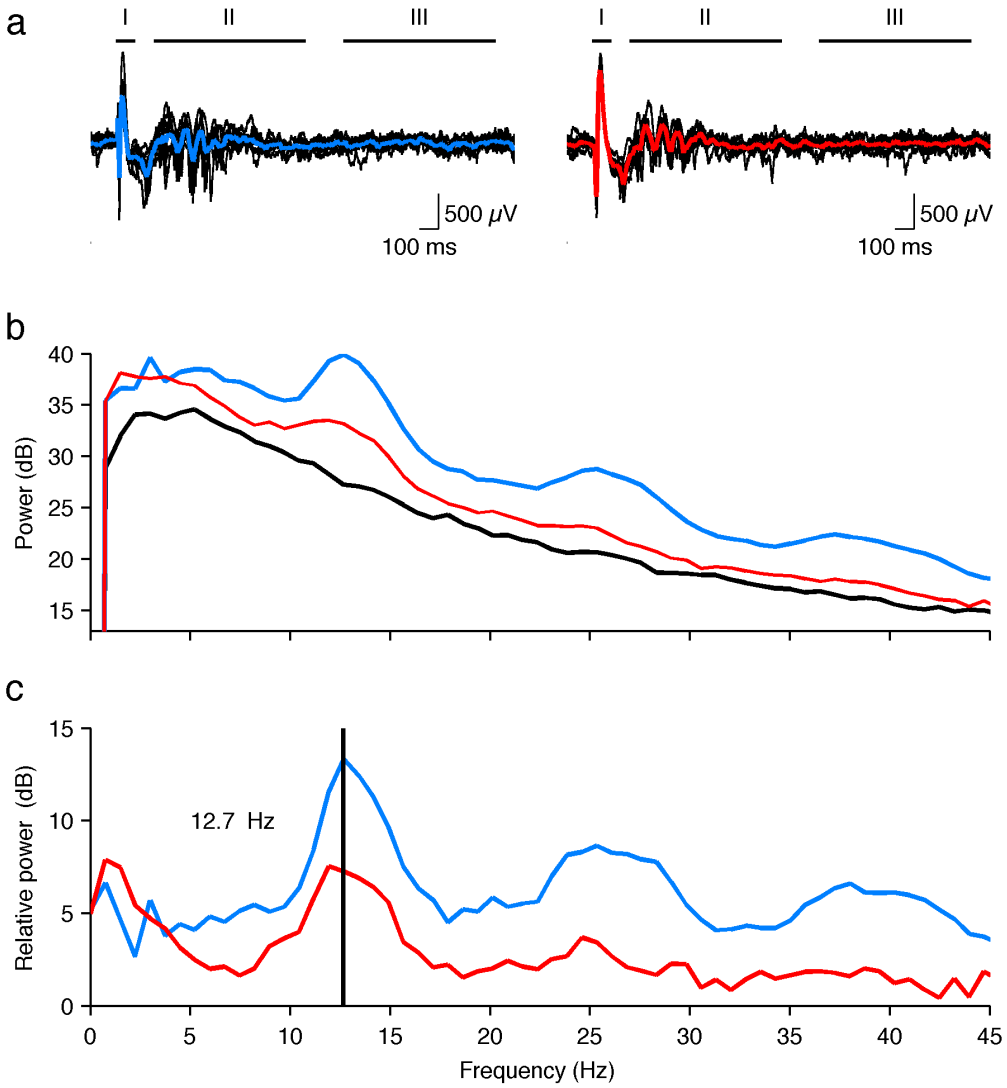

Fig 4.4 Light- and whisker-evoked oscillations lie in the α-range. a) LFP recordings of 10 trials containing light (left panel) and whisker (right panel) stimulation trials. Mean LFP is shown in colour. Sections of recording, from which initial response (I), presence of oscillation (II) and control (III) were calculated, are indicated**. b)** Mean fast Fourier transform (FFT) of all control recordings (black line), light stimulation trials (blue line) and whisker stimulation trials (red line). **c)** Mean FFT of light and whisker trials after subtraction of control values. The black line indicates maximum relative power, which corresponds to the frequency of the light or whisker-induced oscillation.

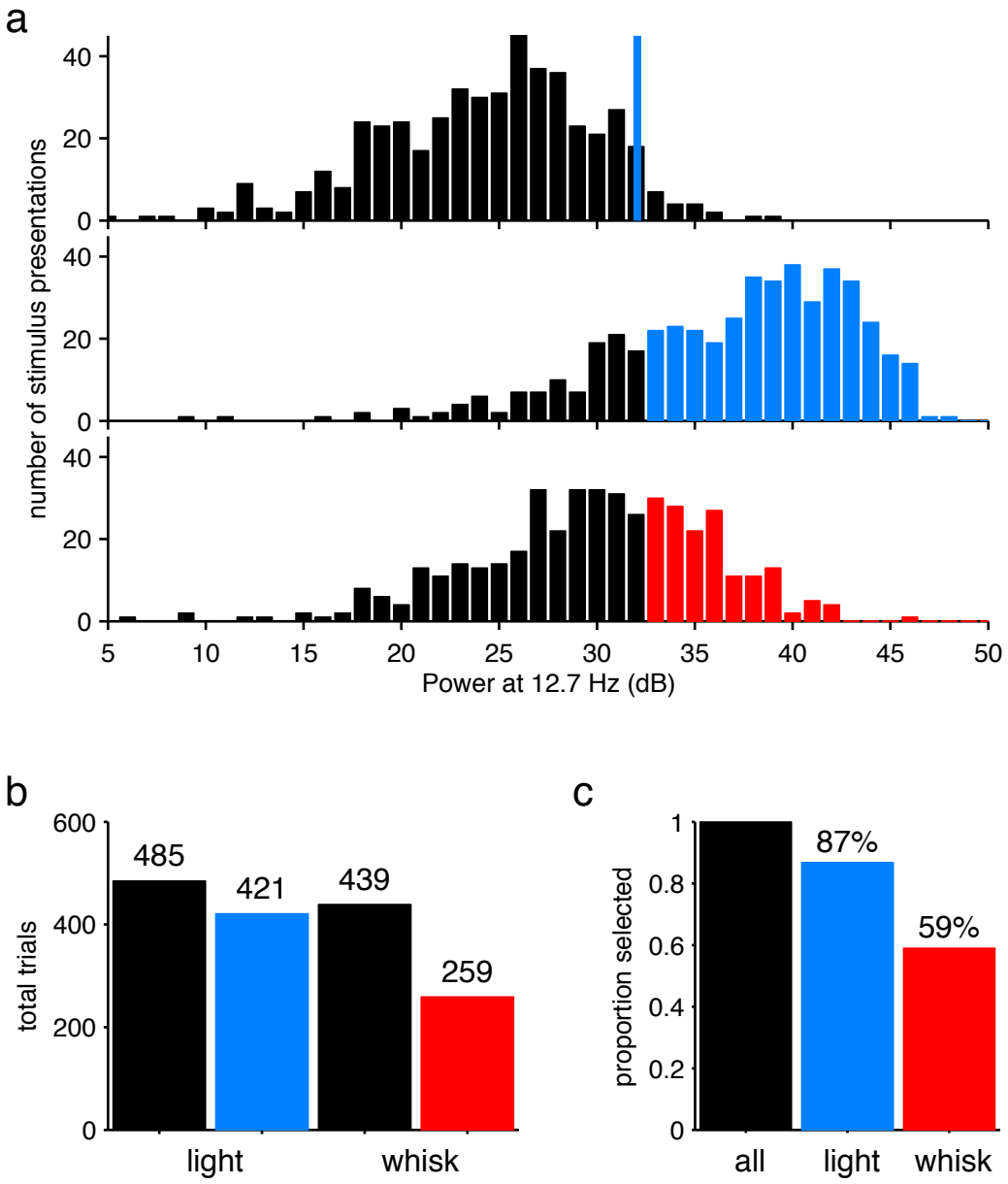

Fig 4.5 Trials can be classified as containing an oscillation or not, based on the power distribution. a) Histogram of the power at 12.7 Hz of all control recordings (top panel), light stimulation trials (middle panel) and whisker stimulation trials (bottom panel) for the example mouse. Blue line in the top panel is located at the power value two standard deviations above the mean, the threshold above which stimulation trials were considered to contain an oscillation. Oscillation-containing trials in lower panels are coloured in blue or red. **b)** The total number of trials for the example mouse, and number of trials containing light- or whisker-induced oscillations**. c)** Proportion of total trials classified as containing an oscillation for the example mouse.

For each trial, there was a small degree of variability in both the delay from the initial response to the beginning of the oscillation and the frequency of the oscillation. The peaks and troughs of the oscillations therefore fell at slightly different times following the stimulus, distorting the mean response. To align all oscillations relative to the initial response, the phase (0 - 2π) of the oscillation in each oscillation-containing trial was extracted from the FFT calculations Trials were then aligned by moving each individual trial along the x-axis by the phase value calculated and the average wavelength calculated for all trials (Fig 4.6 a,b). The resulting mean oscillation amplitude was 199 μV and 109 μV higher than the mean for the unaligned trials for the light-induced and whisker-induced trials, respectively (Fig 4.6c). The aligned control regions showed only a small increase (73 μV) in the amplitude of the mean oscillation, compared to the mean of the unaligned control regions. In all subsequent figures, oscillations will be phase-aligned unless specified.

A total of 10 mice were included in the study (Fig 4.7; example mouse indicated with an arrow). All animals were Thy1-ChR2 mice, except mice 1 and 3, which were C57BL/6 wild-type mice. Mouse 1 received no light stimulation and mouse 3 was used as a control. In mouse 3, light stimulation resulted in oscillations in < 3% of trials.

Different stimulus durations were used for the whisker deflection (10, 20 or 100 ms) and both different durations and intensities were used for the light stimulations. For each animal, the minimum amount of light or deflection required to produce an oscillation varied. For some animals, several different parameters were used and trials with the stimulus parameters with the highest percentage of oscillations produced was analysed further (Fig 4.7).

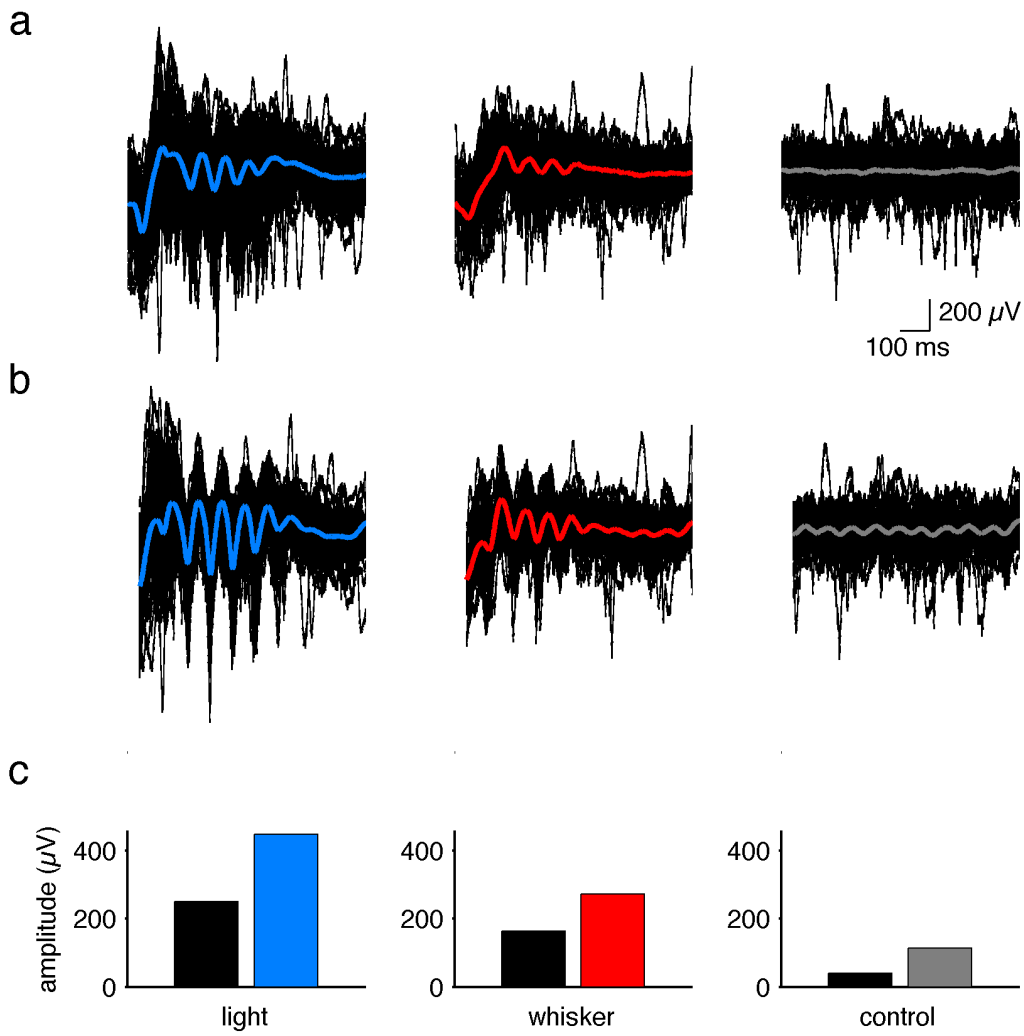

Fig 4.6 Oscillations were aligned according to their phase. **a)** All trials containing oscillations before phase-alignment. Trials are divided into light stimulation (blue mean) or whisker stimulation (red mean). Control recordings are also illustrated (grey mean). **b)** All trials containing oscillations after phase-alignment. **c)** Amplitude of mean LFP recording before (black) and after (colour) phase-alignment.

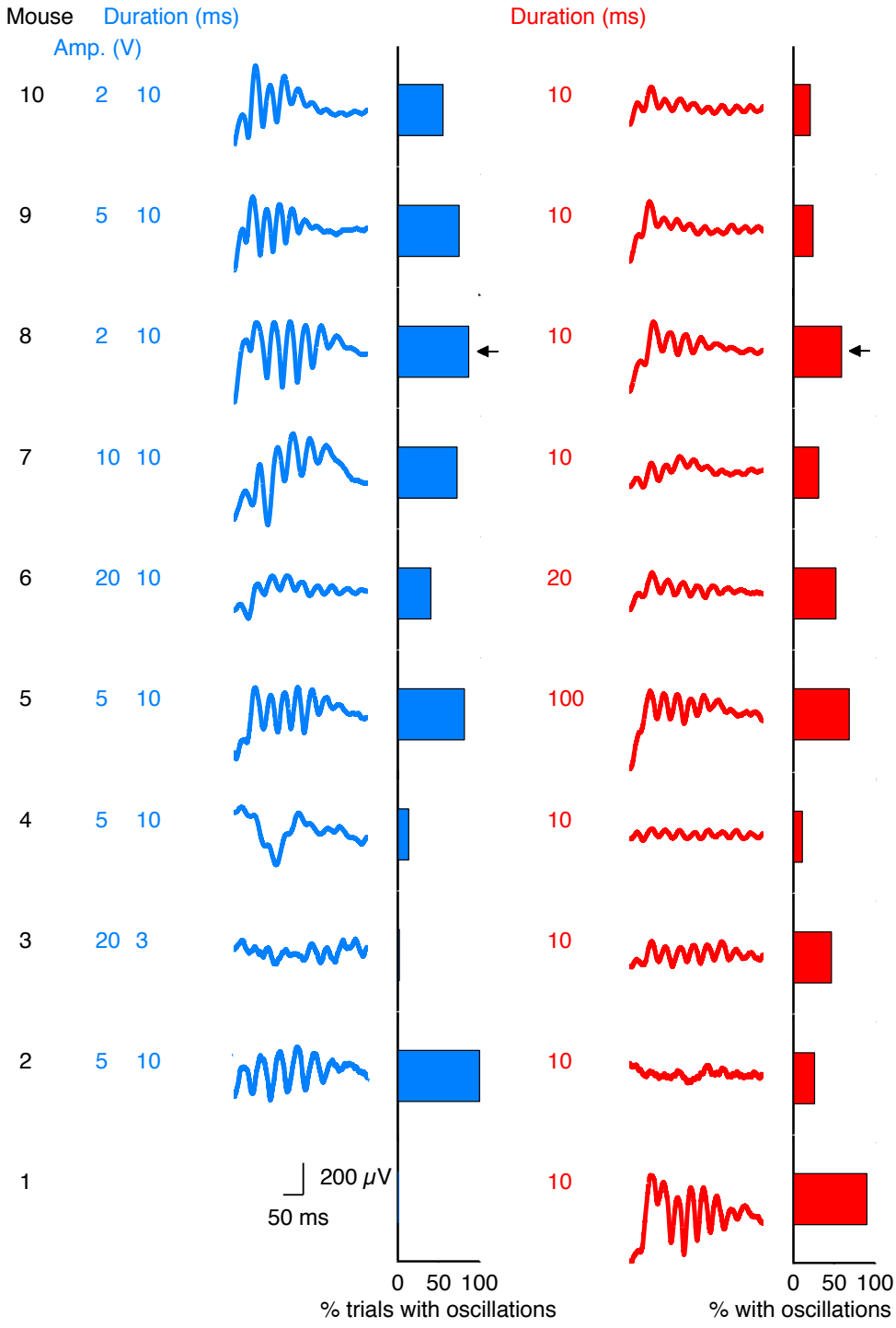

Fig 4.7 Mean LFP recordings showing oscillations from all mice. a) Mean LFP recordings with light stimulation from 10 mice. Left panel: stimulus parameters. Middle Panel: phase-aligned recordings are shown in blue. Right panel: proportion of trials containing an oscillation. A black arrow points to data from the example mouse featured in previous figures. **b)** Mean LFP recordings from 10 mice with whisker stimulation. Phase-aligned recordings are shown in red.

In the example mouse, the frequency of the light-induced oscillations ranges from 9.6 - 14.8 Hz, with a mean of 12.6 ± 1.2 Hz (s.d.; n = 485; Fig 4.9 a). The whisker-induced oscillations have a mean of 12.1 ± 1.3 Hz (s.d.; n = 439). These frequencies were not significantly different.

To detect possible subtle differences, the frequency spectrum between 9.6 Hz and 17.1 Hz was divided into 11 frequency bands with a width of 0.75 Hz, and for all mice the fraction of trials with an oscillation in each of these frequency bands was calculated. The frequency band with the greatest fraction of trials showing oscillations was centred around 11.9 Hz for the light-induced oscillations (n = 1630; Fig 4.9c) and 13.4 Hz for the whisker-induced oscillations (n = 900; Fig 4.9e) over the population of mice tested. However, due to the variability across mice, the difference was not significant. To confirm that the frequency does not depend on the length of either the light stimulation or whisker deflection, the predominant frequency of both types of oscillations was plotted against the length of the stimulation (Fig 4.9 d,f).

A similar analysis was performed on the amplitude of both the light- and whisker-induced oscillations (Fig 4.10). In the example mouse across all trials, the light oscillations had a mean amplitude of 1417 ± 211 μV (s.d.; n = 485; Fig 4.10a). The whisker-evoked oscillations had a mean amplitude of 1042 ± 141 μV (s.d.; n = 439). For this mouse, therefore, the light induced oscillations were of a higher amplitude ($n = 439$, $p < 0.0001$, t-test).

For the population analysis of the mean amplitude, mouse 2 was not included as the amplitudes were far smaller than all the other mice. Only mice were included in which both whisker and light oscillations were present and could be compared. In all mice the mean amplitude was greater for the light-induced oscillations than for the whisker oscillations ($n = 6$, $p < 0.01$, paired t-test).

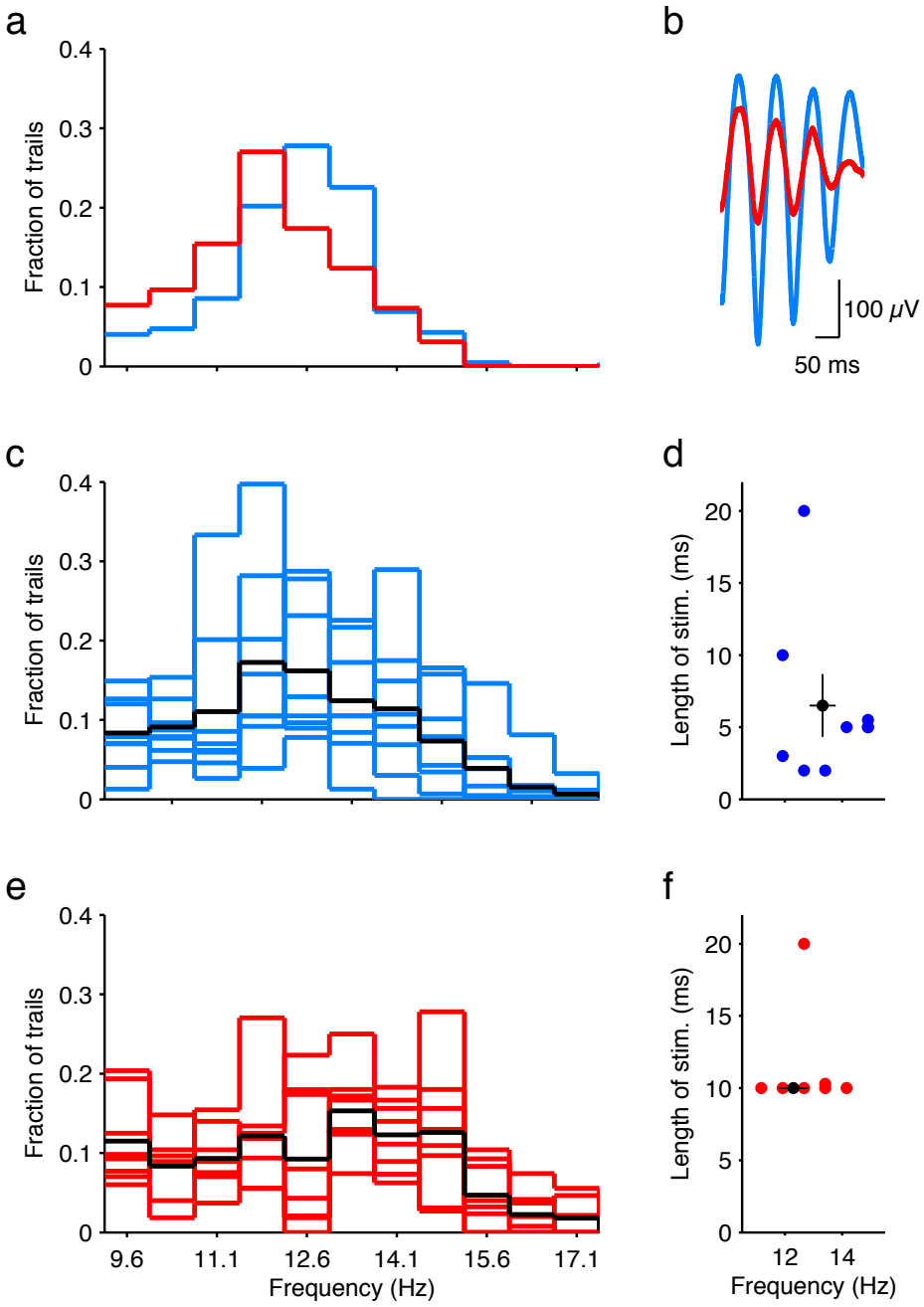

Fig 4.9 Oscillations induced by light and whisker stimulation have similar frequencies. a) Histogram of frequencies for each light- (blue) or whisker- (red) induced oscillation from the example mouse. **b)** Mean light- and whisker-induced oscillations overlaid, allowing direct comparison of frequencies. **c)** Histogram of light-induced oscillation frequencies for each mouse. Black line represents mean of all histograms. **d)** Mean frequency for each mouse, plotted against the length of the light stimulation. **e)** and **f)** Same as **c** and **d** but for whisker-induced oscillations.

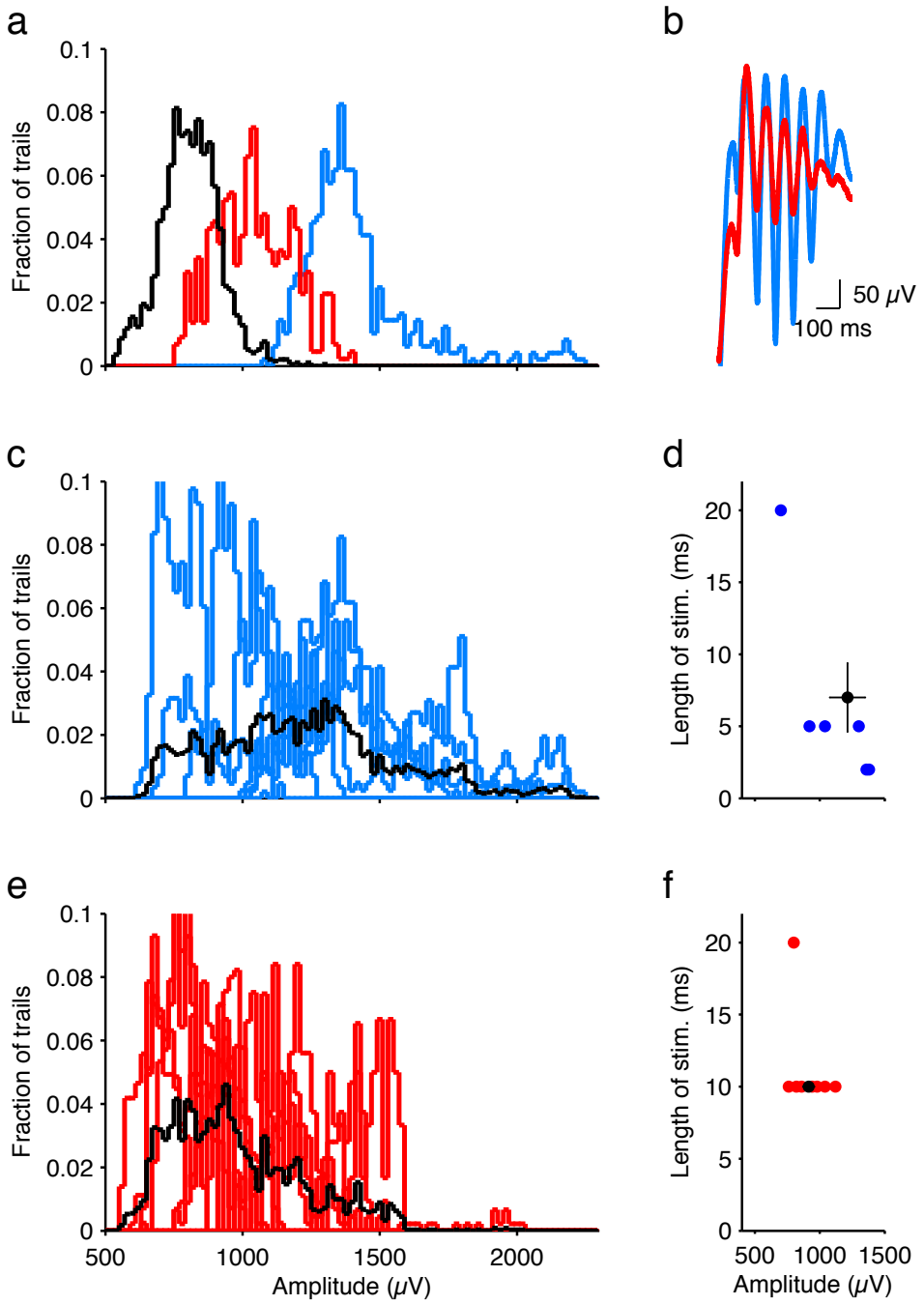

Fig 4.10 Oscillations induced by light have a greater amplitude than oscillations induced by whisker stimulation a) Histogram of amplitudes for each light- (blue) or whisker- (red) induced oscillation from the example mouse. Black line is from the control recordings. **b)** Mean light- and whisker-induced oscillations overlaid, allowing direct comparison of amplitudes. **c)** Histogram of light-induced oscillation amplitudes for each mouse. Black line represents mean of all histograms. **d)** Mean amplitude for each mouse, plotted against the length of the light stimulation. **e)** and **f)** Same as **c** and **d** but for whisker-induced oscillations.

For the same stimulus parameters the initial response to the whisker and light stimulations were variable for each animal. It is possible that the power of the oscillation following the stimulation correlated with the amplitude of the initial response in the same trial. For the example animal, this was not the case, neither for light-induced nor whisker-induced oscillations (r^2= 0.253 and 0.085 respectively; Fig 4.11 a,b). Across all animals in sessions using the same stimulus parameters, there was also no correlation between the initial response and the power of the 12.7 Hz oscillation from trial to trial (r^2= 0.059 and 0.006 respectively; Fig 4.11 c,d).

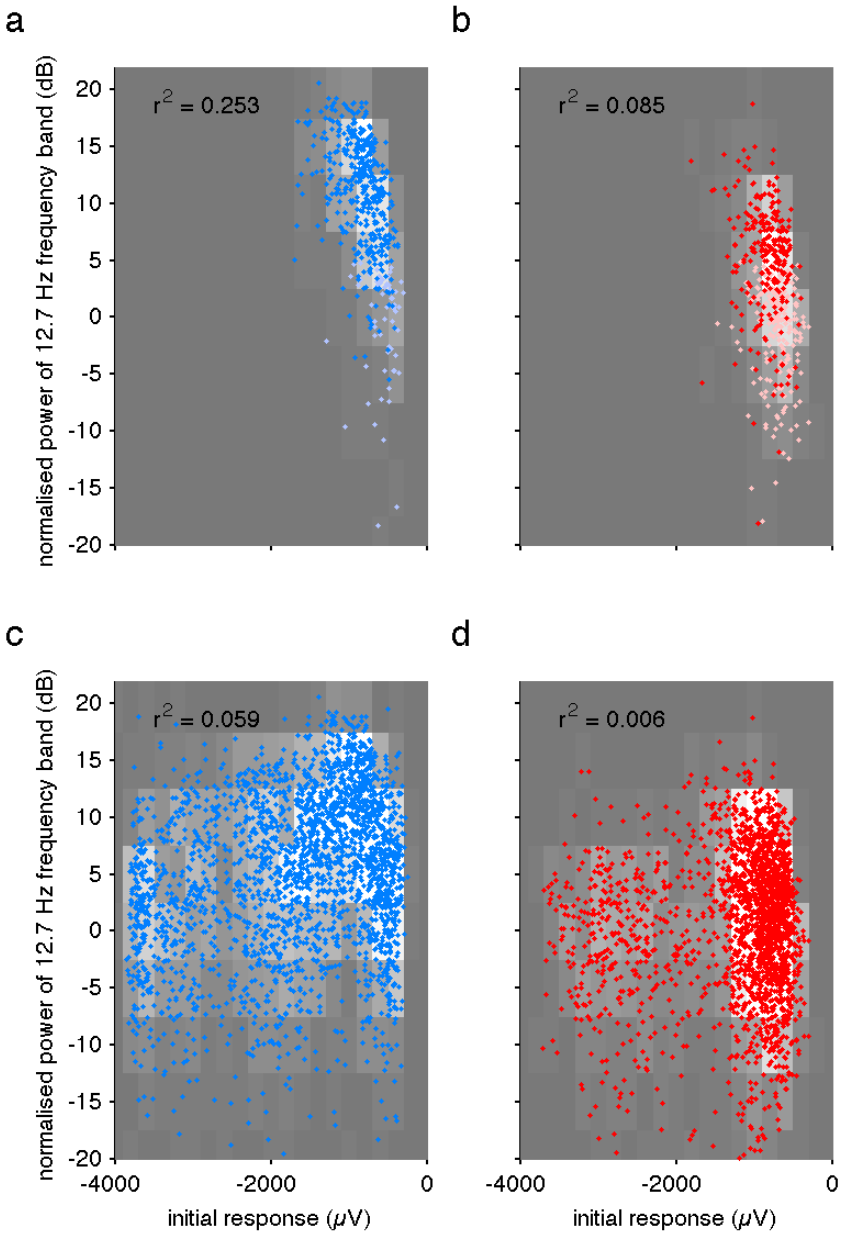

Fig 4.11 A larger initial response does not predict the presence of an oscillation. a) Correlation between the initial response to light stimulation and the power of the light-induced oscillation in the example mouse (n = 485; r^2 = 0.253; n.s.) **b)** Correlation between initial response to whisker deflection and the power of the whisker-induced oscillation in the example mouse (n = 439; r^2 = 0.085; n.s.). **c)** Correlation of initial response to oscillation power across all mice for whisker stimulation trials (n = 2479; n.s.). **d)** Correlation of initial response to oscillation power across all mice for all whisker stimulation trials (n = 2200; n.s.).

4.3.4 Layer-specific oscillation parameters recorded by spiking activity

In the preceding sections I used the LFP data as a useful measurement of the average cortical activity. In order to study how the frequency and timing of the oscillations vary between layers, und thus to potentially determine where the oscillations originate, the local, high pass-filtered extracellular signal revealing the spiking activity was examined (Fig 4.12c).

The extracellular data, sampled at 25 kHz over 16 channels in six mice was filtered between 300 Hz and 5 kHz. Of the mice described in the previous section pertaining to the LFP data, only the mice were included (mice 5-10), for which both whisker stimulation and light stimulation trials were recorded. As for the previous section, only one session with a defined set of stimulation parameters was analysed for each mouse, indicated with an asterisk in Fig 4.7. For each animal, the channels in which no spiking data could be extracted were removed from the analysis.

For mouse 10, extracts of the filtered data taken 100-1100 ms following each light stimulation were overlaid (Fig 4.12a). An increase in spiking activity was observed in the first 600 ms following the stimulation. Due to the high amount of activity in the majority of trials in this section of recording, the individual spikes were very difficult to isolate. An envelope of the data was therefore used to capture the activity. This dispensed with the need for threshold detection of spikes or spike sorting. For each mouse the filtered data was then low-pass filtered and re-sampled at 3 kHz (the same sampling rate as the LFP data), filtered again with a moving window of 20 data points, and the absolute value taken (Fig 4.12b). Finally using the phase information generated from taking the FFT of the re-sampled data, the oscillations were phase-aligned, resulting in a clear oscillation observable in the mean trace in specific channels (Fig 4.12c).

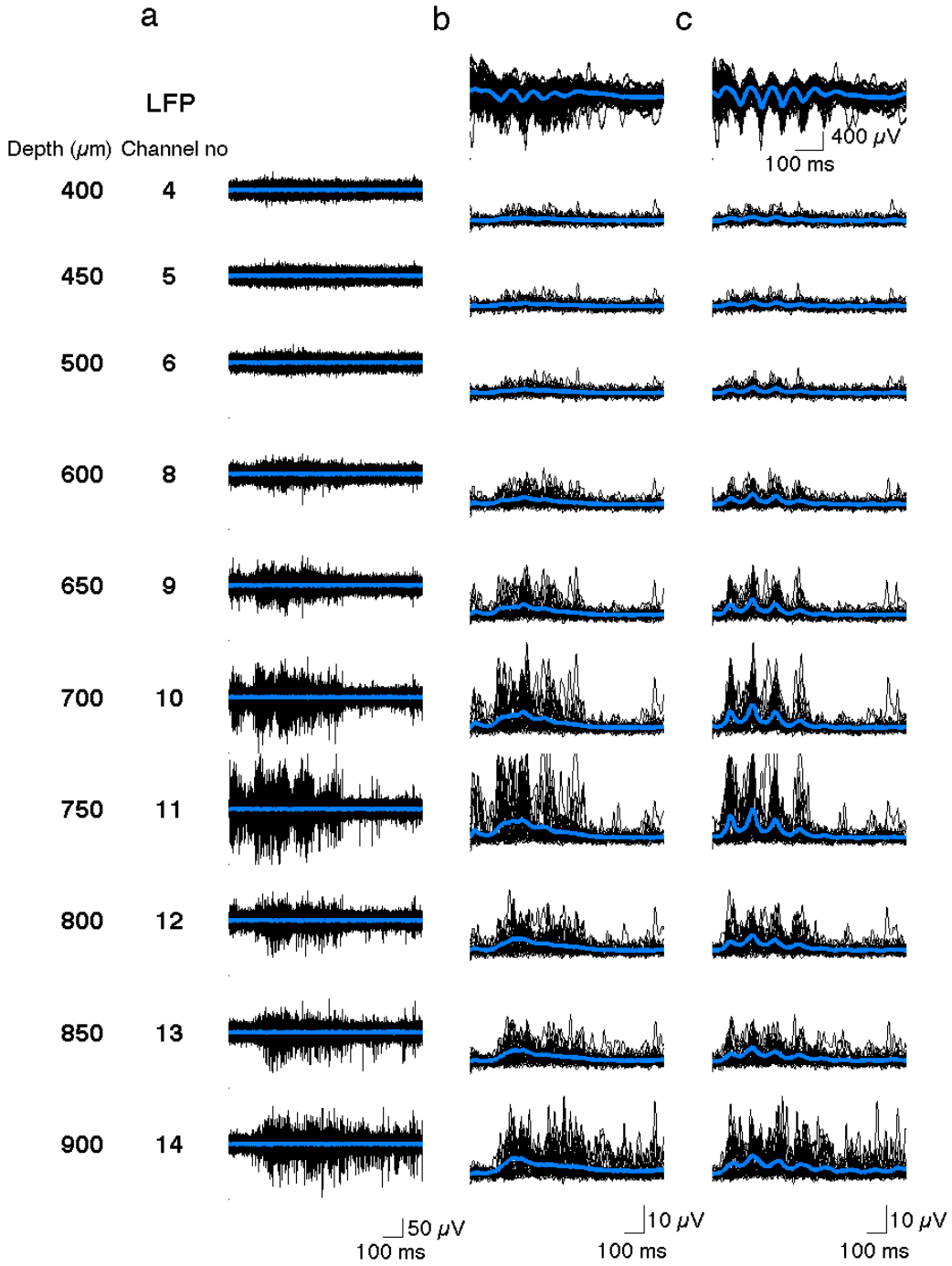

Fig 4.12 Extracellular spiking data following light stimulation of ChR2 expressing neurons. a) Extracellular recordings from mouse 10 from 10 channels of a 16-channel silicon probe, recorded at 24.4 kHz and filtered at 300-5000 Hz. The 50 light stimulation trials displayed (black) and the mean (blue) were extracted 100-1100 ms following ChR2 stimulation. **b)** For later analysis**,** data from **a** was low pass filtered, re-sampled at 3 kHz and converted into absolute value. **c)** Data from **b** was phase-aligned to show oscillations on several channels. The LFP trace from the same recordings is shown in the top panel.

To determine whether or not a trial contained an oscillation, a similar method was used to that described in section 4.2.1. The FFT was taken of the period of processed recording 100-900 ms following all light or all whisker stimulations for a session across all channels individually (Fig 4.13a). An FFT was also taken of the control recording 2000-2800 ms post stimulation, by which time all traces of the oscillatory activity had long subsided (black line; Fig 4.13a). The maximum of the difference between the control and stimulation FFT gave a peak at the dominant frequency and for this frequency a power threshold was set for each channel, based on the control recordings, above which trials were considered to contain an oscillation (Fig 4.13b). In the example in the figure (from mouse 10) channels 8 - 13 show a high proportion of oscillation-containing trials for both light and whisker stimulations.

For each of the six mice, the proportion of light- and whisker-induced oscillations were determined for each channel (Fig 4.14). In both mice 8 and 9 there was a higher proportion of trials containing light-induced oscillations in the central channels than in the most superficial or deepest layers. For mice 7 and 5, this effect was shifted towards the more superficial channels.

While it is clear that for channels in which very few spikes are observed, there is a low probability of an oscillation being detected, a high spiking rate does not necessarily lead to a high proportion of oscillation-containing trials. For mouse 10, the highest spiking rate was observed in channel 14 (Fig 4.12), while the proportion of oscillation-containing trials for this channel was lower than for more superficial channels (10-11) in which fewer spikes were recorded.

The frequency of the oscillations recorded varied across channels, with the mean for each channel ranging between 10 and 14 Hz. The channels were divided into deep (channels 9-16) and superficial (channels 1-8). For mice 5, 6 8 and 9, there was a significant difference between the frequencies of the deep and superficial, light- and whisker- induced oscillations (Fig 4.15b; $n = 8$ for each mouse, $p < 0.05$, $R = 13,5,4$ and 7 respectively, one-way ANOVA with Turkey-Kramer corrections). Across all mice in both deep and superficial channels the frequency

of the light induced oscillations was higher (Fig 4.15b; n = 48, $p < 0.001$, F = 13, one-way ANOVA with Turkey-Kramer corrections).

In order to determine the origin of the oscillation with respect to the layers of the cortex, the delay until the onset of the oscillation following the stimulation was also investigated across channels. The phase of each oscillation from each oscillation-containing trial was computed from the FFT. This was the phase relating to the dominant frequency for that trial. This was then converted individually into time for each trial for each channel, based on the dominant frequency of the oscillation for that individual trial. The cosine function was considered to have a delay of 0, and depending on the phase computed, the delay was assigned a value between 0 and the period of the oscillation (~80 ms).

For mice 10, 8, 7 and 6 there was significant difference between the light- and whisker- induced oscillations in the superficial (channels 1-8) and deep channels of (channels 9-16; Fig 4.16b; n = 8, F = 11, 67, 3 and 7 respectively, $p < 0.05$, one-way ANOVA with Turkey-Kramer corrections). Across the population of 6 mice the delay was shorter for the light-induced oscillations in the deep layers (L5-6) than either type of oscillations in the superficial layers and the whisker-induced in the deep layers. Therefore, overall the light-induced oscillations appeared significantly earlier to the deeper layers (Fig 4.16d; n = 48, $p < 0.001$, F = 13 one-way ANOVA with Turkey-Kramer corrections).

Thus the oscillations could be monitored through the different layers using the spiking data. Both light- and whisker-induced oscillations were found to be more prominent in the superficial and middle layers (L2-4) and have a higher frequency. While the two types of oscillations were found to be very similar, the light-induced oscillations showed a higher frequency and arrived earlier in the deeper layers than the whisker-induced oscillations. They were also present in a greater number of trials.

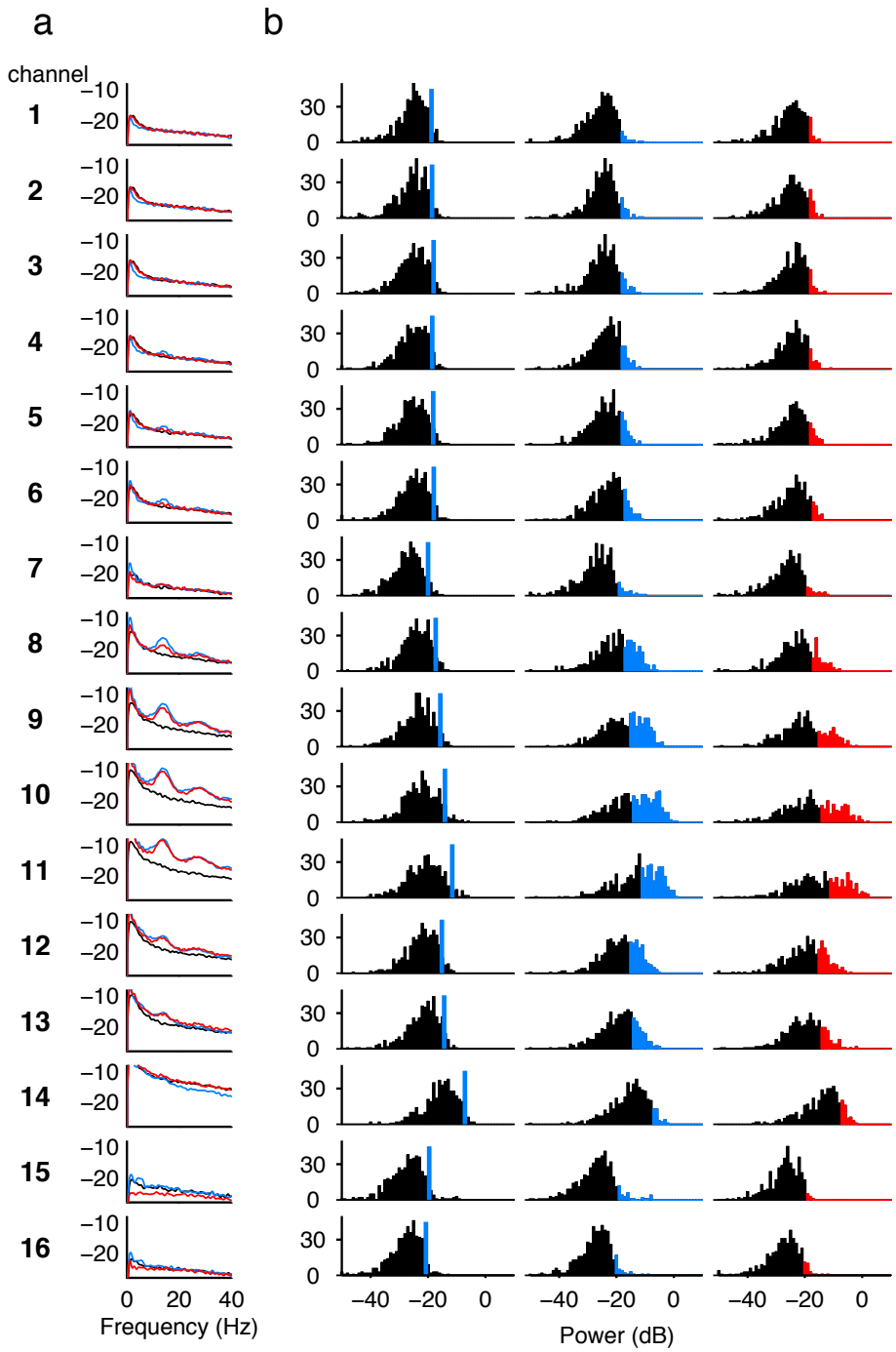

Fig 4.13 Oscillations were identified by a distinctive peak in the FFT. a) The mean FFT for light stimulation trials (blue), whisker stimulation (red) and control recordings (black) was plotted for all channels recorded from mouse 10 (same raw data as in Figure 10c). **b)** Histogram of the power of each trial at the frequency identified by the peak in the FFT for control recordings (left panel) light stimulation trials (middle panel) and whisker stimulation trials (right panel). The noise threshold generated by control recordings (blue line; left panel) was used to identify oscillation-containing trials in light (blue) and whisker (red) stimulation trials.

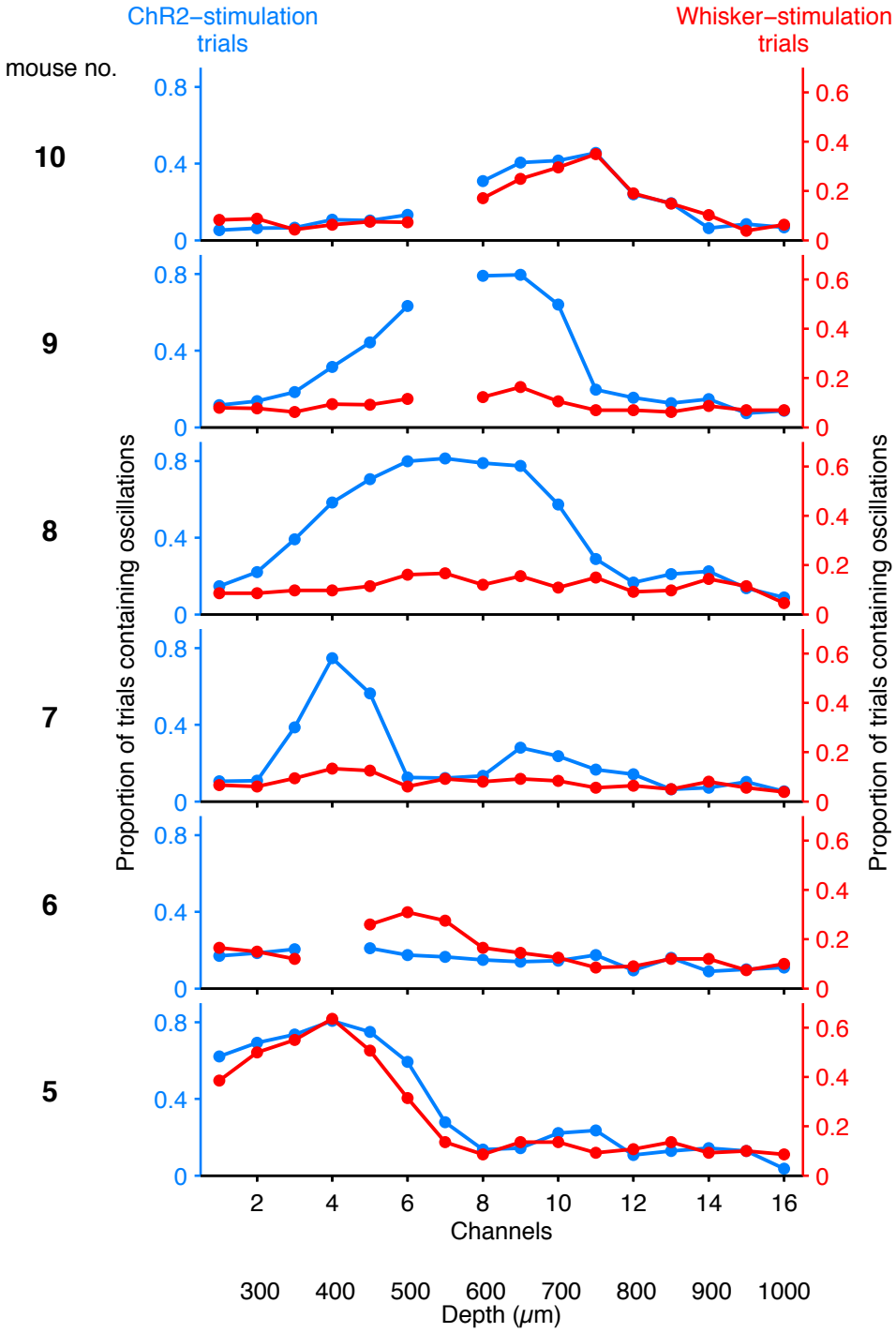

Fig 4.14 Oscillations were identified in specific cortical layers. a) Proportion of trials, which contain oscillations following either light (blue) or whisker (red) stimulation for each channel for 6 mice (mouse numbers refer to mice identified in previous figures of this chapter). Faulty channels were removed from the analysis.

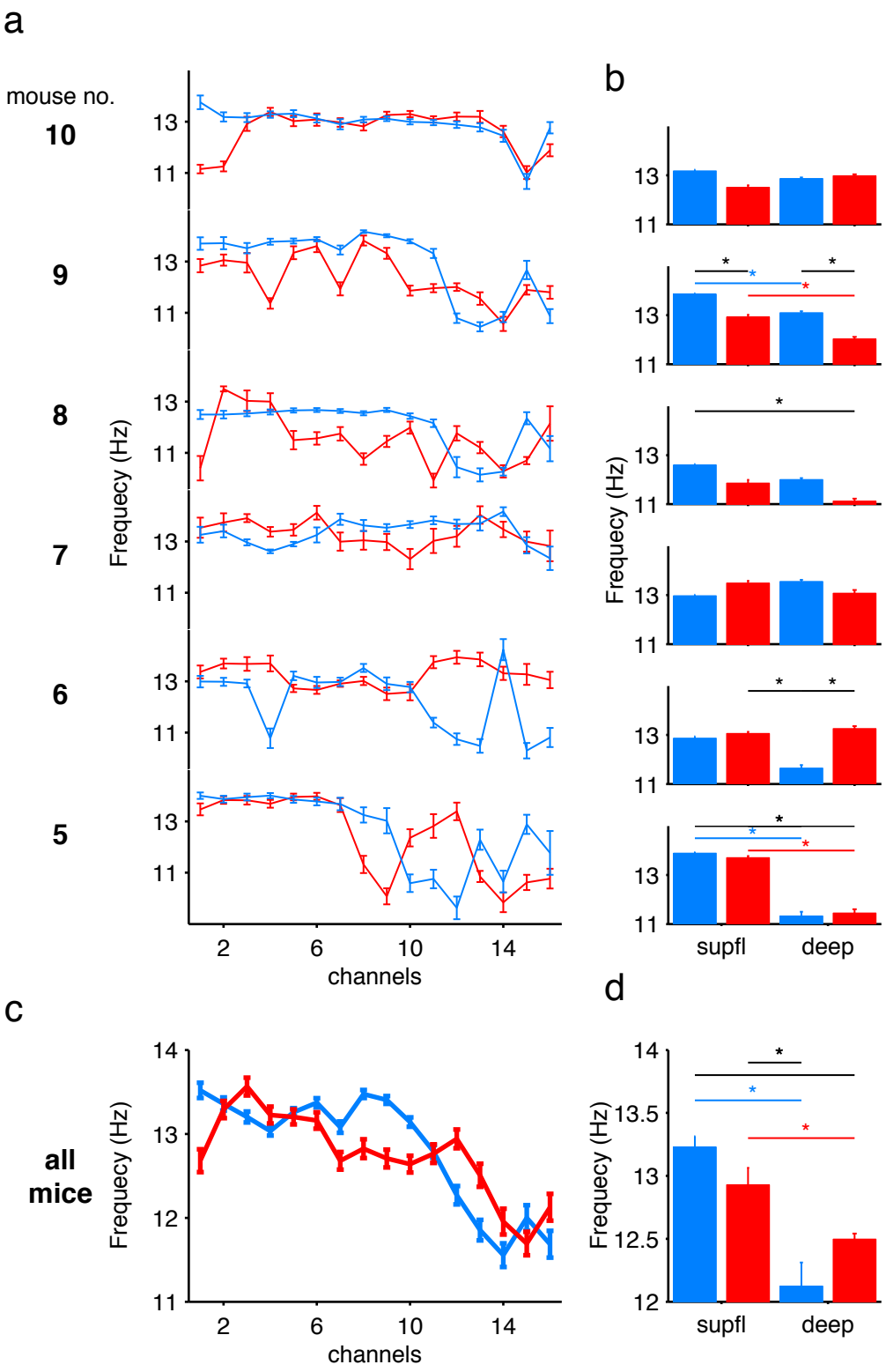
a
mouse no.
10
9
8
7
6
5
Frequecy (Hz)
channels
b
supfl
deep
c
all mice
d

Fig 4.15

Fig 4.15 Oscillations in deeper cortical layers have a lower frequency than in more superficial layers. a) Frequency of the oscillation for only oscillation-containing trials for trials involving light (blue) or whisker (red) stimulation. **b)** Mean frequency for oscillation-containing trials with either light or whisker stimulation over all superficial (1-8; supfl) and deep (9-16) channels for each mouse. Superficial and deep trials for each mouse were compared and indicated with an asterisk when found to be significantly different ($n = 8$, $p < 0.05$, one-way ANOVA with Turkey-Kramer corrections). The difference between whisker and light trials (both superficial and deep) was also tested for significance and indicated with an asterisk. **c)** Mean Frequency over all oscillation-containing trials in all 6 mice. **d)** Mean frequency across all superficial and deep channels in all mice. In both light and whisker stimulation trials oscillations in deeper channels were of a lower frequency than in the superficial channels ($n = 48$, $p < 0.001$, one-way ANOVA with Turkey-Kramer corrections).

Fig 4.16 Light-activated oscillations arrive more rapidly in deeper cortical layers than in more superficial layers. a) Time taken from the onset of stimulation to the beginning of both the light-stimulated (blue) or whisker-stimulated (red) oscillations in each channel of the probe. **b)** Mean delay for oscillations from either light or whisker stimulation over all superficial (1-8; supfl) and deep (9-16) channels for each mouse. Superficial and deep trials for each mouse were compared and indicated with an asterisk when found to be significantly different $n = 8$, $p < 0.05$, one-way ANOVA with Turkey-Kramer corrections). The difference between whisker and light trials (both superficial and deep) was also tested for significance and indicated with an asterisk. c) Mean delay over all oscillation-containing trials in all 6 mice. d) Mean delay across all superficial and deep channels in all mice. In both light and whisker stimulation trials oscillations in deeper channels were detected earlier than in the superficial channels $n = 48$, $p < 0.001$, one-way ANOVA with Turkey-Kramer corrections).

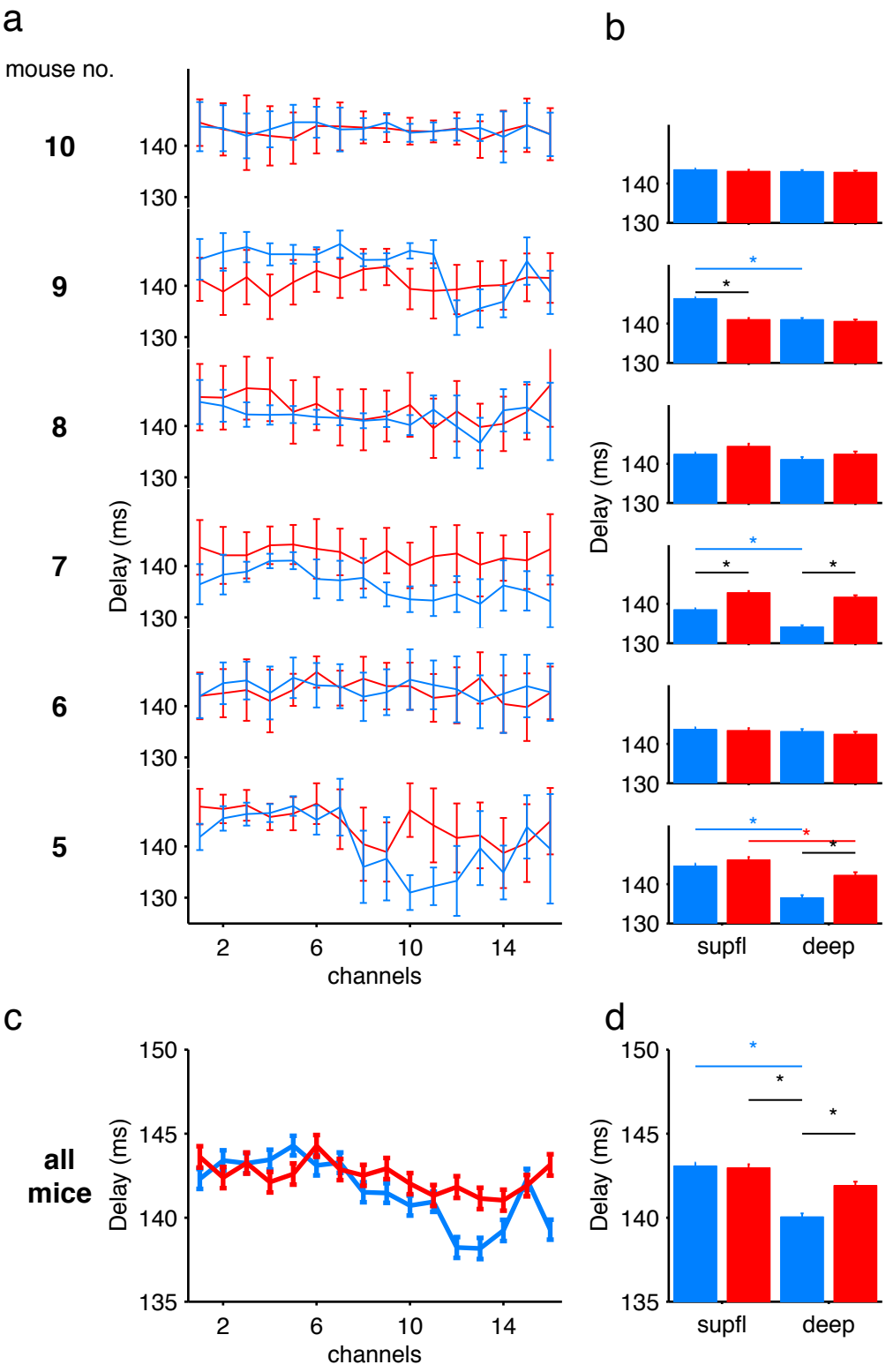
a
mouse no.
10
9
8
7
6
5
Delay (ms)
140
130
2
6
10
14
channels
b
Delay (ms)
supfl
deep
c
all mice
150
145
140
135
Delay (ms)
channels
d
Delay (ms)
supfl
deep

Fig 4.16

4.3.5 Thalamic inactivation eliminates light-induced oscillations

After establishing the presence of both a neuronal response to a whisker deflection and a ChR2-mediated, light-induced 12 Hz oscillation (see Section 4.1), the possible thalamic involvement of these oscillations was examined. For this the thalamus was inactivated by the slow injection of 10 μM TTX or 26 μM muscimol into the VPM of the thalamus in small 20 nl portions with a Nanoinject (see Section 2.8 of Materials and Methods for details of VPM targeting). Included in the solution containing the drug was either 2.5 % dextran or 0.375 % rhodamine, which lightly stained the area through which the pipette passed (due to mild leakage) and strongly stained the site of the injection either green or red respectively. This allowed the precise location of the injection site to be identified post experiment and facilitated the loading and injecting of the solution with the Nanoinject. The change in cortical activity was recorded with a silicon probe previously inserted into the superficial layers of the barrel cortex.

The path of both the silicon probe and the pipette of the Nanoinject, as well as the injection site in the VPM were imaged post experiment for each mouse (Fig 4.17). Animals were only included in the analysis if the drug injection could be clearly confirmed post-experiment to have accurately targeted the VPM.

After recording a baseline of 1618 ± 820 s for the light-induced oscillations and whisker response, TTX was infused into the thalamus (182 ± 70 nl; s.d.; n = 9 mice). An additional 2 mice were injected with muscimol (40 and 280 nl). Small injections (20 nl) were repeated until the whisker-evoked responses were abolished. The amount of drug necessary varied strongly, potentially depending on the precise location within the VPM.

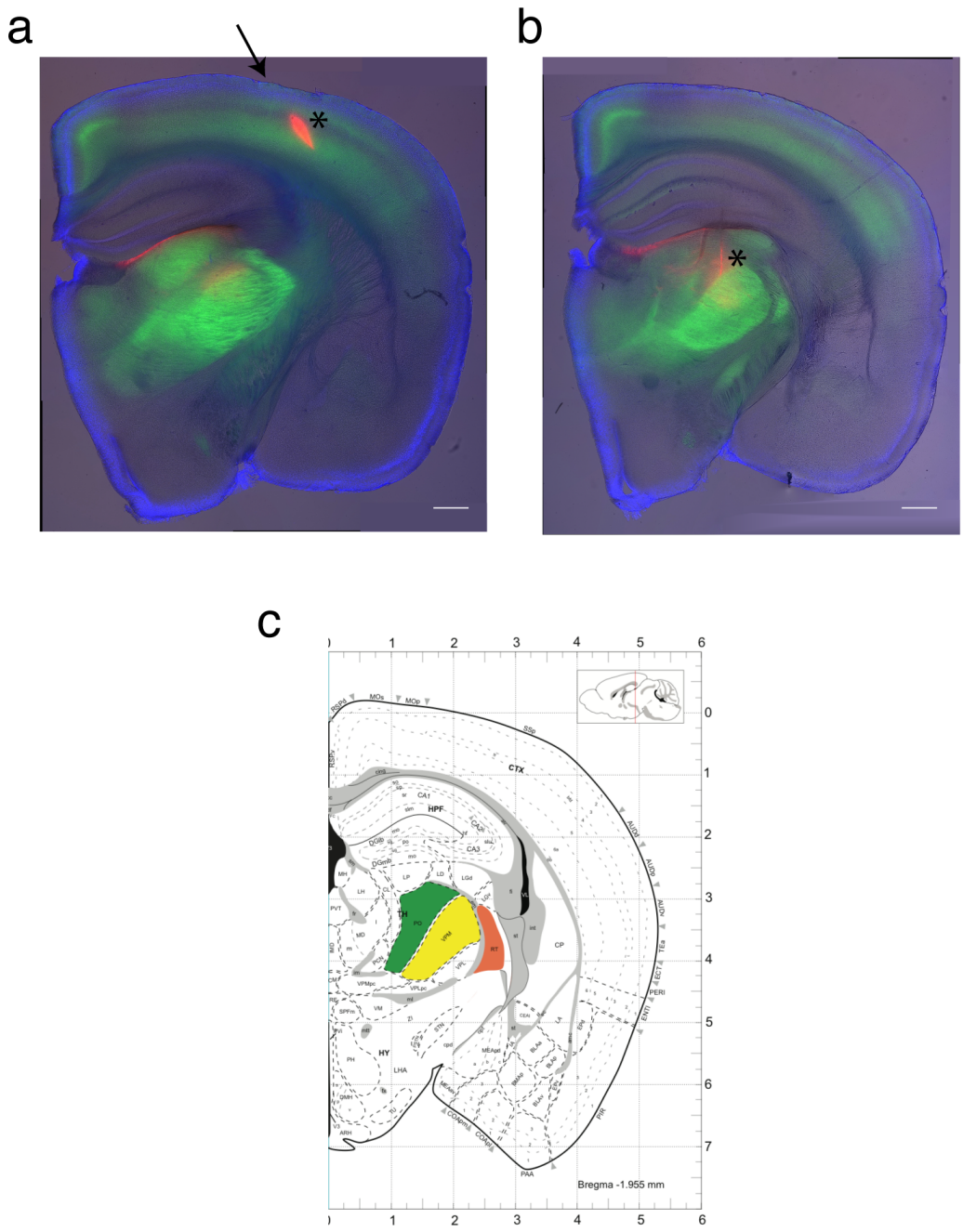

Fig 4.17 Coronal brain slices. a) 300 µM thick coronal slice from mouse taken from 2.2 mm posterior to bregma. Cortex, hippocampus and thalamus can all be clearly seen. Arrow indicates approximate position of silicon probe insertion, the path of which is shown by the red DiI dye (asterisk). Slices were imaged to show DAPI staining (blue), ChR2-YFP expressing neurons (green) and both DiI and rhodamine (red). **b)** Coronal slice taken 1.6 mm posterior to bregma, processed in an identical manner to slice in panel **a**. Asterisk indicates position of path of thalamic drug injection (red line). Scale bars are 0.5 mm.

As in the previous sections, whisker- and light-stimulation trials were interleaved. The whisker stimulation trials were used to measure the presence of thalamic activity and thus the success of the thalamic knockout. The amplitude of the LFP immediately following the whisker deflection was used to measure the whisker response. For both mouse 3 and 9, a clear decrease in the height of the LFP response immediately following whisker stimulation was observed several trials after the first drug injection (each trial was 4 sec long and is represented by a dot in Fig 4.18 a and b). The light stimulation trials were used to measure the light-induced oscillation. This oscillation was extracted from the power in the FFT of the 12 Hz frequency band, with the power from the control recordings of the same band subtracted for each trial. A decrease in the power of the 12 Hz oscillations was also observed following drug injection (panels c and d). The change with time of both the whisker response and oscillation power was filtered over a 20 trial window, making it easier to detect the transition by eye (Fig 4.18 panels e and f). A similar effect was seen in the filtered LFP responses over all trials for all mice except mouse 8 (Fig 4.19), which showed a sudden decrease in both oscillation power and whisker response before the drug injection most likely due to drug leakage from a broken pipette. Due to this lack of a stable baseline, mouse 8 was not included in the further analysis.

To precisely determine the time taken from the beginning of the drug injection to the point at which the whisker response decreased, each point from the whisker response values was filtered with a sliding window calculating the mean value for that point and the hundred trials following it (Fig 4.20a red line). The baseline whisker response (B; red dotted line) was defined as the mean of the hundred trials preceding the drug injection. The threshold (T), after which the response was considered to have decreased, was set as 1.96 standard deviations below the baseline. A decrease in response was defined when the average of the next 100 trials dropped below the threshold (time point indicated by the red dot for the example in Fig 4.20a).

The baseline (red) and final (black) whisker response in the LFP, each calculated over 100 trials, were plotted for each mouse (Fig 4.20b). Each mouse showed a

decrease in whisker response following drug injection, and this effect was significant across the population (Fig 4.20e; $n = 10$, $p < 0.0001$, t-test). As no obvious difference was observed between the inactivation of the thalamus with muscimol (only mouse 6 and 7) and TTX (all other mice), the data was pooled in this and all subsequent analysis.

The LFP power in the light stimulation trials of the 12 Hz oscillation across sessions was analysed in an identical manner as described above (blue lines and dot in Fig 4.20a). The initial oscillation power before the drug injection and final power for each mouse is shown in Fig 4.20c. Although the degree of suppression was variable, all mice showed a significant decrease in oscillation power (Fig 4.20f; $n = 10$, $p = 0.008$, paired t-test).

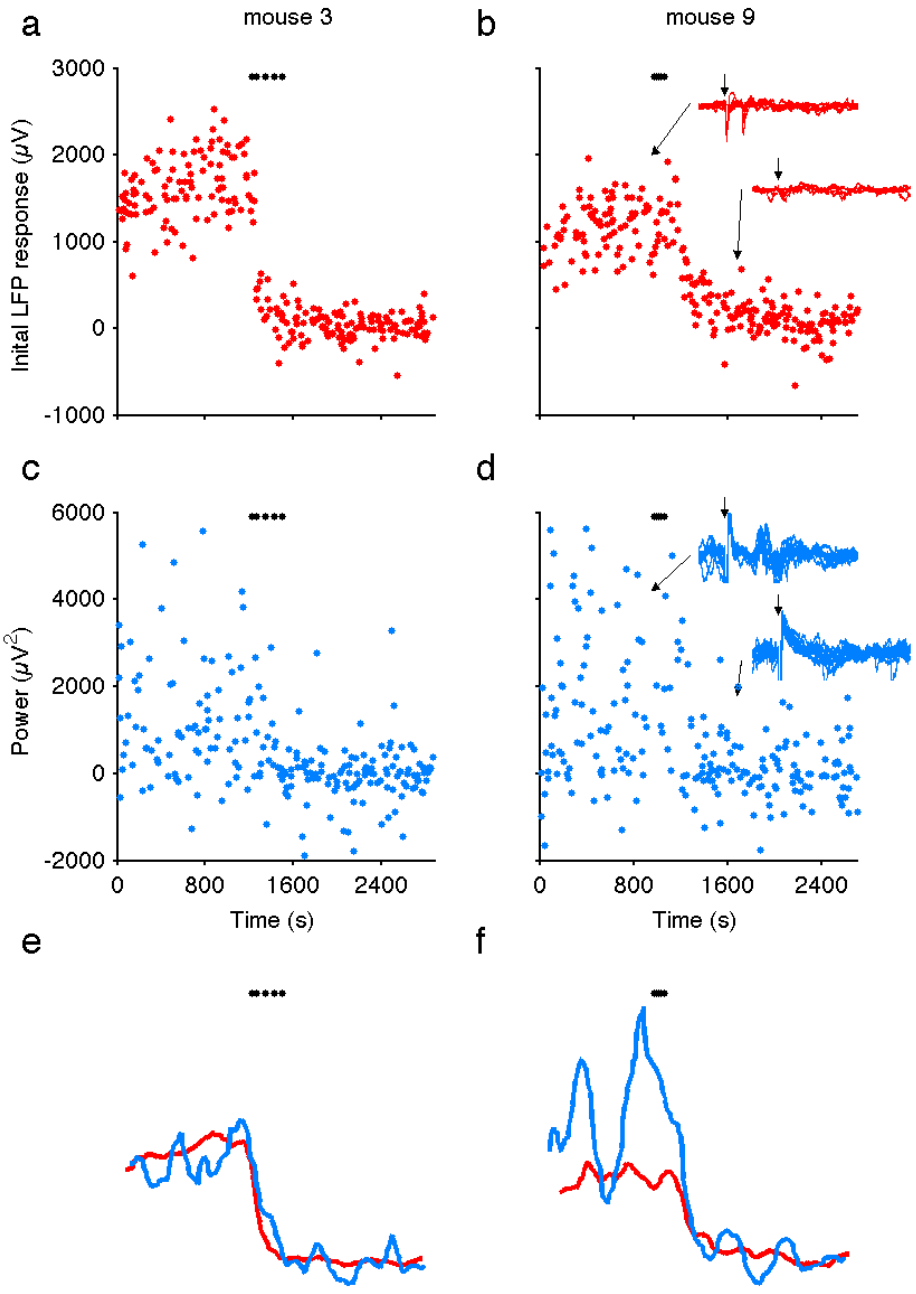

Fig 4.18 Injection of TTX or muscimol into the thalamus leads to a decrease in the whisker response and a decrease in the light-induced oscillation. a) Height of the LFP response to whisker stimulation across 720 4-second trials in mouse 3. Black dots indicate time of each TTX injection. **c)** Strength of 12 Hz oscillation induced by ChR2 stimulation for each trial. **e)** Filtered (20 trial window) responses from panels a and c, permitting detection of the transition from responsive (to whisker and light) to non-responsive (~ trial 310). b,d,f) Identical analysis to panels a, c and e for mouse 9. Transition point here occurs also at ~ trial 310. Inset: 10 sample traces from point in experiment indicated by arrow. Small arrow shows time of whisker or light stimulation.

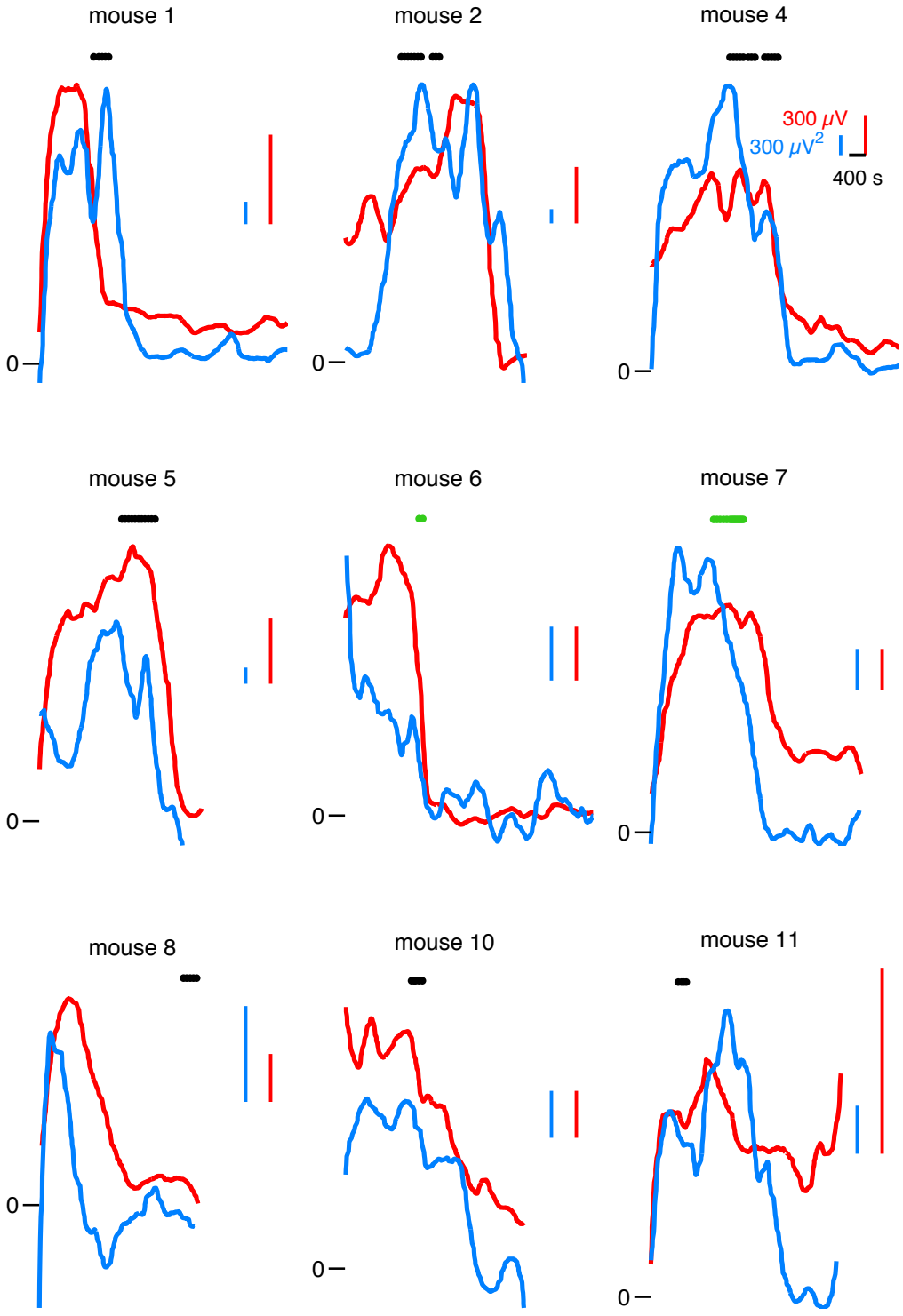

Fig 4.19 Further examples of thalamic inactivation. LFP responses for nine ChR2 positive mice (all remaining mice not included in Fig 4.2.2). The red line plots the height of the whisker LFP response over successive trials. The blue line plots the power of the light-induced oscillations in the LFP over all trials. Scale bars for each mouse are indicated in the corresponding colour. The time of drug injections are indicated by black (TTX) or green (muscimol) dots.

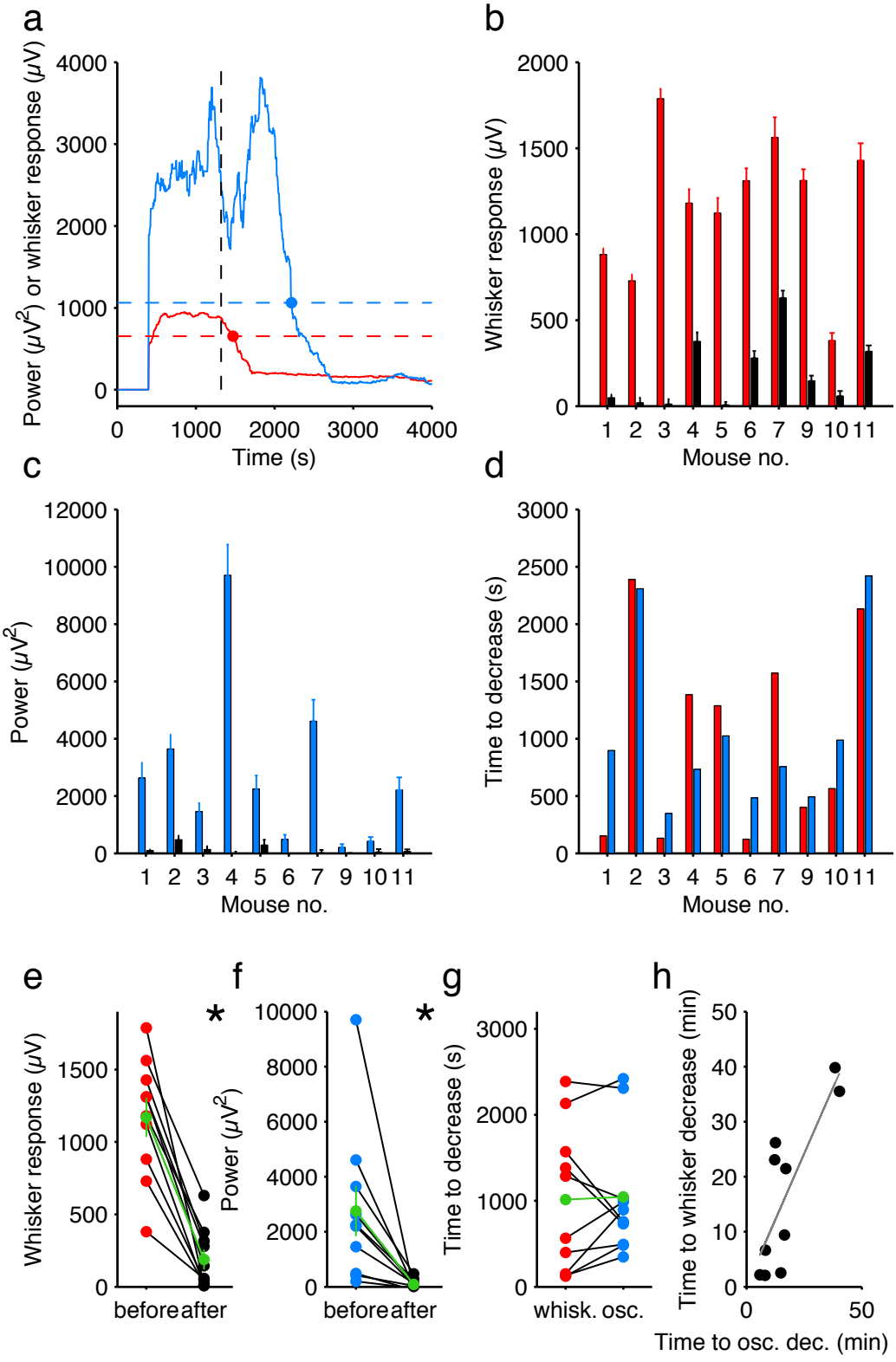
a
Power (μV²) or whisker response (μV)
4000
3000
2000
1000
0
0 1000 2000 3000 4000
Time (s)
b
Whisker response (μV)
2000
1500
1000
500
0
1 2 3 4 5 6 7 9 10 11
Mouse no.
c
Power (μV²)
12000
10000
8000
6000
4000
2000
0
1 2 3 4 5 6 7 9 10 11
Mouse no.
d
Time to decrease (s)
3000
2500
2000
1500
1000
500
0
1 2 3 4 5 6 7 9 10 11
Mouse no.
e
Whisker response (μV)
1500
1000
500
0
*
before after
f
Power (μV²)
10000
8000
6000
4000
2000
0
*
before after
g
Time to decrease (s)
3000
2000
1000
0
whisk. osc.
h
Time to whisker decrease (min)
50
40
30
20
10
0
0 50
Time to osc. dec. (min)

Fig 4.20

Fig 4.20 The time of decrease in light-induced oscillation is correlated with the elimination of the whisker response. a) Height of LFP whisker response (red) and power of light-induced oscillation (blue) for one mouse. Each point represents mean of the 100 following trials. Threshold to detect decrease from baseline for each is shown by dotted line in corresponding colour. Point at which value reaches threshold is indicated by a coloured dot. The trial number of the first drug injection is shown (black dotted line). **b)** Baseline LFP whisker response before drug injection (red) and in final 100 trials (black) for each animal. **c)** Baseline LFP oscillation strength before drug injection (blue) and in final 100 trials (black) for each animal. **d)** Number of trials between time of drug injection and decrease in whisker response (green) and oscillation power (blue) for each mouse. **e)** Summary of panel **b** with mean across all mice (red). Injection of the drug reduces whisker response strength ($n = 10$, $p = 0.008$, t-test). **f)** Summary of panel **c** with mean across all mice (red). Injection of the drug reduces oscillation strength ($n = 10$, $p < 0.0001$, t-test). **g)** Summary of panel **d** across all mice. There is no significant difference between the time taken from drug injection to decrease in either whisker response or oscillation power. **h)** Correlation between time of whisker response decrease and decrease in oscillation power across all animals ($r^2 = 0.66$, $p = 0.0024$).

The time taken from the time of injection to the decrease in whisker response or oscillation power is also variable across mice (Fig 4.20d). There is no significant difference between the time taken for the whisker response to decrease and the time taken for the oscillation to disappear (Fig 4.20g). This suggests that there is a correlation between the times for each decrease for each mouse, a result supported by the correlation plotted in Fig 4.20h ($r^2 = 0.66$, $p = 0.0024$).

The spiking data for each channel of the silicon probe confirms a decrease in both whisker response (Fig 4.21a) and 12 Hz oscillation power (panel b) across all superficial layers. The raw data, sampled at 25 kHz across channels 2-14, was filtered between 300 and 5000 Hz to detect spikes. It was then re-sampled at 3 kHz and further filtered with an envelope of 20 data points. This gave a filtered trace with the same sampling rate as the LFP, but was channel specific, permitting the decrease in responses and oscillations to be tracked across cortical layers.

Recordings from 8 mice were of sufficient quality for the spiking data to be analysed. Across mice there was no significant difference between channels of whisker response (Fig 4.22 a) or oscillation power (Fig 4.22 b). However, in agreement with the LFP analysis, a decrease in both whisker response and oscillation power was observed across all channels. The time taken to observe a decrease in either oscillation power or whisker response did not consistently vary across channels and there was no significant difference between the two (Fig 4.22 c), however across all animals, in the deeper layers the light-induced oscillation decreased before the whisker response (Fig 4.22d; $n = 8$, $p < 0.01$, t-test)

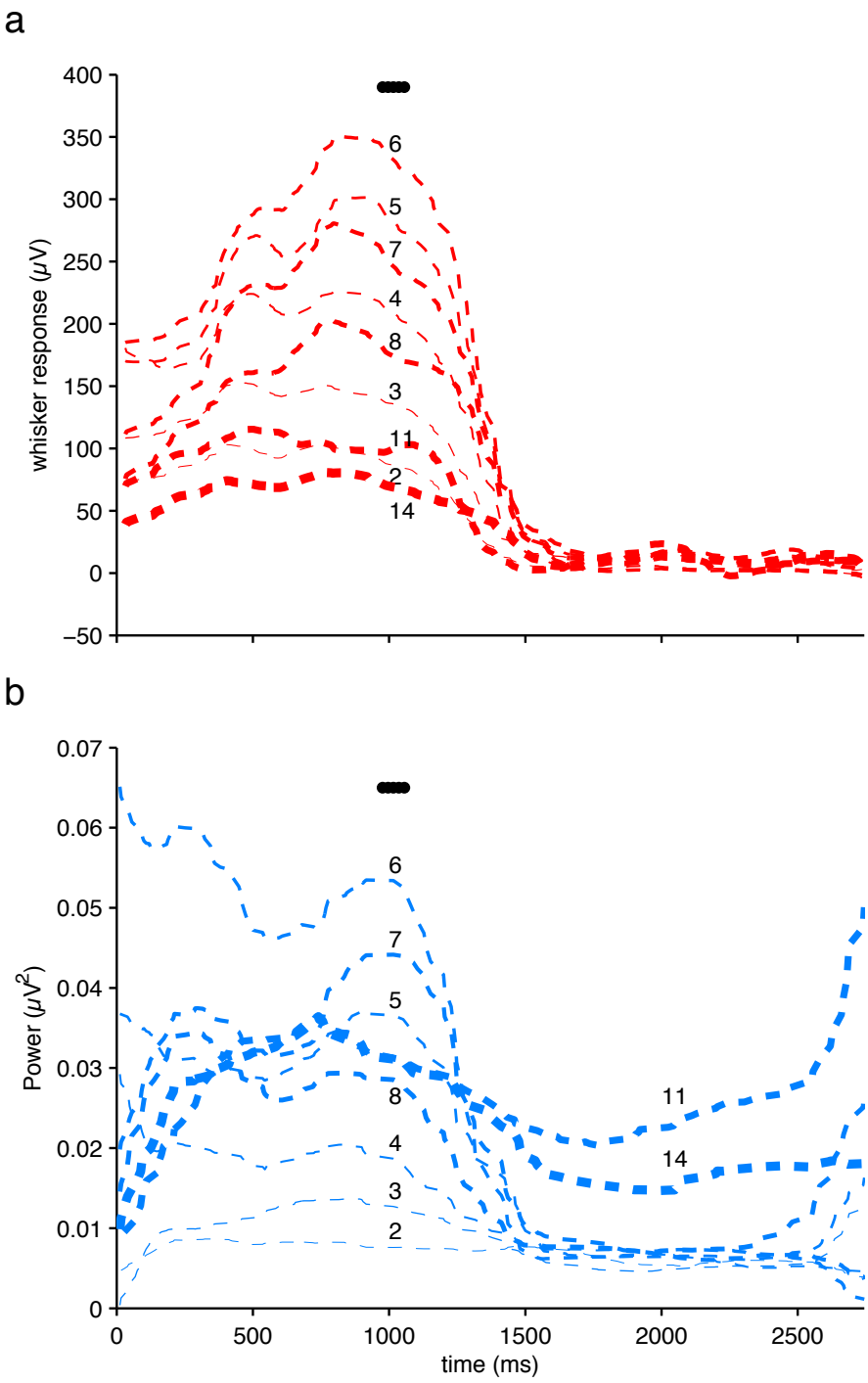

Fig 4.21 Spiking activity of whisker response and oscillations both decrease following drug injection. a) Height of filtered spiking response to whisker stimulation over time, across 13 channels of silicon probe inserted into superficial layers of the barrel in mouse 9. Black dots indicate time of each TTX injection. Thicker lines represent deeper channels. Data is filtered with a 20 trial window. **b)** Power of 12 Hz oscillation induced by ChR2 stimulation over time. Thicker lines represent deeper channels. Data is filtered with a 20 trial window.

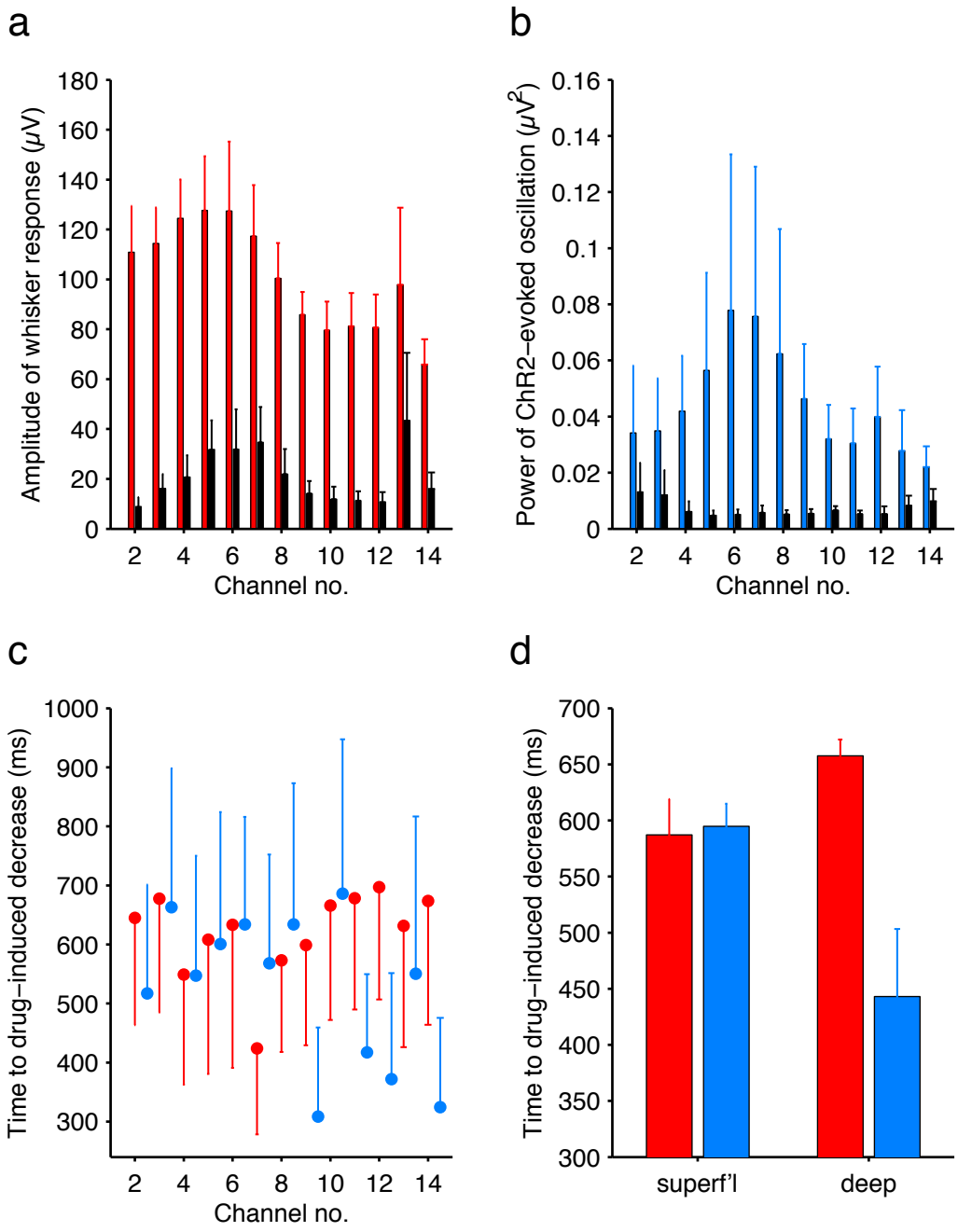

Fig 4.22 Decrease in spiking activity of whisker response and oscillations is correlated across all channels. a) Average baseline spiking whisker response before drug injection (red) and in final 100 trials (black) for all mice across 13 channels. **b)** Average baseline spiking oscillation power before drug injection (blue) and in final 100 trials (black) for each channel. **c)** Time between drug injection and decrease in whisker response (red) and oscillation strength (blue) for each channel. **d)** Mean of time between drug injection and decrease in whisker response for superficial and deep layers across all mice. In the deeper layers the light-induced oscillations disappear before the whisker response.

4.3.6 Oscillations in awake, behaving animals

Until recently, it was believed that sensory-evoked oscillations, arising from interactions between the thalamus and the thalamic reticular nucleus, were only to be found in the anesthetised state (Cotillon-Williams and Edeline, 2003; 2004). The long periods of inhibition necessary for the generation of the burst firing loop, were not thought to be present in the awake animal, due to the high sustained background activity. Two recent papers have demonstrated oscillations generated by micro-stimulation in the cortex of the awake rat and mouse (Venkatraman and Carmena, 2009; Halassa et al., 2011). While these oscillations were artificially induced rather than sensory-evoked, these studies demonstrated that the feedback mechanisms necessary for the propagation of such oscillations are present in the awake animal. In this study, I have investigated this finding by recording oscillations in the somatosensory cortex of awake, unstimulated mice and of mice performing a whisker-related behavioural task. In this case the oscillations were generated by a short 10 ms activation of several thousand putative pyramidal neurons across multiple layers of the barrel cortex and possibly axons from the thalamus, as described in section 4.2.2.

Oscillations were recorded with a 16-channel silicon extracellular electrode in awake animals. The animals were head-fixed via a small metal head-post adhered to their skull and placed on a metal wheel (25 cm diameter, 10 cm wide with crossed rungs every centimetre) with freedom to run backwards and forwards on the spot with very little resistance. Recordings were made both in animals not stimulated on the wheel, while they were alternating between running and sitting quietly, and in animals performing a behavioural task (See Chapter 5 for more details of the task). For the animals undergoing a behavioural task only correct rejection trials, in which the animal did not receive a whisker stimulation and did not lick, were included in the oscillation analysis. Both the licking and, to a lesser extent, the whisker stimulation caused a large electrical artefact which interfered with the recording of the oscillation.

Oscillations in an awake mouse can be observed immediately following the blue light stimulation (Fig 4.23a). These oscillations are confirmed by a peak in the power spectrum at ~15 Hz of the average fast Fourier transform (FFT) over all trials (Fig 4.23c). Oscillations were also observed in animals that were undergoing behavioural training.

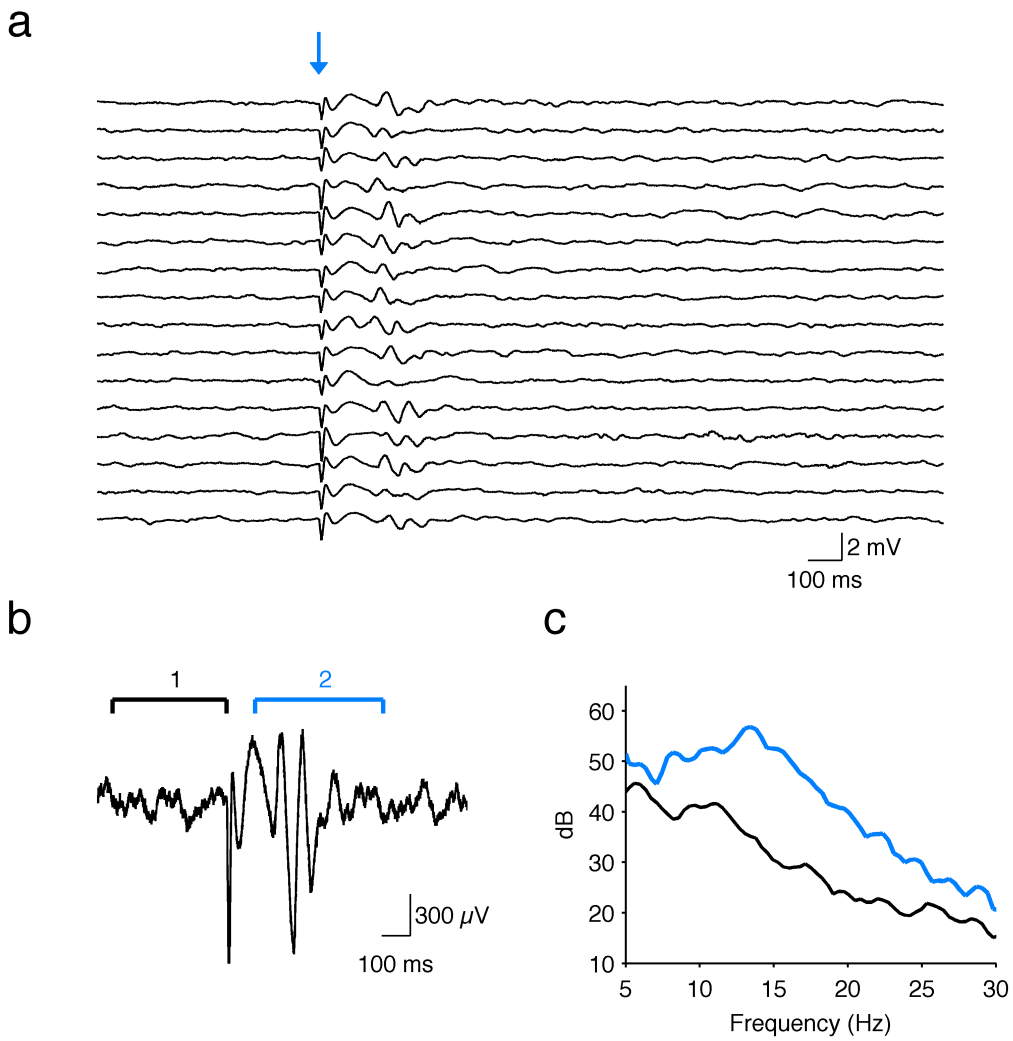

Fig 4.23 Optogenetically evoked oscillations of ~ 15 Hz frequency were recorded in an awake animal. a). Fifteen LFP traces from the barrel cortex (layer 4) of one mouse active on the wheel. Arrow indicate time of 10 ms whisker stimulation. **b)** A single LFP trace for one trial showing the segment prior to light stimulus (marked 1) and immediately after stimulus during the oscillation (marked 2). **c)** Average (n = 98) of fast Fourier transform (FFT) from period 1 (black) and period 2 (blue) shown in black.

Optogenetically-evoked oscillations were recorded in five ChR2 positive animals: four awake mice (mice 1-4), one anesthetised mouse (mouse 5) and one control mouse (mouse 6; Fig 4.24a). The distribution of oscillatory strength in the optimum frequency range for each animal for the period before (left panel) and immediately after (right panel) is plotted (Fig 4.24b) with the trials considered oscillatory highlighted in colour. Oscillatory activity was defined as being above noise level (>0.95 percentile), as described in Section 4.1. The peak frequency of the oscillations varied between animals from 5 to 15 Hz (Fig 4.24e).

Fig 4.24 Oscillations were induced in all ChR2-positive mice but not in the control mouse (following page). a) Average of ~30 traces from six mice; mouse 1 - awake, non-behaving, 2,3,4 - behaving, 5 - anesthetised, 6 - control, behaving. **b)** Left panel: PSTH of oscillation strength for each mouse over all trials during time period before light stimulation (control period). Frequency for each mouse shown in panel e. Right panel: PSTH of oscillation strength during time period immediately after light stimulation. Trials considered showing oscillations displayed in colour. Colours correspond to individual mice shown in panel **a. c)** Oscillation strength for each mouse over all trials during time period before light stimulation **d)** Initial ChR2 response for each mouse. **e)** Frequency of principal oscillation induced for each ChR2-positive mouse.

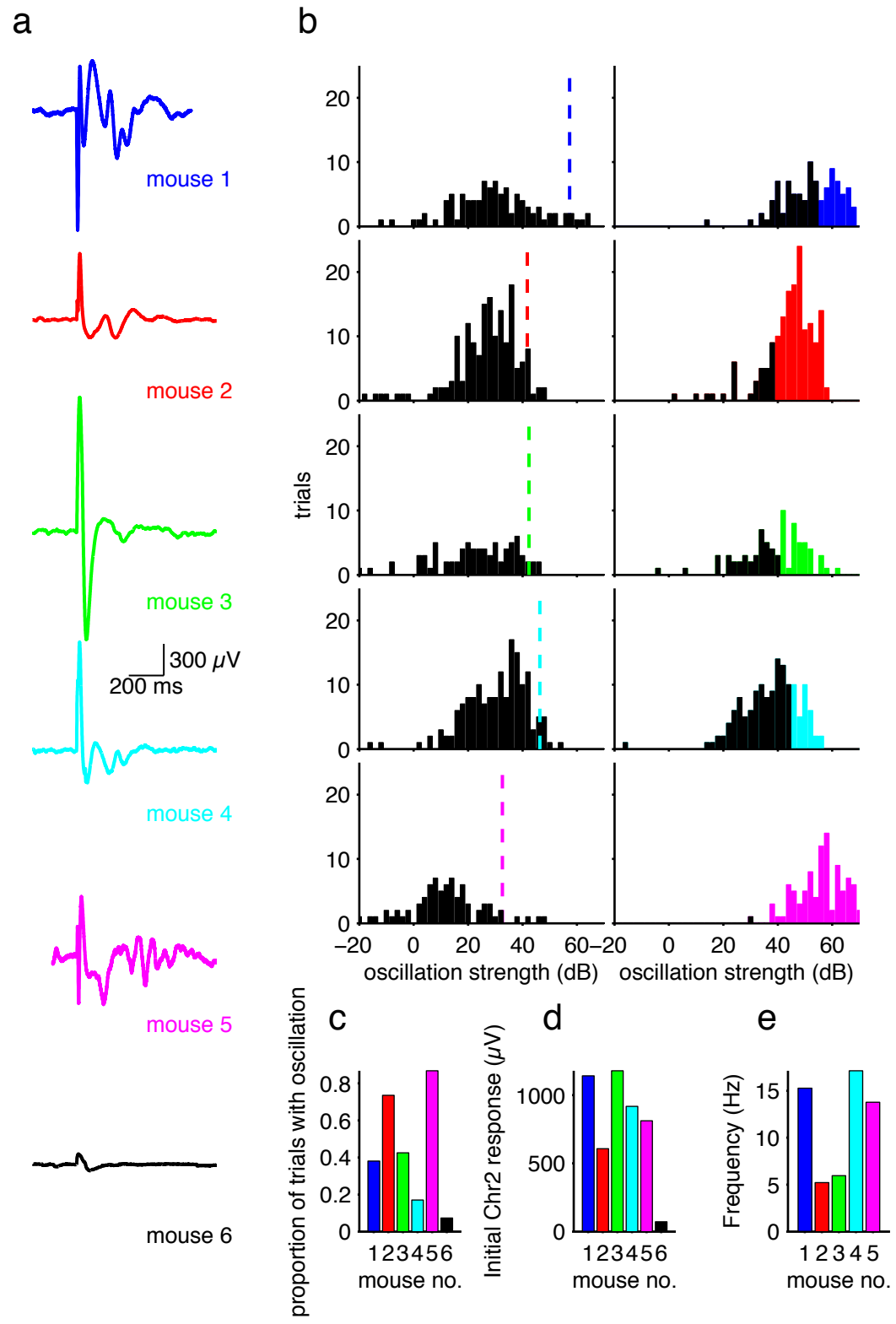
a
b
mouse 1
mouse 2
mouse 3
mouse 4
mouse 5
mouse 6
300 μV
200 ms
trials
oscillation strength (dB)
oscillation strength (dB)
c
d
e
proportion of trials with oscillation
Initial Chr2 response (μV)
Frequency (Hz)
mouse no.
mouse no.
mouse no.

Fig 4.24

4.4 Discussion

4.4.1 What factors determine whether or not an oscillation will take place?

Oscillations in the LFP and the spiking activity, lasting for many hundreds of milliseconds, could often be induced by both whisker deflection and optogenetic stimulation, but not on every trial. From Fig 4.11 it is clear that it is not the size of the initial response to the ChR2 activation or the size of the whisker response that determines whether or not an oscillation will follow. One possible explanation is that the probability of an oscillation forming is determined by the state of the brain prior to stimulation. If the brain is more or less active or engaged in a particular neural process, this could put the neurons in such a state that they are more readily able to be recruited for an oscillation. The oscillations are thought to be caused by strong excitation followed by hyperpolarisation followed by successive bursts of rebound spikes. If the neurons are already very active, they may not be able to be stimulated enough to cause them to hyperpolarise which would prevent the rebound spikes from occurring.

Across mice there was no significant difference in the rate of oscillations evoked with different durations and strengths of stimulus. Within mice, however, longer stimuli or stimuli with greater amplitude were more likely to induce oscillations. This is most likely due to recruitment of a greater number of neurons, due to deeper and longer penetration of the light.

4.4.2 Why do the light oscillations arrive at deeper layers first?

Cortico-thalamic input enters the cortex at several layers. From the VPM, it enters principally in L4, but also in L5a and L3. From the POM the signal enters the cortex in L5a and L1. Based on the layer depths given in Lefort *et al*. (Lefort et al., 2009) the lower boundaries of each layer are L1 - ~130; L2 - ~270; L3 - ~420; L4 - ~600; L5A - ~710; L5B - ~890; L6 - ~1150 μm in the mouse. The 16 channel extracellular multi-site electrode has a linear spacing of electrodes of 50 μm and is positioned such that the channels lie 100-900 μm below the cortical surface. It

is therefore most likely that the superficial channels 1-8 reported activity from layers 1-3 and the superficial parts of layer 4 whereas the deeper channels reported activity from layers 5 and 6 and the deeper parts of layer 4. It is therefore possible that input from the POM into L5a as well as input form the VPM into L4 and L5a contribute to the earlier arrival of the oscillations into the deeper layers. These oscillations could then travel to L2/3 via intra-barrel connections.

A study of laminar organisation in the rat auditory cortex measured the spread of activity across different layers from both evoked responses and spontaneous activity(Sakata and Harris, 2009). They found that evoked responses arrived first to layer 5/6 with a latency of ~10 ms and last to layer 2/3 with a latency of ~30 ms. My work draws similar conclusions, finding that the light-induced oscillations arrive first to the deeper layers. Both studies suggest a fast connection between the thalamus and the deeper cortical layers which challenges the classical view that input arrive first to layer 4 then spread up and down the cortical columns.

4.4.3 Why is there no difference in timing between the decrease in oscillations and whisker response

The whisker response, measured by the amplitude of the initial response in the LFP following whisker deflection, and the light-induced oscillation, measured by the power of the LFP in the ~12 Hz frequency band following light stimulation, disappeared at roughly the same time following drug injection as the whisker induced oscillations (Fig 4.20g). This indicates that the thalamic knockout was swift and precise, reducing the thalamic activity within a few trials (of 4 sec each) sufficiently to prevent the oscillations from propagating through the thalamus. In several cases it appears that the oscillations disappeared before the whisker response. It is highly likely that in these cases the injection site was positioned such that the areas involved in generating the oscillation were removed first, before all the whisker-related thalamus was affected, permitting some whisker signal to still pass through to the cortex while preventing oscillations from propagating. A thorough analysis of the injection site for each animal and its relation to the positions of the VPM, POM and RT would be necessary to confirm this hypothesis.

4.4.4 Oscillations in anesthetised and awake animals

Oscillations were recorded more consistently in the anesthetised animals than in the animals awake on the ball. This could be because the increased activity in awake animals was masking the oscillations and preventing their detection. Alternatively the background ongoing activity in the awake state could prevent the oscillations from forming. The oscillations were generally faster and lasted for a longer amount of time than in the awake animal. While the similarity of the frequency of the oscillations (~12 Hz) suggests that they may be related to whisking, which also has a similar frequency, this is unlikely to be the case, as the oscillations were recorded with more consistency in the anesthetised animal, in which whisking did not take place.

4.4.5 Functional relevance of oscillations

This work has found that oscillations generated by cortical ChR2 activation rely on the thalamus for transmission. This is in agreement with previous work which suggests that the oscillations are a result of interactions between the thalamus and reticular nucleus (Cotillon and Edeline, 2000). Despite the recurrent circuitry within the neocortex, cortical circuitry is not sufficient to generate and maintain the oscillations. Whisker-induced oscillations have a similar profile to those induced by cortical ChR2 activation. This suggests therefore that whisker-induced oscillations are also transmitted through the thalamus and result from thalamic-reticular interactions.

The functional relevance of both the whisker- and ChR2-induced oscillations recorded in this study has been a subject of debate for decades. There have been several conflicting hypothesis (see section 1.4.2). The results from this thesis support the hypothesis that the oscillations result from the interplay between RT neurons and thalamic relay neurons, due to their reliance upon the thalamus for transmission. As described previously in this work, this hypothesis is based upon burst firing leading to IPSPs in thalamic relay cells de-inactivating the I_T current resulting in a further burst of APs. This burst firing activates I_T in the RE cells, thus generating the next burst of the spindle wave. This sequence of bursts back

and forth recruits many of the neurons in both the relevant nucleus of the thalamus and the RE, essentially isolating this area of the brain for as long as the oscillation continues and preventing it from transmitting independent information to the cortex.

In order for the oscillation to take place, the IPSPs must be able to de-inactivate the I_T current without there being too much background excitation preventing the necessary hyperpolarization. The oscillations are therefore more likely to occur in the anesthetised state, as has been shown in this work, although they can occur in awake animals, under certain conditions. So far, it is not possible to determine exactly what conditions in the awake brain permit the oscillations to take place. A thorough study of the state of the brain before each stimulation, both leading to an oscillation or to no oscillation, would be necessary in order to determine the conditions required to generate an oscillation.

4.4.6 Small light responses recorded in control animals

In the awake recordings, a small response was recorded following light stimulation in the control animal. Although the response was far smaller than the response recorded in all the ChR2-positive animals, it represents a form of artefact produced by the stimulation. There are several possible origins for such an artefact: it is possible that the animal was able to see the blue light and the response recorded is a small visual response in the barrel cortex (Fig 3.11). The artefact could also be a photoelectric artefact picked up by the electrode; or it could be the result of the blue light travelling through the brain to reach the retina. Finally, it could be that the neurons themselves are sensitive to constant barrages of light and responded to the direct stimulation. The relatively small size of the response, however, means that in all the ChR2 animals the real signal is far stronger than any artefact and will render the artefact insignificant.

4.5 Conclusion

In this chapter I recorded the response of the barrel cortex to either a whisker deflection or the optogenetic stimulation of thousands of mostly pyramidal

neurons. The initial response to both was large, and this was often followed by strong bursts of spikes, leading to an oscillation in the LFP. These oscillations were characterised in both the LFP and spiking data. They were found to be variable across animals but to have an average frequency of ~ 12.7 Hz and occur in ~ 50% of trials but their presence was not determined by the size of the initial response to the stimulation. The light-induced oscillations arrived earlier in deeper channels and were of a greater amplitude than the whisker induced oscillations. After pharmacologically blocking activity in the thalamus, confirmed by the loss of the whisker response, the light-induced oscillation disappeared indicating that the thalamus is necessary for their propagation. Finally, optogenetic stimulation was able to generate oscillations in the awake animal.

Reproducible oscillations can be recorded in the anaesthetised and awake brain following large-scale perturbations. This suggests that the stimulated area of the brain may be forced to temporarily enter a different coding regime when undergoing a strong, unexpected stimulation. Without the oscillatory regime, the large sensory or mechanical interference could potentially damage the carefully balanced neuronal mechanisms in place during normal behaviour.

5 Can large-scale cortical perturbations affect behaviour?

5.1 Introduction

In the previous chapter it was shown that a 10 ms whisker deflection produced a strong initial response on the population level in the barrel cortex in every trial. In some trials this was followed by an oscillation, visible in both the spiking activity and the LFP, at a frequency of around 12 Hz and lasting approximately 800 ms. The neuronal response was recapitulated in transgenic mice expressing ChR2 under the Thy1 promoter with a 3-10 ms stimulation of ChR2-expressing neurons, producing a similar strong response followed by an oscillation. This oscillation was also present in awake animals and disappeared after silencing activity in the whisker-related thalamus.

The next question was to determine whether this strong oscillation-inducing stimulation would have an effect on behaviour. This was done by training mice in a whisker-based stimulation task and then stimulating the ChR2 expressing neurons while the animal was performing the task. In order to properly investigate the effect of this perturbation on behaviour, it was necessary to develop an appropriate behavioural task. This task had several important requirements. Firstly, the task had to be of sufficient difficulty that the perturbation could have a detrimental effect on behaviour, but simple enough for the animal to learn it in very few sessions. A task in which the animal could reach ~90% performance levels within several days would be ideal. This would give a large window (between 90% and 50%) in which decreases in the animal's performance could be detectable. Secondly, the stimulus had to be of short and very precise duration allowing accurate and reproducible temporal manipulation of the decision process.

For these reasons the task chosen was based loosely on that described in O'Connor *et al*. (O'connor et al., 2010) with important modifications. The task developed by O'Connor et al. measures the animal's ability to detect the position

of a vertical beam with its whiskers. The beam descends from above into one of two positions and is then raised again following the completion of the trial. Several aspects of this task make it suitable for our purpose. The displacement distance between the two pole positions can be manipulated to reach any required performance level. In the task the animals were able to distinguish between distances of as small as 0.95 mm. Furthermore the task was shown to be reliant upon the barrel cortex: after inactivation of the barrel cortex the performance of the animal returns to chance level (O'connor et al., 2010). The task of O'Connor, however, is not temporally precise enough for accurate temporal manipulation. The bar is lowered and the animal is given a time window (2 s) in which it is permitted to sense the bar and then respond. This means that it is not possible to determine when exactly the animal will decide in which position the bar is. It would thus be difficult to reproducibly introduce the cortical noise at a specific time before the whisker made contact with the vertical beam in order to interfere with this decision in a precise way.

5.2 Methods

5.2.1 Animals and Surgery

Fifteen adult (P40-P60) male Thy1-ChR2 mice (Jackson labs) were housed in a ventilated cabinet with reversed light cycle (Tecniplast, UK). All surgeries, experiments and training were carried out in the dark phase. For the initial surgery involving the implantation of the head-post, animals were anesthetised with 2-3% isoflurane and given an injection of Rimadyl analgesia (5% carprofen; 10 mg/kg body weight; Pfizer, UK). Topical EMLA cream, containing lidocaine (Express Chemist, UK) was administered to the head for local anaesthesia ten minutes before surgery begun. A posterior-anterior incision was made in the skin and the two sides separated to reveal the skull. The skull was carefully cleaned of tissue and the edges of the cut skin adhered to the skull with Vetbond (World Precision Instruments, UK). Small incisions were made in the skull with a scalpel blade (Interfocus Research Instruments, UK) to aid the adherence of the dental cement. A small (5 mm diameter, 2-5 mm high) plastic disk, cut from a 1 ml pipette tip

(Starlab, UK) was adhered with superglue over the left C3 barrel in the left barrel cortex (2 mm posterior, 3.5 mm lateral to Bregma). A custom designed stainless-steel head post with base 1 cm long and 0.5 mm wide (see Fig 5.1) was adhered with superglue over the right somatosensory cortex region of skull, as close to the midline as possible (centred 3 mm lateral, 3 mm caudal of Bregma). A very thin metal wire was twisted around the head post and the final 3 mm inserted into the skin posterior to the open skull. This would be later used to ground the head-post to the animal. After the superglue had completely dried (~15 min.) black Jet Denture Repair Acrylic (Lang Dental Manufacturing, USA) was applied to the entire area, covering the sides of the plastic disk and the top and sides of the head-post. The animals were given 3 days to recover before water restrictions and training were commenced.

Six mice (ms 1-6) underwent the behavioural task in its final form. Mice 1,2,4,5 and 6 were transgenic mouse expressing ChR2 under the Thy1 promoter (described in Section 4.2.2) and mouse 3 was a C57BL/6 wild-type control. Mice 1-3 had been previously trained on a similar task and therefore adapted easily to the new task, having been trained already to lick and run on the wheel. Mice 4-6 were naive mice, and their progress on this task from naivety to high levels of performance could thus be monitored.

5.2.2 Behavioural Setup

I modified the task of O'Connor described above (O'connor et al., 2010) to instead use a moving bar that moves in a superior-inferior direction and back again. For every trial the animal must decide to respond (lick) if the bar has moved and refrain from responding if it has not. A thin wooden beam (10 mm diameter) is attached to a piezo bender and positioned very close to the whisker pad, centred on C3. Upon movement of the piezo, the beam lowers for 100 ms, pressing against several whiskers before rising again. This allowed precise control over exactly when the animal was receiving the stimulus. Therefore the subsequent manipulation of behaviour in later sessions via the activation of ChR2 expressing cells with blue light could be precisely timed compared to the stimulus and decision.

For the complete behavioural experimental setup see photo in Fig 5.1. Animals were placed on a free-moving metal wheel (pet shop) with evenly spaced rungs. They were head-fixed with a custom made holder, into which the head-post was screwed. A 1 mm fibre optic coupled cable (Doric Lenses, Canada) was placed inside the plastic disk as close as possible to the skull, depending on the depth of the plastic disk and the position of the probe, this ranged from ~1 mm to 5 mm. External solution or water was place between the end of the fibre and the skull to improve transparency of the skull and allow the light to penetrate deeper into the cortex. A masking blue light emitted from a LED with low dome lens (RS Components, UK) was fixed behind the animal and positioned to hit and reflect off the apparatus in front of the animal, well within its range of vision.

A long wooden pole, fashioned from a single ended cotton bud (RS Components, UK) was glued to a piezo bender, the same as that used in section 4 and 5. The wood moved in a superior-inferior direction (and back again) and maximum displacement of the wooden rod was 12 mm. The bar was positioned so that the movement deflected several whiskers centred on C3. For punishment, a two-way normally closed solenoid valve (01540-01; Cole-Parmer, UK) attached to a custom-made pressure regulator was used to administer an air puff to the animal. The position of the air puff varied depending on the temerity of the animal and how severely its behaviour was affected by the air puff. For very audacious animals the air puff was administered close to the snout. For more timid animals the air puff was given to the body or even into the air near the animal. Reward in the form of a 10 μl drop of water with 10-12.5% sucrose was given through a lickometer (custom-made) driven by a NE-500 Application Syringe Pump (New Era Pump Systems, USA). Excess water was constantly removed by a peristaltic syringe pump (NE-500, Watson Marlow, UK). The lickometer also recorded the licks of the animal, via the closing of a circuit connected to a USB-1208FS Daq Module (Measurement computing, USA). Stimulus, rewards and punishment were all controlled by a combined system involving custom-written Matlab code controlling the Daq box and the Rx5 Pentusa system from Tucker Davis Technologies.

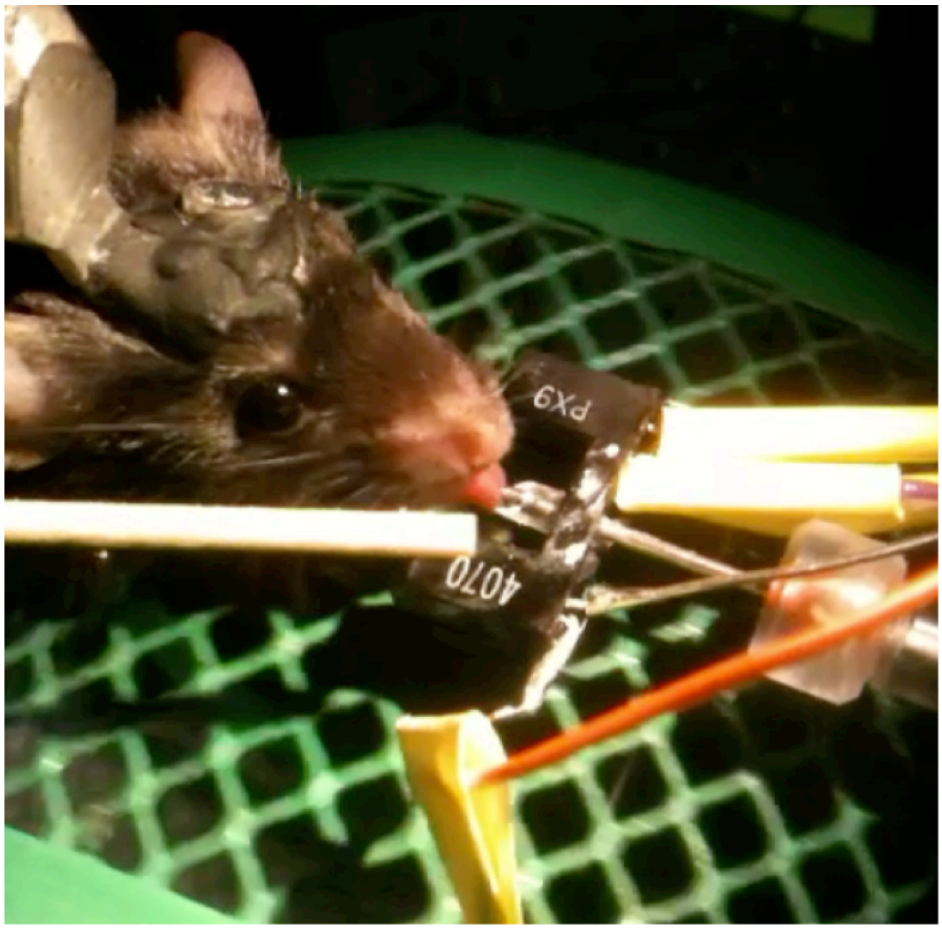

Fig 5.1 Behavioural experimental setup. The mouse is running on a metal wheel and receiving sugar-water reward. The lickometer, as well as dispensing the reward, detects the licks via circuit completion and infrared beam (black box). The mouse is head-fixed via a metal head post adhered to the skull directly with superglue and black dental cement. The whiskers are stimulated with a wooden beam (diameter 0.5 cm, length 20 cm) controlled by a piezo bender. The beam is manipulated in a vertical direction and presses down upon several whiskers from rows A and B.

5.2.3 Training and Behavioural paradigm

Access to unlimited water in their home cage was removed several days before training began and animals were restricted to 1-2 ml of water per day to improve responses to behavioural training and motivation. Typically, animals drink up to 3 ml of water per day when *ad lib*. Once training began, animals received all their water for the day during the training session from rewards in the task. On non-training days, animals were given 1.5-2 ml water at the usual time of training. If the animals did not consume at least 1 ml of water during the training session,

they were given access to "free" water in their box following training for 30 min. The weight of the animals was maintained between 80-90% of their natural weight before the water restriction began. Additional water was given if their weight fell below this level.

Training was divided into several stages. The specific criteria for advancement to the next stage is detailed below for each phase.

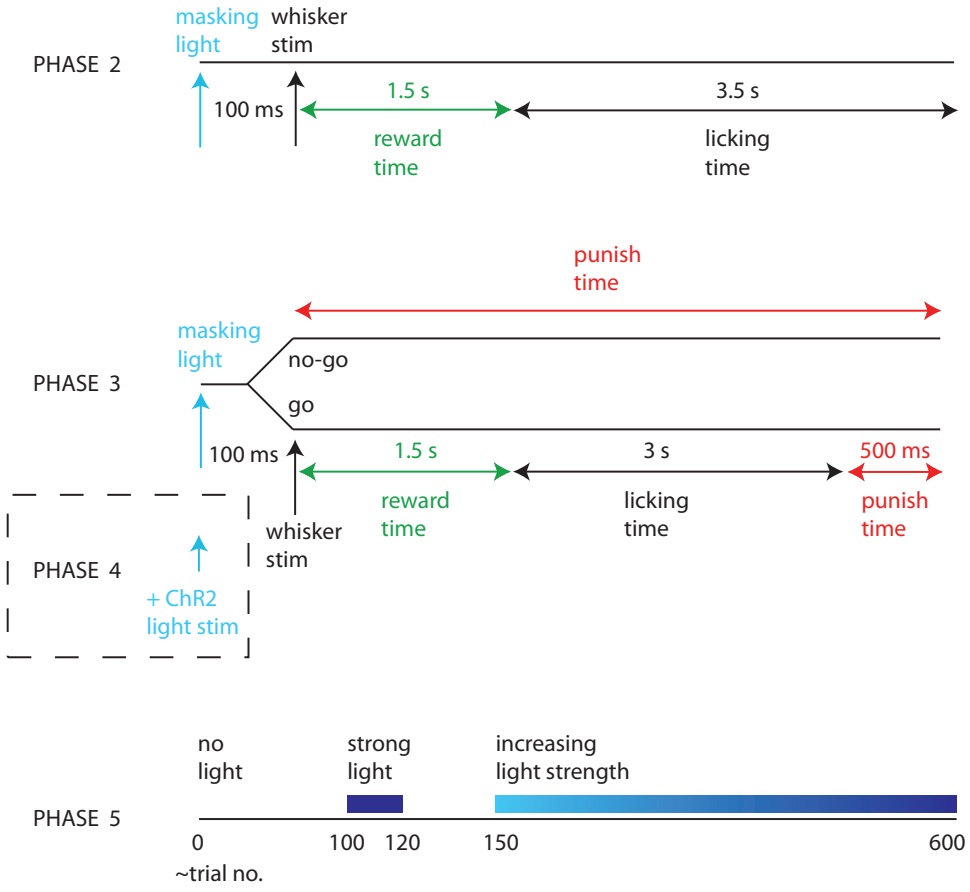

Fig 5.2 Schematic representation of behavioural phases. Phase 1: Masking light followed by whisker stimulation on every trial. The animal has 1.5 s in which to lick to receive the reward. Phase 2: The trials are divided into go and no-go. In the go trials the animal receives a whisker stimulation and must lick to receive a reward. In the no-go trials the animal receives no whisker stimulation and is punished with an air puff if it licks. Phase 4: A blue stimulating light is delivered directly onto the skull at the same time as the masking light to activate ChR2-positive neurons in the brain and interfere with behaviour. Phase 5: The stimulating light is delivered at different intensities, to allow the animal to gradually adapt and perform effectively despite its presence.

Phase 1: A short (~10 min) session on the wheel, to acclimatise the animal. The mouse received sugar water for every lick, with a minimal interval of 200 ms. For every administration of water (also in all other trials) there was an accompanying 100 ms beep with a frequency of 1500Hz. There was no punishment or sensory stimulation. Animals moved to phase 2 when they were running on the ball, licking and drinking the water reward.

Phase 2: The paradigm was divided up into trials of ~5 sec each. Each trial began with a masking light of 200 ms. After a pause of 100 ms, in every trial the piezo was moved in the superior-inferior direction and back again. The displacement was ~12 mm. If the animal licked within 1.5 s it was rewarded with a drop of sugar water. There was no punishment. Animals moved to phase 3 when they were licking at least 80% of the time following the whisker stimulation.

Phase 3: Trials were divided into "go", in which both a whisker stimulus and the masking light were presented and "no go" in which masking light was present but no whisker stimulus. If the animal licked in a go trial (hit), it was given a sugar water reward as above. If it licked in a no-go trial (false alarm), a brief air-puff was given as punishment. If it did not lick in a go trial (miss) or a no-go trial (correct rejection) they were neither rewarded nor punished. Punishment was introduced only once the animal had gained considerable confidence and was accustomed to lick following each whisker stimulus and was also licking in no-go trials. This point typically coincided with sessions in which the animal reached 80 % performance levels. Once the animal had begun to receive punishment in a session, punishment was always administered for that animal for all remaining sessions. It was administered if the animal licked too early or too late in a go trial or anytime during a no go trial. Initially the air puff was directed far from the animal. Once the animal had become acclimatised to the loud noise of the air, it was redirected onto its body or snout. Each punishment was also followed by a time-out of 2 s. If the animal licked during the time-out further time-outs and punishments were given until the mouse stopped licking. The punishment was intended to merely inform the animal that it had made a mistake rather than to cause suffering, since in subsequent trials the animal was induced by the blue

light to lick every trial and therefore received many air puffs (see later phases). If punishment was introduced too early, the animal would sometimes refuse to lick at all or become scared and stop concentrating on the task.

Phase 4: Once the animal had reached performance levels of at least 80%, for every trial at the same time as the masking light (usually 100 ms before the whisker stimulus), a strong 10 ms light pulse of 35 mW from a 1 mm diameter optic fibre (Doric lenses, Canada) was delivered to the surface of the cortex either through the dampened translucent skull or directly onto the brain. After several hundred trials the light is discontinued and the animal performs until it is sated. Phase 4 is only performed once. After one session of phase 4, the animal moves immediately on to phase 5 in the next session on the following day.

Phase 5: The trials begin with no blue light (optogenetic) stimulation (while the masking light is still on) until the animal reaches a sustained performance of over 80%. A maximum power strong blue light (35 mW) is then introduced in the same manner as described in phase 4 for around 20 trials. It is expected that the animal's performance will decrease. The stimulating light is then removed for at least another 20 trials or until the mouse's performance once again exceeds 80%. Once the animals performance has returned to previous levels, the stimulating light is introduced again every trial, but this time at a far lower intensity (7 mW). This low intensity stimulating light is delivered every trial until the performance of the animal once again reaches and is maintained at 80%. The light intensity is then increased in small increments, each time allowing the animal to adjust to the increase and its performance to improve again to 80% accordingly. The light intensity is increased until reaching the maximum intensity (35 mW) after which it is maintained at this strength until the animal is sated.

Following completion of Phase 5 in the previous session, at the start of the next session the animal was anesthetised with isoflurane and placed on the wheel. A small craniotomy (0.5 by 0.5 mm) is made and a 16 channel silicon probe (Neuronexus Technologies, USA) probe inserted into the barrel cortex to a depth of ~1200 μm. The anaesthesia was turned off and the animal left on the wheel to

wake up. Once it had begun licking and walking on the wheel, Phase 5 was run as previously described, this time accompanied by extracellular recording with the silicon probe.

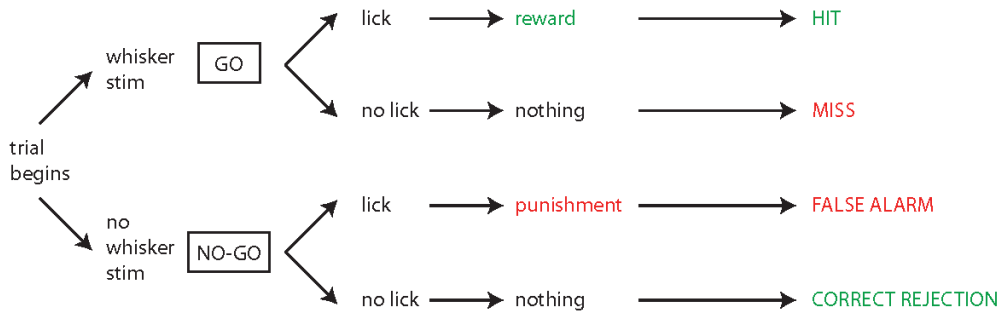

Fig 5.3 Behavioural paradigm and setup. Schematic demonstrating two-choice whisker task resulting in one of four trial types: hit, miss false alarm or correct rejection.

5.2.4 Awake recordings without behaviour

Following training on the wheel, a small craniotomy (0.5 μm by 0.5 μm) was made in the centre of the plastic disc, directly above the C3 barrel. The dura was left intact. The brain was covered in KWIK-seal silicone sealant (World Precision Instruments, UK) and the animal left overnight to recover. The following day the animal was anesthetized briefly with isoflurane and placed on the wheel. While still anesthetised, a 16 channel silicon probe (Neuronexus Technologies, USA) was inserted into the barrel cortex 1200 μm deep at an angle ~30° from the vertical. The isoflurane anaesthesia was removed and, once the animals had regained consciousness, 2-5 ms pulses of light with an ISI of 4 s were administered directly onto the brain, emitted by a 200 μm diameter fibre-coupled LED (Doric Lenses, Canada).

5.3 Results

All six animals were able to achieve high performance levels (>80%) within 4 sessions. Fig 5.4 a-c shows several different sessions at various stages of the learning process. In early session the animals licked randomly with little difference between go and no-go trials (Fig 5.4a). Hits are indicated by trials containing green dots, which show the timing of each lick. Misses are shown by a red line. False alarms are given by red dots and correct rejections are green lines. After a few sessions, however, the animals began to lick more consistently on go trials and incur fewer false alarms (Fig 5.4b). Once the animals learned to lick predominantly on go trials, they still often underwent periods of high performance followed by periods with no licking. During these times there are large sequences of misses and correct rejections (Fig 5.4c). This type of behaviour was seen across all animals and generally occurred later in the sessions, when the animal was becoming sated and was therefore less motivated. Since during resting the animal was not performing the task, its overall performance in the task should not be influenced by its behaviour during resting. These epochs were therefore removed for any further analysis. Fig 5.4d shows the same session as c, with the resting epochs removed. The performance in the session with only active epochs is much higher. Fig 5.4e displays the running performance level, averaged over 25 trials, of the section of the session shown in b.

Fig 5.4 The whisker stimulation task is learned in few trials. a-d) Four different session types, at varying stages of the learning process. Red and green dots show position of individual licks, green in hit trials and red in false alarm trials. A green line indicates a correct rejection and a red line a miss. Black dots show time of whisker stimulation. **a)** An untrained animal. **b)** Animal learning the task within the session. **c)** Animal has learned the task, but has epochs of trials in which it does not respond for 5 consecutive trials due to a lack of motivation. **d)** Same session as in **c** but with resting epochs removed. **e)** Running average of 25 trials for session in **b. f)** Training session for the 3 naive animals. Black panels indicate sessions of Phase 2, in which every trial contained a whisker stimulation. Green panels are sessions of Phase 3 in which the animal reached a performance level of > 80%. Red panels are Phase 3 sessions in which it did not perform above 80%. For both green and red panels the resting periods were removed before the analysis of performance.

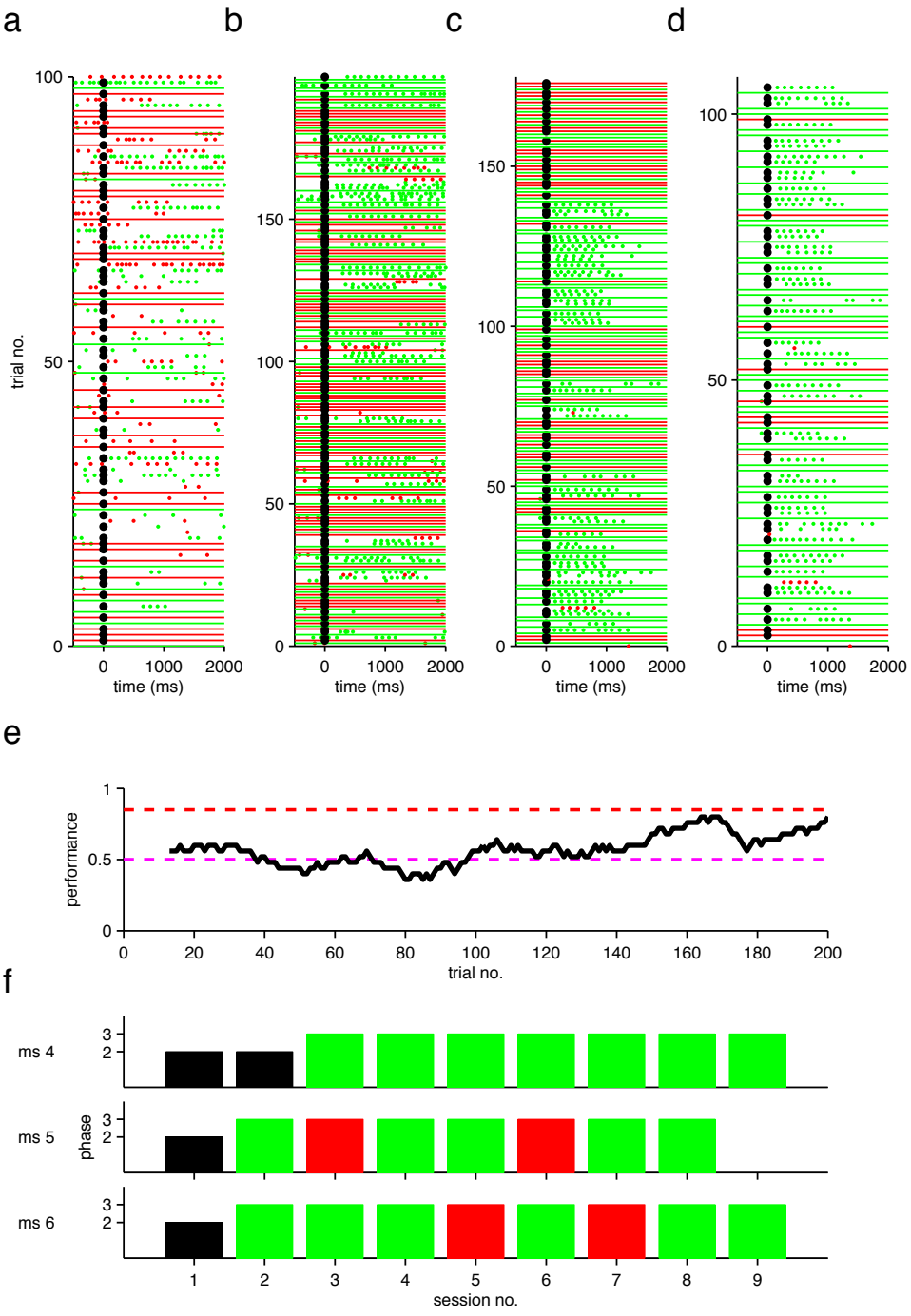
a
b
c
d
trial no.
time (ms)
e
performance
trial no.
f
ms 4
ms 5
ms 6
phase
session no.

Fig 5.4

For the three animals for which this task was their first experience on the wheel (mice 4-6), their overall training schedule over all sessions is displayed in Fig 5.4f. All animals began with at least one session of Phase 1 or 2. If the animals appeared calm and were licking consistently they were moved immediately onto Phase 2 in their first session to allow them to rapidly become accustomed to the whisker stimulation. Mice 5 and 6 both performed at a high enough level in their first session to be moved to Phase 3 in their second session, with Mouse 4 requiring another adaptation session. The mice then varied between sessions in which they reached performance levels of > 80% when averaged over 25 trials (green) and sessions in which they did not (red). Surprisingly, in some sessions the animals performed above 80% but failed to do so in the following session. All three mice underwent 8-9 sessions in total.

The performance levels of all six mice in all Phase 3 sessions are shown in Fig 5.5a. Each line represents the running average over 25 trials. Trials are separated into sessions and all epochs in which the animal did not lick for more than 8 trials in a row were removed as resting periods. In some sessions, most of the trials were used to measure the effect of noise on performance and were not considered learning trials. The number of trials per session for each mouse was variable. The amount of time each mouse remained on the wheel was dependent upon how thirsty (and therefore motivated) the mouse was at the beginning of the trial and how quickly it took the water reward before the suction pump removed it. Mice which consumed a large amount of water early in the session became satiated more quickly, leading to a drop in performance. Fig 5.5a indicates the number of learning trials for each session, following removal of trials in which the animal was quiet and trials used for noise experiments. It can therefore give only a general idea of the number of trials per session possible, with an approximate range of 300 to 700.

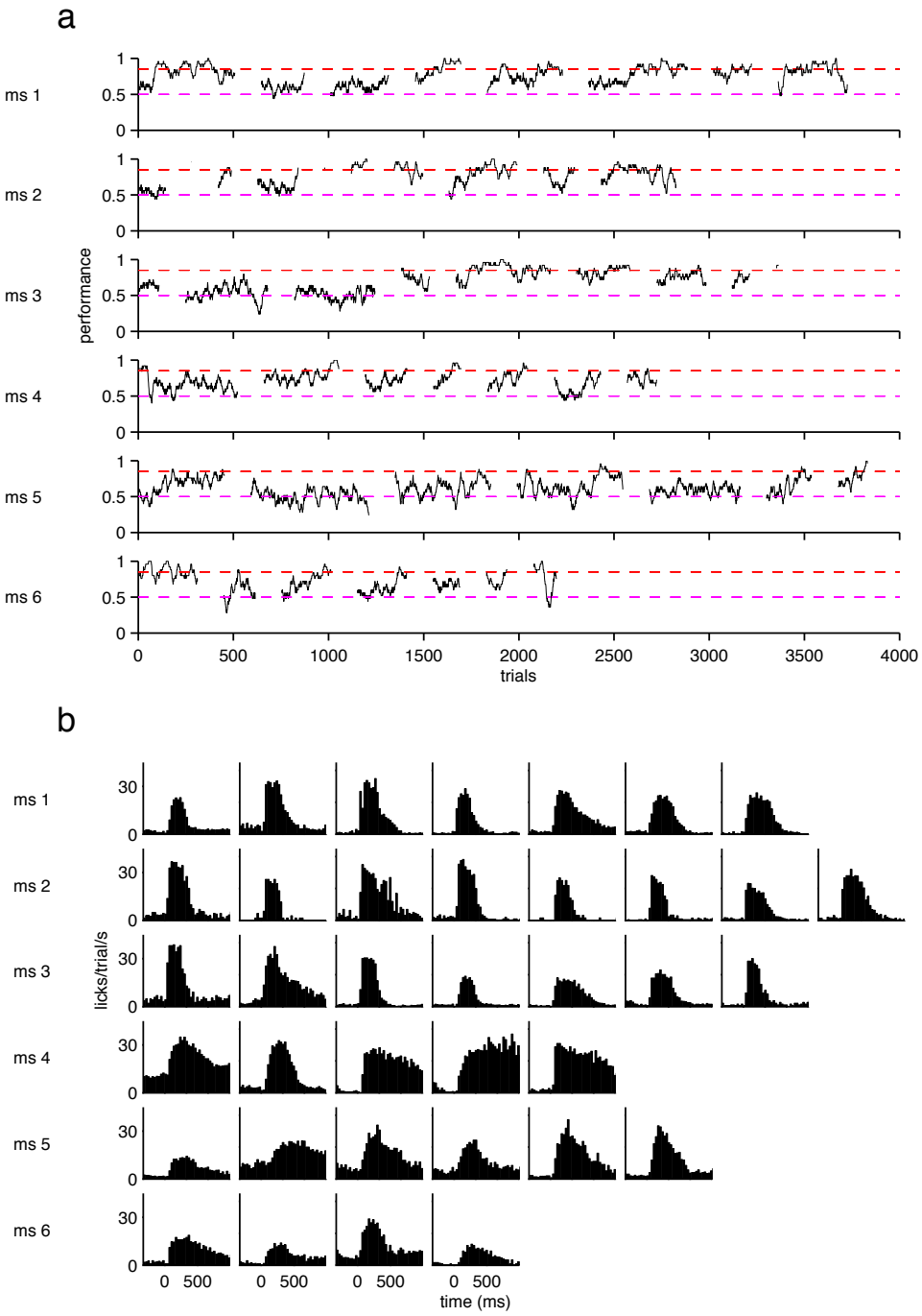

Fig 5.5 Performance levels across all sessions for all animals. a) Running average over 25 trials for each session for mice 1-6. Trials are divided into sessions. 50% performance and 80% performance levels are indicated by dotted lines. Only trials without added ChR2-induced noise and with resting epochs removed are included. **b**) PSTH for licks in hit trials for each session across all animals. Sessions in which there were not enough licks or too much electrical noise for accurate lick detection were not included.

Improvements in learning can be measured not only in the performance level of each session but also in the timing and reproducibility of licking. When an animal is well trained it will lick only following the stimuli and only for the amount of time necessary to receive the water droplet. Fig 5.5b plots the licking patterns for each animal for each session in which there were enough trials to construct a reliable PSTH of licking. Only correct trials (hits) were included. For some sessions, electrical noise prevented the precise number of licks to be counted and these sessions were excluded. All three animals that had been trained previously (ms 1-3) learned rapidly to lick following the stimulus. The corresponding PSTHs show a sharp incline following the whisker stimulus (at time = 0 ms) and often falls off sharply 500 ms post-stimulus when the animal has removed all the water reward from the lickometer. The behaviour of the naive animals (ms 4-6) was less consistent. Mouse 4 continued licking far after the reward had been received (Fig 5.5b), indicating a failure to comprehend the exact nature of the reward, however its performance levels were high (Fig 5.5a). Mouse 5 began with random licking, with only a small increase in the PSTH following the stimulus. By the last session plotted, the mouse was licking consistently following the stimulus and ceasing to lick once the reward had been consumed. However, it showed less improvement in performance (Fig 5.5a) than mouse 4.

Mice can learn this task within 2-3 days, and all six mice achieved high levels of performance within 4 sessions. The mice learned to lick only when appropriate and to refrain from licking the remaining time, ideal behaviour for recording studies, in which early licking could interfere electrically with the quality of the data recorded. The animals were able to perform for up to 700 trials per session before becoming sated and losing motivation. The whisker deflection stimulus was rapid (100 ms) and reproducible, which would allow perturbations to be introduced precisely every trial. This task is therefore suitable for investigations into the effect of introduced noise on behaviour, which will be explored in the following section.

5.3.1 Large scale perturbation of the network activity alters the behavioural response

Having established that mice were able to reach high levels of performance in a head-fixed whisker-stimulation behavioural task, I introduced large-scale perturbations into the network in order to investigate its effect on the behaviour of the animal. Would the neuronal noise prevent the animal from detecting the whisker deflection? Would the animal be able to adapt to the perturbation and perform efficiently despite the noise? What would the limit of noise be at which the animal would still be able to perform?

To introduce the perturbations, a 1 mm fibre optic cable was placed just above the surface of the transparent skull or craniotomy centred on the C3 barrel. Once the animal had reached performance levels of > 80% in the session, the 10 ms pulse of blue light was shone at the beginning of both go and no-go trials, usually 100 ms before the whisker stimulus (Fig 5.2) at the same time as the blue light flash indicating the beginning of the trial, which also served as masking light.

For a trained animal, it was possible to reach 80% performance within 100 trials in the absence of the optogenetic stimulation. The blue light was then delivered for at least 200 trials (Fig 5.6a). At this point the performance of the animal decreased to ~50% as the animal responded to every trial, rather than just the trials in which there was a whisker stimulus (Fig 5.6b). This behaviour continued for as long as the strong blue light was maintained. Once the blue light was removed the animal returned to licking only following whisker stimulus and its performance returned to > 80% (Fig 5.6 a,b). The same effect was seen in the behaviour across the population of ChR2 +ve animals (mouse 1-5; Fig 5.6c). Once the blue light stimulus was removed, the animals' performance returned to previous levels, or even beyond (mice 2 and 4). The decrease in performance was significant for all mice ($n = 10$ for all mice, $p < 0.01$, t-test). The return to previous levels was significant for mice 1,2,4 ($p < 0.01$, t-test). The behaviour of the control animal did not change with the addition or removal of the blue light stimulus, indicating that the change in behaviour is caused by activation of the ChR2-expressing neurons, rather than a visual response to the light.

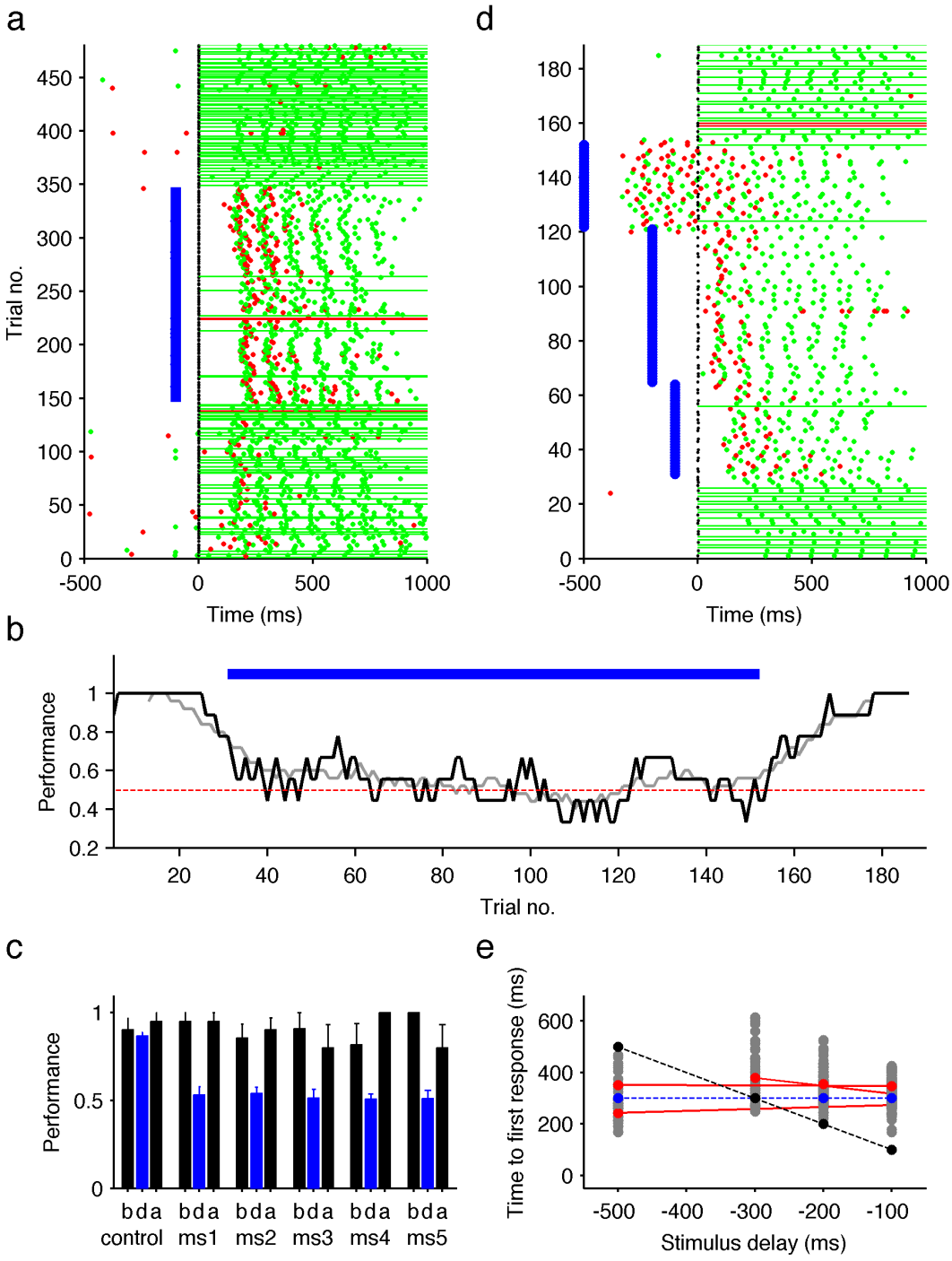
a
d
Trial no.
Time (ms)
b
Performance
Trial no.
c
e
Time to first response (ms)
Stimulus delay (ms)
bda control
bda ms1
bda ms2
bda ms3
bda ms4
bda ms5

Fig 5.6

Fig 5.6 ChR2 excitation of several thousand neurons alters the behavioural responses. a) Trials for one animal presented in similar way to Fig 5.4. 10 ms blue light stimulus is given for ~200 consecutive trials, 100 ms before the whisker stimulus (black dots). Light stimulation occurs from trials 150-350, indicated by blue line. Animal responds by licking almost every trial. **b)** Performance for a different session to that shown in a. Blue light decreased performance rate to ~ 50%. **c)** Performance rate for all trials before (b) during (d) and after (a) light stimulation for 6 different mice. Mice 1-5 are ChR2 +ve mice, control is ChR2 -ve mouse. While the performance of all ChR2 +ve mice drops to chance level with blue light stimulation, the performance of the control is not affected. **d)** Trials for a session with blue light stimulation (blue line) occurring at different time points before the whisker stimulation. Time on the x-axis is measured from the whisker stimulus. **e)** Delay from light stimulus to first response for 3 different mice (grey dots. Average for each mouse is indicated by red dots. Expected line if animals were responding consistently to whisker stimulus (black dotted line) or light stimulus (blue dotted line).

The loss of performance was caused by the animals responding to the light every trial instead of to the whisker stimulation. This can be seen when the interval between the light and whisker stimuli is increased. The animals licked at a fixed delay following the light stimulus, regardless of when the whisker stimulus occurred (Fig 5.6d). All three animals, in which different intervals were tested, responded with consistent delay to the light stimulus. Intervals of 100, 200, 300 and 500 ms were investigated. Fig 5.6e shows the delay to lick following light stimulus for three animals across different light-whisker intervals, indicated by the red dots. If the animals were responding to the whisker stimulus, a constant delay to the whisker stimulus would be expected, and the response time measured from the light stimulus should decrease with decreasing light-whisker intervals (indicated by the black dots). If, on the other hand the animals followed the light, but not the whisker stimulus, the response delay should be independent of the light-whisker interval (indicated by blue dots). The gradients for all three animals are closer to the blue line, confirming that the animals are following the blue light, rather than the whisker stimulation.

5.3.2 Gradual adaptation of the animal to the perturbation improves performance

Once it had been confirmed that the performance of the ChR2 +ve animals was consistently worsened by the addition of a strong blue light stimulus, it was investigated whether or not the animals were able to learn to adjust to the blue-light-induced noise and perform the task despite its presence, if they were first allowed to adapt gradually to a lower perturbation level.

For the first session involving blue light, the mouse received only the strongest stimulus intensity for several hundreds of trials. In the following session, the strong light stimulus was given for around 20 trials, enough to confirm that the performance level had dropped to chance (50%). The animal was then allowed to recover to previous high performance levels by switching off the light. The light was then reintroduced, but this time at the lowest level. Once the animal was able to perform well with this amount of light present, the amplitude of the light was increased in small steps, each time allowing the animal time to adjust and regain previous performance levels before increasing the intensity again. In sessions with sufficient trials, the light was gradually increased to the highest level and the animal was able to perform with this level of noise present for many trials.

Fig 5.7a presents the performance measure of part of a typical session in which the amplitude of light is increased gradually. Changes in light strength are indicated by arrows. In each case the performance of the animal drops with each increase in light stimulus intensity, and steadily climbs again in subsequent trials as the animal learns to ignore this new level of introduced noise. Within several hundred trials, with gradually introduced light perturbation, the animal is performing with 100% accuracy despite the strongest light stimulus being delivered 100 ms before the whisker stimulus. For one animal, the only one in which this specific analysis was done, the amount of trials required to regain performance is increased with increasing light intensities (Fig 5.7b).

The level of performance achieved with the light stimulus present can be compared for sessions in which the animal received the strongest light gradually,

in small intensity increments, or immediately. The number of trials containing light stimulation was the same in each case. In all four animals in which strong light was delivered in both manners the animal was able to achieve higher performance levels when the light was delivered gradually (Fig 5.7c).

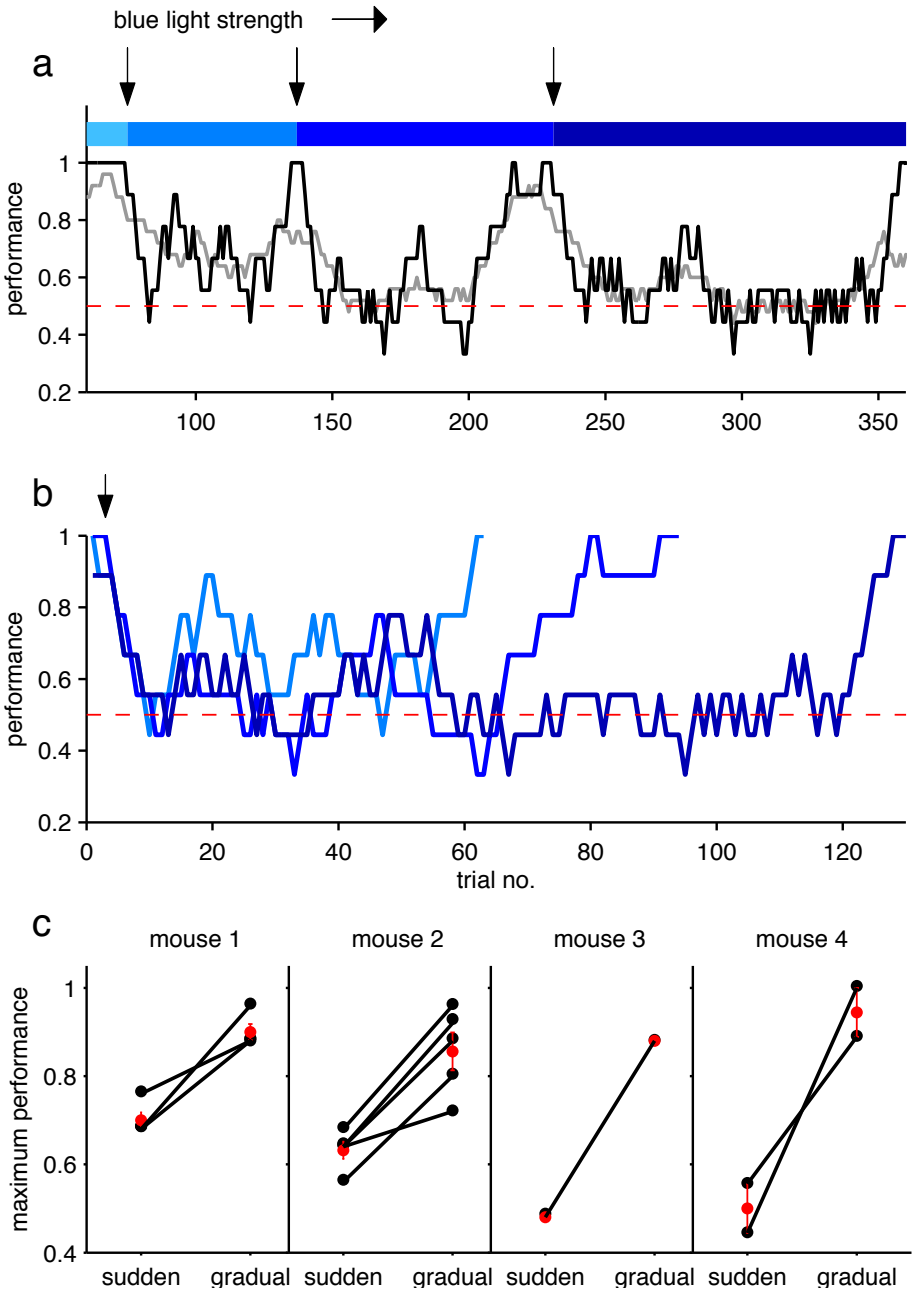

Fig 5.7 Gradual increase in light intensity allows adaptation. a) Performance in one session in which the light intensity used for ChR2 activation was increased in steps. Darker blue line indicates stronger light. Arrows show point of transition. The black line shows the running average over the last 10 trials. The grey line shows the running average over the last 25 trials. **b)** The running average over 10 trials. All three adaptation sections of same session as in a) overlaid. Arrow shows light transition. Blue colour of line corresponds to light strength. **c)** Maximum performance level reached for four mice in sessions in which strongest light intensity was given suddenly, or arrived at gradually over hundreds of trials. Each black dot represents a training session. The mean is plotted in red.

5.3.3 Extracellular recording during task performance

For one animal, the extracellular neuronal activity of layers 3-5 of the barrel cortex was recorded while the animal was performing using the 16-channel multi-site electrode described previously. The recordings were done in later sessions in which the animal had adapted to the blue light, and therefore did not lick in response to every ChR2 stimulation. Both LFP and spiking activity could be extracted from this data. In all sessions a large licking artefact caused by a grounding loop between the lickometer and the extracellular electrode circuit was recorded (Fig 5.8a) and subsequently removed from further analysis. For each trial, a large ChR2-evoked (blue arrow) response can be seen, often inducing an oscillation. The whisker response (black arrow) is less clear, but can be observed in the average over many trials (Fig 5.8b).

In the beginning of the first recording session, the neuronal activity for the trials with an without a licking response was distinctive (Fig 5.8b). Both trial types that involved the animal licking (hits and false alarms) showed an increased response to the ChR2 activation, although the stimulation intensity and manner of delivery was identical. Both the initial peak (Fig 5.8 c,e; $n = 173$, $p < 0.01$, t-test,) and the subsequent inhibitory trough (Fig 5.8 d,f; $p < 0.001$, t-test;) were significantly increased in the licking trials over the session indicating that a stronger neuronal activation was correlated with a behavioural response.

In order to investigate the correlation between licking and a larger ChR2 response, a large section in which there was no licking (resting period) was compared to a section with interspersed licking (active period). Fig 5.9a displays the section of the session from which these periods were taken. The resting period (R) was trials 250-300 and the two active sessions (A1 and A2) were trials 150-200 and 340-390. The trials from each of these sections were averaged, and the peaks (Fig 5.9b) and trough responses (Fig 5.9c) examined.

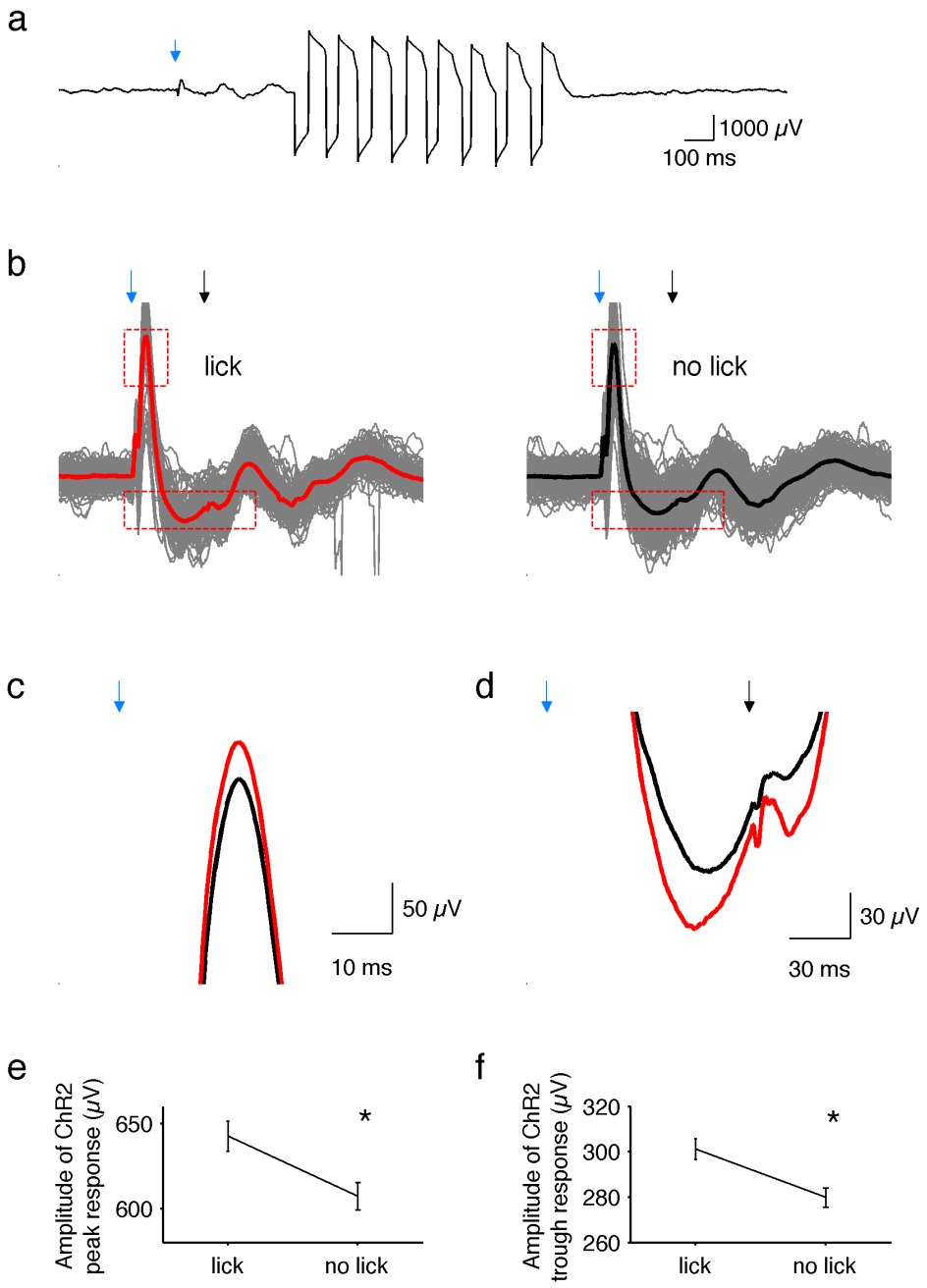

Fig 5.8 Extracellular recordings predict behavioural responses. a) LFP recording from layer 4 using a 16 channel multi-unit silicon probe with licking artefact. In all panels the blue arrow indicates the time of light stimulation, the black arrow shows the time of whisker stimulation, if present. The large licking artefact present in **a** was removed for further analysis. **b)** All trials (grey) and average (red or black) for trials involving licking (left panel) and no licking (right panel). **c,e)** Mean size of peak ChR2 response, immediately following light stimulation, for lick and no-lick trials (n = 173, $p < 0.01$, t-test) **d,f)** Mean size of trough following peak in light response for lick and no lick trials ($p < 0.001$, t-test).

The depth of the trough response for the resting periods was greater than for both the active periods (Fig 5.9d; $n = 173$, $p < 0.001$, t-test). Equally, the peak was higher for the active periods (Fig 5.9e; $n = 173$; $p < 0.001$, t-test). The delay to peak response from start of ChR2 activation was greater for the quiet period (Fig 5.9f; $n = 173$, $p < 0.05$, t-test).

Later in the session, there was no significant difference between the lick and no-lick trials (data not shown). However, two different responses to the light were observed and the trials could be therefore divided into two distinct populations based on their LFP profile (Fig 5.10a). The light is indicated with a black arrow. Both populations began with a trough immediately following the light response. This was followed by a peak of similar height. The response of population A (orange) then dropped to the level of the initial trough, whereas the response of population B (black) descended gradually. Raw traces for each population are displayed in Fig 5.10b. The first derivative (taken around the arrow in Fig 5.10b) allows the two populations to be easily divided (Fig 5.10c). The mean derivative before and after the arrow in Fig 5.10c illustrates the two distinct populations (Fig 5.10d) Surprisingly, the two populations are spread over the session section (Fig 5.10e), and there is no significant difference between the amount of the trials involving licking in the two populations (Fig 5.10f). Furthermore, there is no significant difference in performance in the two trial populations (Fig 5.10g).

These two distinct populations of LFP responses to ChR2 stimulation are correlated with neither the licking behaviour of the animal nor the accuracy of the response. It is unknown what caused the responses to the ChR2 activation to be so variable and separate into such clear populations. Possibly the state of the animal, unrelated to the specific behavioural task, contributed to the responsiveness of the cortex to each ChR2 stimulation.

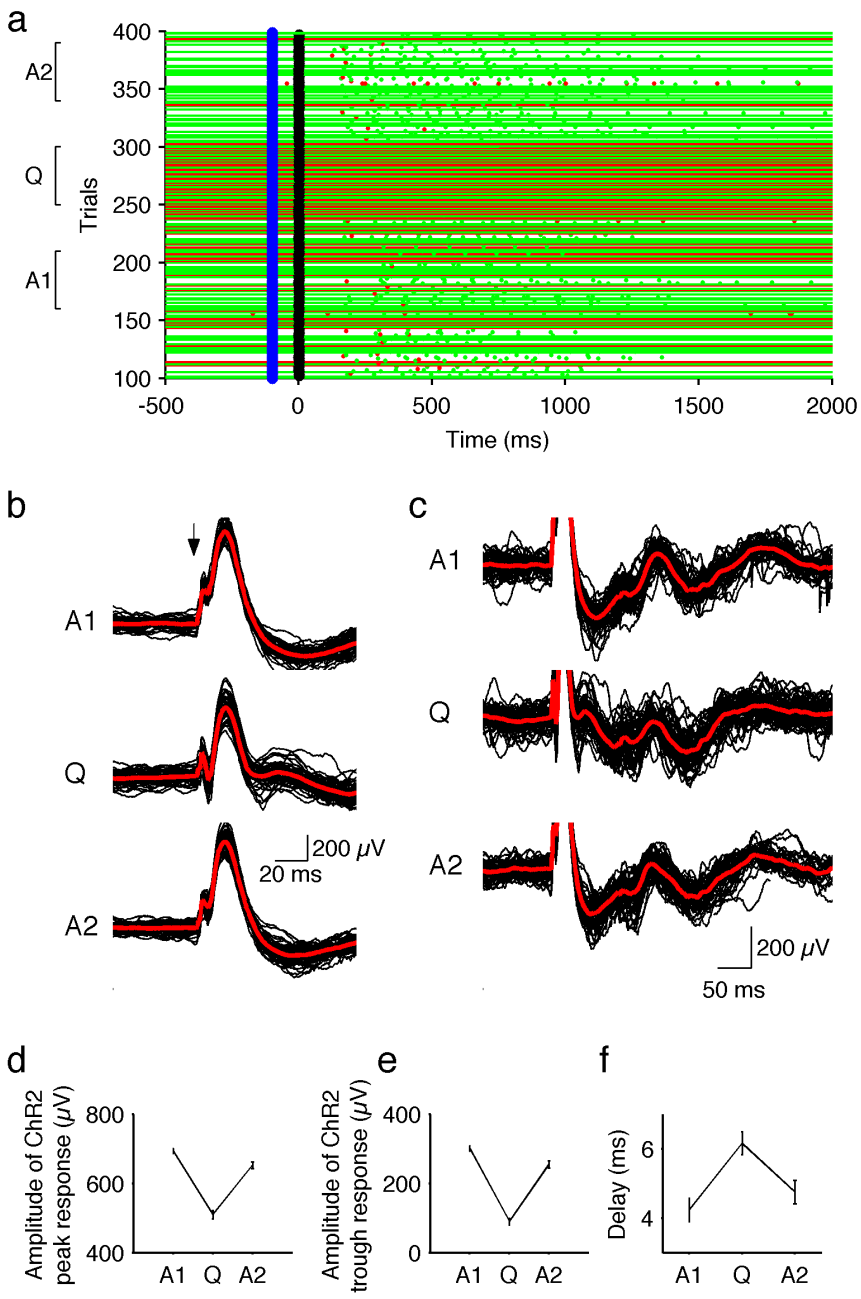

Fig 5.9 Time period in which animal does not respond has different ChR2 activation profile. a) Section of session used for further panels. Light (blue) and whisker (black) stimulations are indicated. **b)** Individual trials and average for trials in active section of trials 150-200 (A1). Trials from quiet section covering trials 250-300 (Q). Trials from active section (A2) following passive (quiet) section (trials 340-390). **c)** Same as **b** except showing response trough following peak for the three sections. **d)** Size of peak ChR2 response from active (A1 and A2) and quiet (Q) sections plotted in **b** and **c**. **e)** Size of response trough for the three different sections. **f)** Delay to peak of response for the three sections.

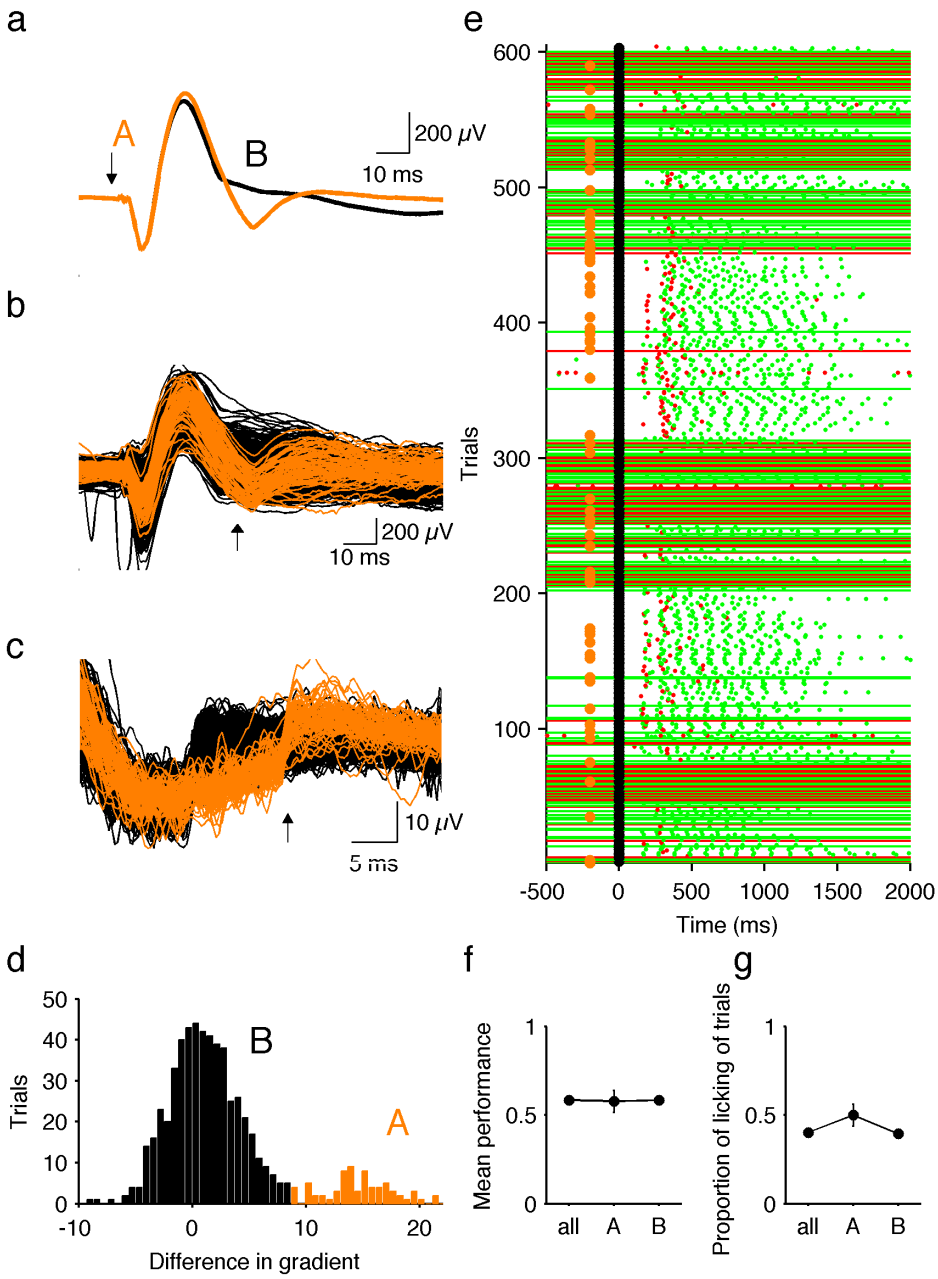

Fig 5.10 Two populations of ChR2 responses based on LFP profile a) Average of two populations of responses to ChR2 activation. Population A is shown in orange, population B is black. Arrow indicates blue light stimulation. **b)** Individual traces for two distinct populations. Arrow indicates centre of section used in **c. c)** First derivative of traces in **b.** Arrow indicates section used in **d. d)** Histogram of difference in mean value for each trial between 5 ms before and 5 ms after arrow in **c.** Two distinct populations are revealed. **e)** Section of session used in analysis displayed in **f** and **g**. Same animal and session as used in Fig 5.7. Orange dots indicate trials from population A. **f)** Mean performance for all trials from **e** and only trials in population A or B**. g)** Fraction of trials in which the animal licked; all trials, only population A and only population B.

5.4 Discussion

5.4.1 Possible contribution of other modalities to solving whisker-based task

In this chapter I have developed a decision-based whisker stimulation task and used this task as a tool to investigate the effects of large-scale perturbations of cortical networks on behaviour. The stimulation consisted of a wooden beam deflecting several whiskers and the perturbation was delivered by optogenetic stimulation of several thousand neurons in the barrel cortex or possibly in the thalamus. While this task was designed to be whisker-based it is possible, however, that the animal did not rely solely upon its whisker system to perform accurately in the task. The task was performed in the light, to prevent as far as possible the animal from seeing the optogenetic blue light stimulation and the wooden rod was positioned such that it was possible for the animal to view its movement. Furthermore, while other louder noises, caused by the suction pump, might have prevented the animal from hearing the beam movement, the deflection of the whisker was accompanied by a distinctive noise. It is therefore highly likely that both the auditory and visual modalities were also helping the animal to perform in the task.

For this study, however, the first objective was to investigate if the perturbation of several thousand neurons interferes with an animal's performance. For this objective, inputs from other modalities must only improve the animals' performance. Therefore if the performance decreases to chance level despite possible help from other modalities it must also do so when the animal is only relying upon its whiskers. Whether or not the animal was only receiving whisker input or whether it could hear and see the deflection as well does not detract from the conclusion that perturbations affect behaviour. Furthermore, if selective disturbance of the activity in the barrel cortex lets the animal's performance drop to chance level, the whisker system appears to be the primary (and potentially only) modality the mouse uses to detect the stimulus applied.

The second objective was to study whether or not the animal could learn to distinguish the perturbation from the real sensory stimulation and thus learn to perform despite the perturbation. For this objective, inputs from other modalities are also irrelevant. For these experiments, I compared the ability of the animal to perform well under strong optogenetic light stimulation when the light had been introduced gradually, to when it had been introduced at maximum intensity and sustained at that level. The perturbation is introduced into the barrel cortex. Therefore contributions to the decision by information from the visual and auditory systems should not be affected by the strength of presence of the perturbation, and should therefore be the same in both cases. Only the information from the whiskers coming into the barrel cortex should be affected by the amount of perturbation. Therefore a direct comparison is being made between the animals' ability to detect the whisker information under the two different light introduction regimes.

While it would be ideal to develop a task that relies solely upon the whisker system, for the objectives of this study, the experimental setup using a moving wooden rod for whisker deflection was sufficient and the possible engagement of other sensory modalities does not affect the final conclusions.

5.4.2 Stimulation of neurons other than cortical pyramidal cells with blue light

As described in Chapter 4, the transgenic mice used in this task contained ChR2-expressing neurons in layer 2/3 and layer 5 of the cortex as well as in the thalamus, most particularly the whisker-related nuclei of the thalamus, VPM and POM, and the reticular thalamic nucleus. The optogenetic stimulation was given in the form of a blue light delivered onto the moistened skull or brain. Cortical neurons are expected to be the principal recipients of this stimulation, most strongly in layers 2/3 but also possibly in layer 5, given the distribution of the ChR2 expressing neurons reported (Arenkiel et al., 2007; Wang et al., 2007). It is unlikely that the blue light penetrated deeply enough to stimulate the neurons of the thalamus directly but it is possible that axons from the VPM/POM to the cortex were stimulated. Furthermore, while characterisation of these animals has determined

that the majority of ChR2-expressing neurons in the cortex are pyramidal, and interneurons rarely express ChR2 (Wang et al., 2007), it is possible that some interneurons were directly activated by the light stimulation. Viral injection of ChR2 plasmids directly into the barrel cortex or the use of a more specific transgenic mouse would resolve the issue of the scale of neuronal activation by the stimulus. For the purposes of this set of experiments, however, with this line of mice I was able to deliver a strong perturbation and activate many neurons. The precise number and type of neurons activated is unknown, but not relevant for the conclusions drawn.

It is also possible that the stimulation of the neurons leads to a physical movement of the whiskers which is detected by the animal. A similar idea was proposed in a study by Houwelling and Brecht (Houweling and Brecht, 2008) in which the animal learnt to report the stimulation of a single neuron. In my study, no movement of the whiskers was observed during the same ChR2 stimulation in the anesthetised animal. However, it is indeed possible that small whisker movements could be undetected by eye but still felt by the animal and could be thus inducing a behavioural response in the animal. To rule out this possibility a thorough investigation of high-speed video of the whiskers during ChR2 stimulation would need to be performed. In the study by Houwelling and Brecht, whisker movement during microstimulation of the barrel cortex was measured with a high precision tracking system. While movement was indeed reported, it was not evoked by the microstimulation.

5.4.3 Implications for neural coding

In this task the animal was able to adapt to the perturbation and learn to perform in the task despite its presence. This means that the whisker information travelling through the barrel cortex must be encoded with sufficient redundancy that the presence of a large amount of extra activity does not prevent the animal from receiving it. A neural code, which relied upon precise spiking activity in few neurons could not withstand the large scale perturbation even if its delivery were introduced gradually. It is most likely, therefore, that for stimulations as coarse as the deflection of multiple whiskers, the animal is able to accumulate information

from many thousands of neurons and integrate this information over time to reach a decision of whether or not whiskers were deflected. A more difficult task, e.g. texture discrimination using the whiskers, might be expected to be more easily disrupted.

The neuronal mechanisms underlying the adaptation to the ChR2 stimulation are still unclear. There is most probably some form of plasticity taking place, however it has yet to be determined of what form this plasticity might take. It is possible that the neural code is changing to be more "robust" or resistant to the perturbation. Synapses could be strengthening. Inhibition could be switching off the 'offending' neurons. Further recording studies while the animal is performing the task would help to elucidate this question. They would allow direct comparisons between the neuronal responses during constant strong optogenetic stimulation and during gradually increasing stimulation. This would identify if the neuronal changes underlying the changes in behavior were occurring in the barrel cortex itself or further downstream.

5.4.4 Potential contribution of electrophysiological recordings

The electrophysiological recordings in this study, while preliminary and from only one animal, give certain insights into the neuronal activity underlying the behaviour. The ChR2 response measured in the cortex was larger for trials in which the animal responded with a lick (Fig. 5.8). Later in the same session for the same animal, the ChR2 responses were different (both in size and timing) in the quiet section of trials in which the animal was not responding. This suggests that when the animal was unresponsive, possibly not concentrating on the task, the cortex was also less responsive to the ChR2 stimulation (Fig 5.9). Later still, two distinct populations of ChR2 responses were recorded, although no correlation between the responses and the behavioural response was detected (Fig 5.10). Furthermore, no differences in licking or accuracy of response was found to explain the reason for the distinct populations.

Together, these recordings suggest that the behaviour of the animal could possibly be explained by the recorded neuronal response to ChR2 stimulation. The ongoing

background activity in the cortex immediately preceding the ChR2 stimulation could alter the direct response of the cortex to the stimulation, which could subsequently alter the behavioural of the animal. In order to investigate these ideas further, the neuronal activity immediately preceding ChR2 stimulation should be investigated across several animals in times of responsiveness and unresponsiveness. It is possible that certain characteristics of the spontaneous or background cortical activity could be identified which would predict an accurate response in the behaving animal.

5.5 Conclusion

In this chapter I have developed a behavioural task, which has allowed me to investigate the effect of large-scale perturbations on behaviour. It was found that the performance of mice in a whisker-based stimulation task initially dropped to chance level if a strong perturbation was delivered 100ms before the sensory stimulation. If the strong perturbation was sustained for every trial, the performance of the mouse did not improve. If the perturbing stimulation was removed and then introduced gradually, the animal was able to adapt to the stimulation and learn to perform in the task despite the perturbation.

6 General discussion

The work presented in this thesis has spanned a range of neuronal perturbation methods with different orders of magnitude, with the final aim of investigating how the brain reacts to unexpected inputs. From the introduction of one spike in the anesthetised animal to the introduction of thousands of spikes in the behaving mouse, I have probed the concepts of absorbance and adaptation, techniques the brain might employ to allow it to continue functioning at an efficient level despite the perturbation. These mechanisms put limits on the neural coding schemes the brain can employ.

6.1 Introducing a single spike leads to extra spikes in the network

A single spike was introduced electrically into a cortical network with a patch electrode and the network activity monitored simultaneously with extracellular recordings. It was found that this single extra spike causes a short-lived increase in the spiking rate of neurons in the local network (London et al., 2010). Due to subsequent extra inhibitory spikes cancelling out future excitatory spikes, however, this perturbation did not cause a long-term increase in spike rate. Overall it was determined that an extra ~28 spikes had been introduced into the network. This finding supported the idea that the cortex in the anesthetised state must only rely on a rate code rather than precise spike timing. If precise spike timing were necessary for efficient function, the natural noise generated in the brain would constantly produce extra spikes and interfere with the precise code, preventing the brain from functioning. The brain does function, however, and therefore must exist in a regime in which a few extra random spikes do not make a difference, most likely by using a rate code. In an awake animal performing a complicated task, it is possible that more precise timing of spikes in specific neurons might be necessary. However, at least in the anesthetised state, a rate code is the more likely regime of neural coding employed by the brain.

6.2 Perturbing several cells with light temporarily changes the network dynamics

To permit the introduction of perturbations into several specific cells, I changed technique from the electrical stimulation of one cell to the optogenetic stimulation of neurons electroporated with ChR2. It was clear that inducing several excitatory neurons to spike did produce an increase in the local network spike rate that was detectable in nearby cells, both with the cell-attached configuration and with the extracellular multi-site probe.

It has been shown in previous studies that the stimulation of a single neuron can be both detected by the rat (Houweling and Brecht, 2008) and can result in the detectable movement of a whisker (Brecht et al., 2004). While these studies give important insight into the power of a single cell to cut through the general chaotic cortical activity from thousands of neurons in order to be noticed by the animal, they do not address the question of the power of a single cell during natural behaviour. The animal can be trained to detect the stimulation of a single cell (Houweling and Brecht, 2008), but this does not mean that the performance of a naive animal engaged in another task would be affected by the activity of one or several cells. Indeed, further studies have shown that the introduction of single spikes into ~300 neurons is required before the animal can even detect the stimulation (Huber et al., 2008). It is most likely that the perturbation of even more cells would be required to alter behaviour. Therefore, the small increase in firing rate from the stimulation of ~10 neurons, shown in Chapter 3, is unlikely to cause a change in an animal's behaviour, with a possible exception if the extra spikes came at exactly the precise time and in the specific neurons involved in the task. A study by Brecht *et al*. (Brecht et al., 2004) demonstrates that a train of APs in a single motor neuron can result in the detectable movement of a whisker. These experiments however, even though they involve the stimulation of a single neuron, do not contradict the claims made above. The neurons stimulated were in the motor cortex, rather than the somatosensory cortex, and their stimulation results in the direct physical movement of a whisker rather than the behavioural interference described above. Just as the stimulation of a single neuron can move a whisker, the animals may be able to sense the stimulation of a single

sensory neuron but it unlikely that this sensation will be strong enough to prevent their completion of an unrelated behavioural task.

This is, of course, only one possibility. A contrasting view might suggest that to detect a very small stimulation, this stimulation must be sufficiently amplified by the brain to allow it to reach the consciousness of the animal. To affect behaviour, however, the perturbation needs only to modify the unconscious sensory input in some way. If follows therefore that to modify behaviour, a smaller perturbation would be necessary than the strength of stimulation required for detection mentioned in the previous studies (Huberd, 2007; Houweling and Brecht, 2008)

6.3 Sudden whisker deflection or activation of thousand of neurons produces an oscillation

To take a step closer towards investigating perturbations during behaviour, the next step was to look at the effects of larger perturbations on the network. These perturbations were introduced either with the sudden deflection of the C2 whisker or the optogenetic activation of thousands of neurons, mostly pyramidal neurons in the barrel cortex but with possible additional indirect stimulation of the VPM and POM. Both of these stimulations were expected to produce a strong spiking excitatory response in all layers of the barrel cortex. In addition to this expected response, in many trials an oscillation followed, caused by rhythmic bursts of spikes detectable intracellularly, in the spiking activity of the network and the LFP. The oscillations from the whisker deflection and the optogenetic stimulation were similar enough that it is most likely that the same neurons are involved and once initiated, the oscillations employ similar mechanisms of propagation through the cortex and thalamic nuclei.

The functional significance of these oscillations remains unknown. Some studies have suggested that oscillations may provide better signal-to-noise and thus facilitate detection of a stimulus (Sherman, 2001). Other studies have shown the thalamus is insensitive to external inputs during spindles and that the spindles could represent a cut-off from the external world (Llinás and Steriade, 2006). Another suggestion is that they are a means of sustaining the memory of a stimulus, supported by the idea that

the oscillation can continue several hundreds of milliseconds after the initial stimulus has stopped.

The strong stimulus, in contrast to the perturbation of a few neurons, appears to set the cortex into a completely new regime of firing, recruiting a large proportion of the cells into a fairly rigid behavioural pattern. This would suggest that the animal is unable to function efficiently and perform a task while this firing regime is in place. The strong bursting followed by periods of silence followed by bursting should not leave the involved neurons with enough freedom to encode a specific sensory stimulus.

Oscillations have been observed in the awake animal however, without leading to any noticeable behavioural deficiency, suggesting that the animal is able to function at least sufficiently, if not optimally, during an oscillation. In order to determine whether or not the animal function more or less efficiently during an oscillation, a direct link between the presence of an oscillation and performance accuracy needs to be found.

6.4 Large-scale disturbances can affect behaviour, but can be overcome by the animal

To test the hypothesis that the initial response to strong stimulation (inducing oscillations) would prevent the neurons from encoding sufficient information to allow the animal to perform a task, I introduced such a strong perturbation at a precise point during a behaviour task, 100 ms before the sensory input. The reaction of the animal to such a large perturbation was to initially be overwhelmed and follow every perturbation with a response. Either the neural response to the perturbation was similar enough to the response to a whisker deflection that the animal was unable to distinguish between the two and reacted to the optogenetic activation as though it were whisker stimulation and responded accordingly, or the stimulation was so strong that the animal was disorientated and simply responded every time without trying to perform the task at all. Indeed if the punishment is greatly outweighed by the potential reward the best strategy is to respond every time if the sensory information does give no clue about the reward.

With the gradual introduction of the perturbation, slowly increasing the intensity of the light over many trials, and thus presumably slowly increasing the amount of neurons recruited and the scale of the neural response, the animals were able to learn to distinguish between perturbation and signal, and to return to their former high levels of performance despite the presence of the perturbation. It is possible that it is the simple nature of the task, which permits the animals to continue to perform. Since many of the neurons must be occupied with the perturbation and the subsequent oscillation, the level of redundancy in the encoding of this task appears to be very high. Sufficient numbers of neurons normally recruited and encoding the sensory stimulus would thus be left unaffected by the perturbation to still perform the task. The encoding of this task is clearly robust and difficult to permanently perturb. This level of robustness and redundancy has many advantages, as certain physical disruptions such as strokes or lesions would also be more readily overcome.

It is quite possible that a more complicated task such as whisker-based texture discrimination might require more precise timing of the signal in smaller, well-defined networks in order to transmit the information, and might therefore be more affected by the perturbation, even if it is introduced gradually. The next step therefore would be to increase the complexity of the task, or vary the timing of the optogenetic light stimulus to whisker stimulus delay to try to find the limit at which the animal cannot learn to adapt to the light.

As mentioned in Chapter 5, further recording studies during the task are also essential. While the adaptation behaviour described in the Chapter is clear and consistent across animals, the reason for this change is unknown. It is possible that the neurons themselves in the barrel cortex are undergoing a form of plasticity which permits them to distinguish between the optogenetic and whisker stimulations. Alternatively, the outputs of these neurons could be identical during both the constantly strong and the gradually increasing optogenetic stimulus and the changes underlying behaviour could be taking place downstream in another brain region. With recordings, direct comparisons of the neuronal responses to the stimulus of strongest intensity under both conditions (constant and gradually increasing) could be made.

6.5 Final comments

In this thesis I have shown that small perturbations have a significant effect on the local network, implying the use of a rate code for at least some brain states in the barrel cortex. I have shown that a large perturbation produces a strong response, which often leads to a strong oscillation. The same stimulus interferes with the behaviour of a performing mouse, but the mouse can learn to perform despite the noise. All of these findings suggest a coding regime with high degrees of redundancy and robustness. Although the neural coding patterns are easily perturbed - even a single spike causes a temporary increase in firing rate - this disturbance does not have debilitating effects on the behaviour or the experience of the animal.

List Of Abreviations

AP	action potential
ChR2	channelrhodopsin2
DAPI	4',6-diamidino-2-phenylindole
FFT	fast Fourier transform
GABA	γ-aminobutyric acid
GFP	green fluorescent protein
HEPES	4-(2-hydroxyethyl)-1-piperazine-ethanesulfonic acid
I	current
ISI	inter-stimulus interval
i.p.	intraperitoneal
IPSP	inhibitory postsynaptic potential
LFP	local field potentialf
M1	primary motor cortex
MGB	medial geniculate body
MT	middle temporal
n.s.	not significant
NpHR	halorhodopsin
P	postnatal day
POM	posterior medial nucleus of the thalamus
PSTH	peri-stimulus time histogram
RFP	red fluorescent protein
RT	reticular nucleus of the thalamus
S1	primary somatosensory cortex
S2	secondary somatosensory cortex
s.d.	standard deviation
SEM	standard error of the mean
TTX	tetrodotoxin
vM1	whisker-related motor cortex
VPM	ventro posteriormedial nucleus of the thalamus
VPL	ventral posterolateral nucleus of the thalamus
YFP	yellow fluorescent protein

References

Ahissar E, Kleinfeld D (2003) Closed-loop neuronal computations: focus on vibrissa somatosensation in rat. Cereb Cortex 13:53–62.

Ahissar E, Sosnik R, Haidarliu S (2000) Transformation from temporal to rate coding in a somatosensory thalamocortical pathway. Nature 406:302–306.

Andermann ML, Moore CI (2006) A somatotopic map of vibrissa motion direction within a barrel column. Nat Neurosci 9:543–551.

Andersen P, Andersson SA, Lomo T (1967) Nature of thalamo-cortical relations during spontaneous barbiturate spindle activity. J Physiol (Lond) 192:283–307.

Arabzadeh E, Zorzin E, Diamond ME (2005) Neuronal encoding of texture in the whisker sensory pathway. PLoS Biol 3:e17.

Arenkiel BR, Peca J, Davison IG, Feliciano C, Deisseroth K, Augustine GJ, Ehlers MD, Feng G (2007) In vivo light-induced activation of neural circuitry in transgenic mice expressing channelrhodopsin-2. Neuron 54:205–218.

Arnold PB, Li CX, Waters RS (2001) Thalamocortical arbors extend beyond single cortical barrels: an in vivo intracellular tracing study in rat. Exp Brain Res 136:152–168.

Aronoff R, Matyas F, Mateo C, Ciron C, Schneider B, Petersen CC (2010) Long-range connectivity of mouse primary somatosensory barrel cortex. European Journal of Neuroscience 31:2221–2233.

Aronoff R, Petersen C (2007) Layer- and column-specific knockout of NMDA receptors in pyramidal neurons of the mouse barrel cortex. Front Integr Neurosci 1:1.

Avanzini G, de Curtis M, Panzica F, Spreafico R (1989) Intrinsic properties of nucleus reticularis thalami neurones of the rat studied in vitro. J Physiol (Lond) 416:111–122.

Averbeck BB, Latham PE, Pouget A (2006) Neural correlations, population coding and computation. Nat Rev Neurosci 7:358–366.

Averbeck BB, Lee D (2006) Effects of noise correlations on information encoding and decoding. J Neurophysiol 95:3633–3644.

Bal T, Krosigk von M, Mccormick DA (1995a) Role of the ferret perigeniculate nucleus in the generation of synchronized oscillations in vitro. J Physiol (Lond) 483 (Pt 3):665–685.

Bal T, Krosigk von M, Mccormick DA (1995b) Synaptic and membrane mechanisms underlying synchronized oscillations in the ferret lateral geniculate nucleus in vitro. J Physiol (Lond) 483 (Pt 3):641–663.

Bal T, Mccormick DA (1993) Mechanisms of oscillatory activity in guinea-pig nucleus reticularis thalami in vitro: a mammalian pacemaker. J Physiol (Lond) 468:669–691.

Bishop GH, O'Leary J (1936) Components of the electrical response of the optic cortex in the rabbit. :1–17.

Bourassa J, Pinault D, Deschênes M (1995) Corticothalamic projections from the cortical barrel field to the somatosensory thalamus in rats: a single-fibre study using biocytin as an anterograde tracer. Eur J Neurosci 7:19–30.

Boyden ES, Zhang F, Bamberg E, Nagel G, Deisseroth K (2005) Millisecond-timescale, genetically targeted optical control of neural activity. Nat Neurosci 8:1263–1268.

Brecht M (2007) Barrel cortex and whisker-mediated behaviors. Curr Opin Neurobiol 17:408–416.

Brecht M, Grinevich V, Jin TE, Margrie T, Osten P (2006) Cellular mechanisms of motor control in the vibrissal system. Pflugers Arch 453:269–281.

Brecht M, Roth A, Sakmann B (2003) Dynamic receptive fields of reconstructed pyramidal cells in layers 3 and 2 of rat somatosensory barrel cortex. J Physiol (Lond) 553:243–265.

Brecht M, Schneider M, Sakmann B, Margrie TW (2004) Whisker movements evoked by stimulation of single pyramidal cells in rat motor cortex. Nature 427:704–710.

Bruno RM, Khatri V, Land PW, Simons DJ (2003) Thalamocortical angular tuning domains within individual barrels of rat somatosensory cortex. J Neurosci 23:9565–9574.

Chiaia NL, Rhoades RW, Fish SE, Killackey HP (1991) Thalamic processing of vibrissal information in the rat: II. Morphological and functional properties of medial ventral posterior nucleus and posterior nucleus neurons. J Comp Neurol 314:217–236.

Cohen MR, Newsome WT (2004) What electrical microstimulation has revealed about the neural basis of cognition. Curr Opin Neurobiol 14:169–177.

Cohen MR, Newsome WT (2009) Estimates of the contribution of single neurons to perception depend on timescale and noise correlation. J Neurosci 29:6635–6648.

Contreras D, Destexhe A, Sejnowski TJ, Steriade M (1997) Spatiotemporal patterns of spindle oscillations in cortex and thalamus. J Neurosci 17:1179–1196.

Contreras D, Steriade M (1996) Spindle oscillation in cats: the role of corticothalamic feedback in a thalamically generated rhythm. J Physiol (Lond) 490 (Pt 1):159–179.

Cotillon N, Edeline JM (2000) Tone-evoked oscillations in the rat auditory cortex

result from interactions between the thalamus and reticular nucleus. Eur J Neurosci 12:3637–3650.

Cotillon N, Nafati M, Edeline JM (2000) Characteristics of reliable tone-evoked oscillations in the rat thalamo-cortical auditory system. Hear Res 142:113–130.

Cotillon-Williams N, Edeline J-M (2003) Evoked oscillations in the thalamo-cortical auditory system are present in anesthetized but not in unanesthetized rats. J Neurophysiol 89:1968–1984.

Cotillon-Williams N, Edeline J-M (2004) Evoked oscillations in unit recordings from the thalamo-cortical auditory system: an aspect of temporal processing or the reflection of hyperpolarized brain states? Acta Neurobiol Exp (Wars) 64:253–270.

Curtis JC, Kleinfeld D (2009) Phase-to-rate transformations encode touch in cortical neurons of a scanning sensorimotor system. Nat Neurosci:10.

de Kock CPJ, Bruno RM, Spors H, Sakmann B (2007) Layer- and cell-type-specific suprathreshold stimulus representation in rat primary somatosensory cortex. J Physiol (Lond) 581:139–154.

de Kock CPJ, Sakmann B (2009) Spiking in primary somatosensory cortex during natural whisking in awake head-restrained rats is cell-type specific. Proc Natl Acad Sci USA 106:16446–16450.

de Ruyter Van Steveninck RR, Lewen GD, Strong SP, Koberle R, Bialek W (1997) Reproducibility and variability in neural spike trains. Science 275:1805–1808.

DeAngelis GC, Newsome WT (2004) Perceptual “read-out” of conjoined direction and disparity maps in extrastriate area MT. PLoS Biol 2:E77.

deCharms RC, Zador A (2000) Neural representation and the cortical code. Annu Rev Neurosci 23:613–647.

Destexhe A, Contreras D, Sejnowski TJ, Steriade M (1994) A model of spindle rhythmicity in the isolated thalamic reticular nucleus. J Neurophysiol 72:803–818.

Destexhe A, Hughes SW, Rudolph M, Crunelli V (2007) Are corticothalamic “up” states fragments of wakefulness? Trends Neurosci 30:334–342.

Diamond I (1995) Cerebral cortex: The barrel cortex of rodents.

Diamond ME, Armstrong-James M, Budway MJ, Ebner FF (1992) Somatic sensory responses in the rostral sector of the posterior group (POm) and in the ventral posterior medial nucleus (VPM) of the rat thalamus: dependence on the barrel field cortex. J Comp Neurol 319:66–84.

Diamond ME, Heimendahl Von M, Knutsen PM, Kleinfeld D, Ahissar E (2008) 'Where' and “what” in the whisker sensorimotor system. Nat Rev Neurosci 9:601–612.

Dinse HR, Krüger K, Akhavan AC, Spengler F, Schöner G, Schreiner CE (1997)

Low-frequency oscillations of visual, auditory and somatosensory cortical neurons evoked by sensory stimulation. Int J Psychophysiol 26:205–227.

Fee MS, Mitra PP, Kleinfeld D (1997) Central versus peripheral determinants of patterned spike activity in rat vibrissa cortex during whisking. J Neurophysiol 78:1144–1149.

Feldmeyer D, Egger V, Lübke J, Sakmann B (1999) Reliable synaptic connections between pairs of excitatory layer 4 neurones within a single "barrel" of developing rat somatosensory cortex. J Physiol (Lond) 521 Pt 1:169–190.

Feldmeyer D, Lübke J, Sakmann B (2006) Efficacy and connectivity of intracolumnar pairs of layer 2/3 pyramidal cells in the barrel cortex of juvenile rats. J Physiol (Lond) 575:583–602.

Feldmeyer D, Lübke J, Silver RA, Sakmann B (2002) Synaptic connections between layer 4 spiny neurone-layer 2/3 pyramidal cell pairs in juvenile rat barrel cortex: physiology and anatomy of interlaminar signalling within a cortical column. J Physiol (Lond) 538:803–822.

Golomb D (2006) Coding of Stimulus Frequency by Latency in Thalamic Networks Through the Interplay of GABAB-Mediated Feedback and Stimulus Shape. J Neurophysiol 95:1735–1750.

Halassa MM, Siegle JH, Ritt JT, Ting JT, Feng G, Moore CI (2011) Selective optical drive of thalamic reticular nucleus generates thalamic bursts and cortical spindles. Nat Neurosci 14:1118–1120.

Helmstaedter M, Sakmann B, Feldmeyer D (2008) The Relation between Dendritic Geometry, Electrical Excitability, and Axonal Projections of L2/3 Interneurons in Rat Barrel Cortex. Cerebral Cortex.

Holmgren C, Harkany T, Svennenfors B, Zilberter Y (2003) Pyramidal cell communication within local networks in layer 2/3 of rat neocortex. J Physiol (Lond) 551:139–153.

Houweling AR, Brecht M (2008) Behavioural report of single neuron stimulation in somatosensory cortex. Nature 451:65–68.

Huber D, Petreanu L, Ghitani N, Ranade S, Hromádka T, Mainen Z, Svoboda K (2008) Sparse optical microstimulation in barrel cortex drives learned behaviour in freely moving mice. Nature 451:61–64.

Huberd (2007) Microsoft Word - Suppl_Methods_Figures_Nature06445.doc. :1–12.

Jadhav SP, Wolfe J, Feldman DE (2009) Sparse temporal coding of elementary tactile features during active whisker sensation. Nat Neurosci 12:792–800.

Jones EG (1985) The thalamus. Plenum Publishing Corporation.

Judkewitz B, Rizzi M, Kitamura K, Häusser M (2009) Targeted single-cell electroporation of mammalian neurons in vivo. Nat Protoc 4:862–869.

Kajikawa Y, Schroeder CE (2011) How Local Is the Local Field Potential? Neuron 72:847–858.

Kerr JND, de Kock CPJ, Greenberg DS, Bruno RM, Sakmann B, Helmchen F (2007) Spatial organization of neuronal population responses in layer 2/3 of rat barrel cortex. J Neurosci 27:13316–13328.

Kitamura K, Judkewitz B, Kano M, Denk W, Häusser M (2008) Targeted patch-clamp recordings and single-cell electroporation of unlabeled neurons in vivo. Nat Meth 5:61–67.

Kleinfeld D, Ahissar E, Diamond M (2006) Active sensation: insights from the rodent vibrissa sensorimotor system. Curr Opin Neurobiol 16:435–444.

Konig P, Engel AK, Singer W (1996) Integrator or coincidence detector? The role of the cortical neuron revisited. Trends Neurosci 19:130–137.

Koralek KA, Jensen KF, Killackey HP (1988) Evidence for two complementary patterns of thalamic input to the rat somatosensory cortex. Brain Res 463:346–351.

Krogsgaard-Larsen P, Johnston GA, Curtis DR, Game CJ, McCulloch RM (1975) Structure and biological activity of a series of conformationally restricted analogues of GABA. J Neurochem 25:803–809.

Landisman CE, Connors BW (2007) VPM and PoM nuclei of the rat somatosensory thalamus: intrinsic neuronal properties and corticothalamic feedback. Cerebral Cortex 17:2853–2865.

Lefort S, Tomm C, Floyd Sarria J-C, Petersen CC (2009) The Excitatory Neuronal Network of the C2 Barrel Column in Mouse Primary Somatosensory Cortex. Neuron 61:301–316.

Li CYT, Poo MM, Dan Y (2009) Burst Spiking of a Single Cortical Neuron Modifies Global Brain State. Science 324:643–646.

Li X, Gutierrez DV, Hanson MG, Han J, Mark MD, Chiel H, Hegemann P, Landmesser LT, Herlitze S (2005) Fast noninvasive activation and inhibition of neural and network activity by vertebrate rhodopsin and green algae channelrhodopsin. Proc Natl Acad Sci USA 102:17816–17821.

Lindén H, Tetzlaff T, Potjans TC, Pettersen KH, Grün S, Diesmann M, Einevoll GT (2011) Modeling the spatial reach of the LFP. Neuron 72:859–872.

Llinás R, Jahnsen H (1982) Electrophysiology of mammalian thalamic neurones in vitro. Nature 297:406–408.

Llinás RR, Steriade M (2006) Bursting of Thalamic Neurons and States of Vigilance. J Neurophysiol 95:3297–3308.

London M, Roth A, Beeren L, Häusser M, Latham PE (2010) Sensitivity to perturbations in vivo implies high noise and suggests rate coding in cortex.

Nature 466:123–127.

Luo L, Callaway EM, Svoboda K (2008) Genetic dissection of neural circuits. Neuron 57:634–660.

Lübke J, Egger V, Sakmann B, Feldmeyer D (2000) Columnar organization of dendrites and axons of single and synaptically coupled excitatory spiny neurons in layer 4 of the rat barrel cortex. J Neurosci 20:5300–5311.

Manns ID, Sakmann B, Brecht M (2004) Sub- and suprathreshold receptive field properties of pyramidal neurones in layers 5A and 5B of rat somatosensory barrel cortex. J Physiol (Lond) 556:601–622.

Margrie TW, Brecht M, Sakmann B (2002) In vivo, low-resistance, whole-cell recordings from neurons in the anaesthetized and awake mammalian brain. Pflugers Arch 444:491–498.

Matyas F, Sreenivasan V, Marbach F, Wacongne C, Barsy B, Mateo C, Aronoff R, Petersen CCH (2010) Motor control by sensory cortex. Science 330:1240–1243.

Mccormick DA, Bal T (1997) Sleep and arousal: thalamocortical mechanisms. Annu Rev Neurosci 20:185–215.

Murasugi CM, Salzman CD, Newsome WT (1993) Microstimulation in visual area MT: effects of varying pulse amplitude and frequency. J Neurosci 13:1719–1729.

Muthuswamy J, Tran P, Rangarajan R, Lenz FA, Hanley DF, Thakor NV (1999) Somatosensory stimulus entrains spindle oscillations in the thalamic VPL nucleus in barbiturate anesthetized rats. Neurosci Lett 262:191–194.

Nagel G, Szellas T, Huhn W, Kateriya S, Adeishvili N, Berthold P, Ollig D, Hegemann P, Bamberg E (2003) Channelrhodopsin-2, a directly light-gated cation-selective membrane channel. Proc Natl Acad Sci USA 100:13940–13945.

NARAHASHI T, MOORE JW, SCOTT WR (1964) Tetrodotoxin Blockage Of Sodium Conductance Increase In Lobster Giant Axons. J Gen Physiol 47:965–974.

O'connor DH, Clack NG, Huber D, Komiyama T, Myers EW, Svoboda K (2010) Vibrissa-Based Object Localization in Head-Fixed Mice. J Neurosci 30:1947–1967.

O'connor DH, Huber D, Svoboda K (2009) Reverse engineering the mouse brain. Nature 461:923–929.

Paxinos G, Franklin KBJ (2007) The Mouse Brain in Stereotaxic Coordinates, Third Edition, 3rd ed. Academic Press.

Petersen CC, Sakmann B (2000) The excitatory neuronal network of rat layer 4 barrel cortex. J Neurosci 20:7579–7586.

Petersen CC, Sakmann B (2001) Functionally independent columns of rat

somatosensory barrel cortex revealed with voltage-sensitive dye imaging. J Neurosci 21:8435–8446.

Petersen CCH (2003) The barrel cortex--integrating molecular, cellular and systems physiology. Pflugers Arch 447:126–134.

Petersen CCH (2007) The functional organization of the barrel cortex. Neuron 56:339–355.

Petersen CCH, Hahn TTG, Mehta M, Grinvald A, Sakmann B (2003) Interaction of sensory responses with spontaneous depolarization in layer 2/3 barrel cortex. Proc Natl Acad Sci USA 100:13638–13643.

Pierret T, Lavallée P, Deschênes M (2000) Parallel streams for the relay of vibrissal information through thalamic barreloids. J Neurosci 20:7455–7462.

Ramcharan EJ, Gnadt JW, Sherman SM (2000) Burst and tonic firing in thalamic cells of unanesthetized, behaving monkeys. Vis Neurosci 17:55–62.

Reichova I (2004) Somatosensory Corticothalamic Projections: Distinguishing Drivers From Modulators. J Neurophysiol 92:2185–2197.

Reppas JB, Newsome WT (2007) Brain stimulation: feeling the buzz. Curr Biol 17:R358–60.

Sakata S, Harris KD (2009) Laminar structure of spontaneous and sensory-evoked population activity in auditory cortex. Neuron 64:404–418.

Salzman CD, Britten KH, Newsome WT (1990) Cortical microstimulation influences perceptual judgements of motion direction. Nature 346:174–177.

Shadlen MN, Newsome WT (1994) Noise, neural codes and cortical organization. Curr Opin Neurobiol 4:569–579.

Sherman SM (2001) Tonic and burst firing: dual modes of thalamocortical relay. Trends Neurosci 24:122–126.

Sherman SM, Koch C (1998) Thalamus. Oxford University Press.

Simons DJ, Carvell GE (1989) Thalamocortical response transformation in the rat vibrissa/barrel system. J Neurophysiol 61:311–330.

Softky WR (1995) Simple codes versus efficient codes. Curr Opin Neurobiol 5:239–247.

Spengler F, Dinse HR (1994) Reversible relocation of representational boundaries of adult rats by intracortical microstimulation. Neuroreport 5:949–953.

Steriade M (1995) Thalamic origin of sleep spindles: Morison and Bassett (1945). J Neurophysiol 73:921–922.

Steriade M (2005) Sleep, epilepsy and thalamic reticular inhibitory neurons. Trends

Neurosci 28:317–324.

Steriade M, Deschênes M, Domich L, Mulle C (1985) Abolition of spindle oscillations in thalamic neurons disconnected from nucleus reticularis thalami. J Neurophysiol 54:1473–1497.

Steriade M, Domich L, Oakson G, Deschênes M (1987) The deafferented reticular thalamic nucleus generates spindle rhythmicity. J Neurophysiol 57:260–273.

Steriade M, Gloor P, Llinás RR, Lopes de Silva FH, Mesulam MM (1990) Report of IFCN Committee on Basic Mechanisms. Basic mechanisms of cerebral rhythmic activities. Electroencephalogr Clin Neurophysiol 76:481–508.

Steriade M, Mccormick DA, Sejnowski TJ (1993) Thalamocortical oscillations in the sleeping and aroused brain. Science 262:679–685.

Swadlow HA, Gusev AG (2001) The impact of "bursting" thalamic impulses at a neocortical synapse. Nat Neurosci 4:402–408.

Temereanca S, Simons DJ (2004) Functional topography of corticothalamic feedback enhances thalamic spatial response tuning in the somatosensory whisker/barrel system. Neuron 41:639–651.

Timofeev I, Steriade M (1996) Low-frequency rhythms in the thalamus of intact-cortex and decorticated cats. J Neurophysiol 76:4152–4168.

Van der Loos H (1976) Neuronal circuitry and its development. Prog Brain Res 45:259–278.

Veinante P, Deschênes M (1999) Single- and multi-whisker channels in the ascending projections from the principal trigeminal nucleus in the rat. J Neurosci 19:5085–5095.

Venkatraman S, Carmena JM (2009) Behavioral modulation of stimulus-evoked oscillations in barrel cortex of alert rats. Front Integr Neurosci 3:10.

Voigt BC, Brecht M, Houweling AR (2008) Behavioral Detectability of Single-Cell Stimulation in the Ventral Posterior Medial Nucleus of the Thalamus. J Neurosci 28:12362–12367.

Wang H, Peca J, Matsuzaki M, Matsuzaki K, Noguchi J, Qiu L, Wang D, Zhang F, Boyden E, Deisseroth K, Kasai H, Hall WC, Feng G, Augustine GJ (2007) High-speed mapping of synaptic connectivity using photostimulation in Channelrhodopsin-2 transgenic mice. Proc Natl Acad Sci USA 104:8143–8148.

Wong-Riley MT, Welt C (1980) Histochemical changes in cytochrome oxidase of cortical barrels after vibrissal removal in neonatal and adult mice. Proc Natl Acad Sci USA 77:2333–2337.

Woolsey TA, Van der Loos H (1970) The structural organization of layer IV in the somatosensory region (SI) of mouse cerebral cortex. The description of a cortical field composed of discrete cytoarchitectonic units. Brain Res 17:205–242.

Yu C, Derdikman D, Haidarliu S, Ahissar E (2006) Parallel thalamic pathways for whisking and touch signals in the rat. PLoS Biol 4:e124.